

**A MODEL FOR FLUID FLOW BETWEEN
PARALLEL, CO-ROTATING
ANNULAR DISKS**

Thesis
Submitted to
Graduate Engineering and Research
School of Engineering

UNIVERSITY OF DAYTON

In Partial Fulfillment of the Requirements for
The Degree
Master of Science in Mechanical Engineering

by
Jeffrey Stuart Allen

University of Dayton
Dayton, Ohio
July, 1990

A MODEL FOR FLUID FLOW BETWEEN
PARALLEL, CO-ROTATING ANNUALAR DISKS

Approved by:



Kevin Hallinan, Ph.D.
Advisory Committee, Chairman



Gary A. Thiele, Ph.D.
Associate Dean/Director
Graduate Engineering and Research
School of Engineering



Gordon A. Sargent, Ph.D.
Dean, School of Engineering

Acknowledgements

I am deeply indebted to my family, friends, and associates for their support during the course of this work and my education. In particular, I would like to thank Dr. John Schauer for getting me started on this project and for his continual guidance and support. And I greatly appreciate the faculty and staff of the mechanical engineering department for their assistance and patience. I would also like to thank Dr. Costandy Saba and Dr. Vinod Jain for providing me with the financial means to pursue my master studies. An enormous debt of gratitude goes to my good friend Frank Lung for his technical assistance and for his help in preparing this thesis. I can not thank enough Dr. Kevin Hallinan who inherited the role of my thesis advisor. Without his considerable time and effort I would have never finished. Finally, I would especially thank my parents, Bryant and Carol, for their patience, understanding, and support; to them I dedicate this work.

Abstract

A MODEL FOR FLUID FLOW BETWEEN PARALLEL, CO-ROTATING ANNULAR DISKS

Allen, Jeffrey Stuart
University of Dayton, 1990
Advisor: Dr. Kevin Hallinan

A model for fluid flow between parallel, co-rotating annular disks is developed from conservation of mass and conservation of momentum principles. Through the assumption of fully-developed boundary layer flow a closed form solution is found for the velocity components and the pressure. These solutions are then applied to the conservation of angular momentum principle from which a closed form solution for the torque of the system is found.

The model can be used to analyze the fluid/disk system in either a pump or a turbine configuration. The only change necessary is a slight modification of the boundary conditions. The accuracy of the results in both cases improves as the dimensionless parameter R^* increases. An R^* on the order of or greater than 1 indicates that viscous effects are important and the model appears to be very accurate in this range.

Other dimensionless parameters similar to R^* appear in the development which also describe various aspects of the model. These parameters are discussed with respect to the force effects (momentum, Coriolis, centripetal, viscous, and pressure) that each describe. In addition, the performance of a turbine configuration is investigated with the model and the moment of momentum relationship developed from the model.

The results of this analysis appear to be promising for describing rotating viscous flows and justify further investigation.

Contents

Table of Contents	v
List of Figures	viii
List of Tables	ix
Nomenclature	x
1 INTRODUCTION	1
1.1 Background	1
1.1.1 History	3
1.1.2 Model Geometry	3
1.2 Scope of Work	6
2 ANALYTICAL MODEL	9
2.1 Differential Equations of Motion	10
2.2 Velocity Profile	12
2.3 Solution to Continuity	15
2.4 The R -Constant	16
2.5 Solution to Momentum Equations	18
2.6 Summary	20
3 BOUNDARY CONDITIONS	21
3.1 Mass Flow Rate and Angular Velocity	21
3.2 Tangential Velocity and Angle of Tangency	24
4 CHARACTERISTICS PARAMETERS	28
4.1 Dimensionless Parameters γ and Re_δ	29
4.2 R^*	29
4.3 Angular Velocity Constant, c	31
4.4 Rossby Number	32
4.5 Summary	33

5	PATHLINES	35
5.1	Change In Angular Position of Fluid	35
5.2	Pathlines And Relative Velocities	38
6	TORQUE AND POWER	41
6.1	Conservation of Angular Momentum	41
6.2	Torque	44
6.3	Power	47
7	RESULTS AND DISCUSSION	48
7.1	Model Verification	48
7.2	System Performance	50
7.3	Model Behavior	53
7.4	Summary	60
8	CONCLUSION	61
8.1	Summary of Model	61
8.2	Recommendations	62
A	Conservation of Mass	65
A.1	Reduction of Continuity	65
A.2	Solution for the Radial Velocity Component	66
B	Conservation of Momentum	68
B.1	Reduction of the Navier-Stokes Equations	68
B.2	Velocity Profile Function	71
B.3	Incorporating Continuity	72
	B.3.1 r -momentum	73
	B.3.2 θ -momentum	73
B.4	γ vs. Re_δ	75
B.5	The R Constant	77
B.6	Summary	77
C	Solution to θ-Momentum	79
C.1	Homogeneous Solution	80
C.2	Particular Solution	82
C.3	Total Solution	84
D	Solution to r-Momentum	85
D.1	Integrations	86
D.2	Solution	92

E	Conservation of Angular Momentum	94
E.1	Rotating Control Volume	94
E.2	Conservation of Angular Momentum	97
E.3	Solution to Moment of Momentum	100
E.3.1	Surface Integral Evaluation	103
E.3.2	Volume Integral Evaluation	105
F	Program Listing	108
G	Data Files	129

List of Figures

1.1	Basic Rotor Construction for System	2
1.2	Geometry of Model for Rotor	5
1.3	Fluid Element: Orientation, Forces, and Velocities	7
3.1	Directions of the Radial Velocity Component	23
3.2	Angle of Tangency	26
5.1	Incremental Change in Fluid Particle Position	37
5.2	Typical Pathline For Turbine Configuration	39
6.1	Control Volume Definition for System Model ($N = 0$)	43
7.1	Torque versus Angular Velocity for Various δ	51
7.2	Power versus Angular Velocity for Various δ	54
7.3	Normalized Pressure for Various R^*	55
7.4	Pathlines for Various R^*	57
7.5	R^* versus r^*	58
7.6	\bar{V} versus r^*	59
E.1	Rotating Control Volume Relative to Inertial Frame of Reference	95
E.2	Control Volume Definition	102

List of Tables

1.1	Coordinate and Velocity Components	4
1.2	Specifying Parameters for Rotor	6
2.1	λ -Coefficient Values	14
3.1	Determination of System Constants	27
7.1	System Specification for Figures 7.1 and 7.2	50
B.1	Typical Rotor and Fluid Parameters for Turbine Configuration . . .	76
D.1	Values of Functions F_m and G_m for Various m	89

Nomenclature

Variables

A	cross-sectional area
a	constant for $U(r)$
b	constant for $\bar{V}(r)$
c	constant for $\bar{V}(r)$
d	constant for P
\hat{e}	unit vector
g	body force
g_c	gravitational constant
hp	horsepower
\dot{m}	mass flow rate
m, n	series indices
N	number of disks on rotor
P	pressure
\mathcal{P}	power
r	radial position
R	system constant
Re	Reynold's number
T	torque
u, U	radial velocity
v, V	absolute tangential velocity
\bar{v}, \bar{V}	relative tangential velocity
\forall	volume
w	axial velocity
z	axial position
α	angle of tangency
γ	aspect ratio
δ	half-disk spacing
η	axial position, z/δ
θ	angular position
ω	angular velocity of rotor
Ω	angular velocity of fluid
λ	velocity profile constant

Functions

$\mathcal{F}(\eta)$	velocity profile function
F_m, G_m	factorial functions
$S_m(r)$	series function
∇	gradient function
Δ	incremental change

Subscripts

$C.V.$	control volume
i	inner radius
j	vector indice
m	series function indicator
o	outer radius
r	radial, or based on radius
z	axial
δ	based on half-disk spacing
θ	tangential

Superscripts

*	dimensionless
---	---------------

Chapter 1

INTRODUCTION

1.1 Background

The system under study consists of fluid flowing between parallel, co-rotating annular disks. The rotor, or rotating assemblage, of the system is constructed by attaching a stack of annular disks to a central shaft. Figure 1 illustrates the basic rotor configuration. This fluid-rotor system can operate either as a pump or as a turbine. In both instances energy transfer between the fluid and the rotor occurs through viscous effects. The operation of this system, as either as a pump or as a turbine, utilizes shear stresses in the fluid at the disk face which are created by a velocity differential between the fluid and the rotor. In the pump configuration, the velocity of the disks at a given radius is greater than the tangential velocity of the fluid at that radius; therefore, kinetic energy is transferred from the rotor to the fluid through viscous interaction at the disk face. In the turbine configuration, the disks are rotating slower than the tangential velocity of the fluid for a given radius and kinetic energy is transferred from the fluid to the rotor.

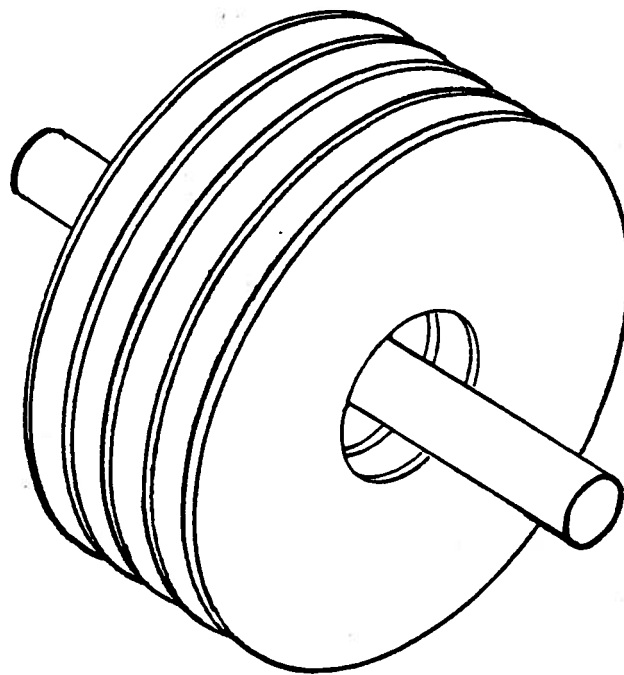


Figure 1.1: Basic Rotor Construction for System

1.1.1 History

The system under investigation in this study was first introduced in 1911 by Nikola Tesla as a turbine. In 1913 he demonstrated the concept with a steam powered, eight inch diameter turbine that developed over 200 horsepower[1,2]. A patent was issued to Tesla for both the concept and the device[3,4], hence the name Tesla Turbine. The turbine configuration is also referred to as the shear-torque turbine and the bladeless turbine. Since Tesla's original work the turbine has been more of a curiosity of acadamia than a practical device; although it has been developed for use in dentist drills. Some other applications that have been considered involve small propulsive devices for expendable weapons, such as torpedoes[5].

The pump configuration has been developed much more extensively both practically and analytically. This attention results from the long operating life this type of pump would exhibit in harsh environments. With a no-slip condition at the fluid-disk interface there would be less wear on components than found in typical pumps which rely upon direct momentum exchange for inducing fluid motion. In other words, with a typical pump the fluid impinges upon the rotor and this impingement accelerates rotor wear; whereas, the pump configuration of the system under study does not have this collision between the fluid and the rotor. This style of pump has been commercially developed for slurries or fluids containing solid objects that would damage either conventional pumps or the objects being pumped. One such application is in fisheries where this type of pump allows fish and rocks to pass through without damage to the pump or fish.

1.1.2 Model Geometry

Studying the performance of the device shown in Figure 1.1 requires that the interaction between the fluid and the rotor be modelled. In general, when the interaction

Table 1.1: Coordinate and Velocity Components

Coordinate	Component	Velocity
radial:	r	u
tangential:	θ	v
axial:	z	w

between the fluid and the rotor is being discussed the term *system* will be used. When the operation of this device, as a pump or as a turbine, is being discussed the term *configuration* will be used. The term *model* refers to the application of the equations of motion to the two-disk system shown in Figure 1.2. The model can be used in either a turbine configuration or a pump configuration.

Figure 1.2 illustrates the geometry of the rotor. A cylindrical coordinate system where the z-axis coincides with the axis of rotation. The notation used for coordinates and velocities is shown in Table 1.1.

Figure 1.2 illustrates the model geometry of the rotor. A single pair of disks will be used to model the fluid-disk interface; for actual rotors the model results will be multiplied by a coefficient corresponding to the number of disk pairs on the rotor:

$$ROTOR_{actual} = C(\# \text{ of disks}) * ROTOR_{model}.$$

If the disk faces are parallel to one another and the distance between the disks is constant over the radius of the rotor, then four parameters will completely specify the rotor geometry. These four parameters are outer radius, inner radius, disk spacing, and the number of disks. Table 1.2 defines the nomenclature used for these parameters. The coefficient corresponding to the number of disks, N , is defined such that for a single pair of disks (the model geometry) N is equal to zero:

$$C(\# \text{ of disks}) = N + 1.$$

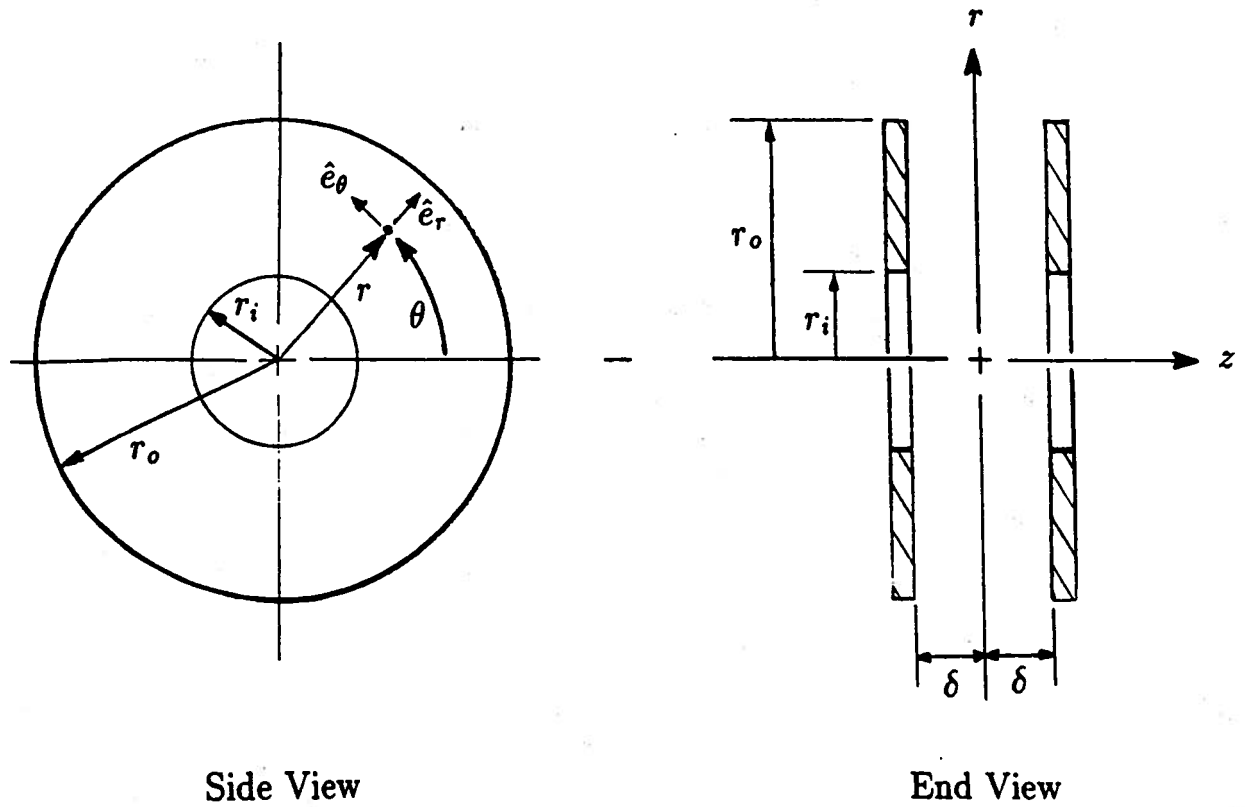


Figure 1.2: Geometry of Model for Rotor

Table 1.2: Specifying Parameters for Rotor

Outer Radius:	r_o
Inner Radius:	r_i
Half-Disk Spacing:	δ
Number of Disks:	N

Therefore, the performance of $ROTOR_{actual}$ must equal the $ROTOR_{model}$ performance for a system having only two disks.

Figure 1.3 illustrates the shear stresses on a fluid element in the turbine configuration. The shear stress in the radial direction is defined as τ_r and the shear stress in the tangential direction is defined as τ_t . The shear stresses arise from the velocity differential between the fluid and rotor and are the primary source of energy transfer for this system. This study focuses on finding the velocity differential responsible for the shear stresses.

1.2 Scope of Work

The goal of this study is to develop a procedure to predict the exchange in energy between the fluid and the rotor for various fluid properties, rotor configurations, and operating conditions. With the energy transfer known, the performance of the system as either a pump or a turbine can be calculated. The procedure will be to determine the velocity components of the fluid relative to the rotor and then to calculate the torque resulting from the sum of the shear forces across the disk faces.

The emphasis of this study is on the development of a new model and not on the use of the model. Several different rotor configurations and system operating conditions are studied, but even the study of these few systems is far from complete. The use of the model is concentrated on gaseous fluids in a turbine configuration since

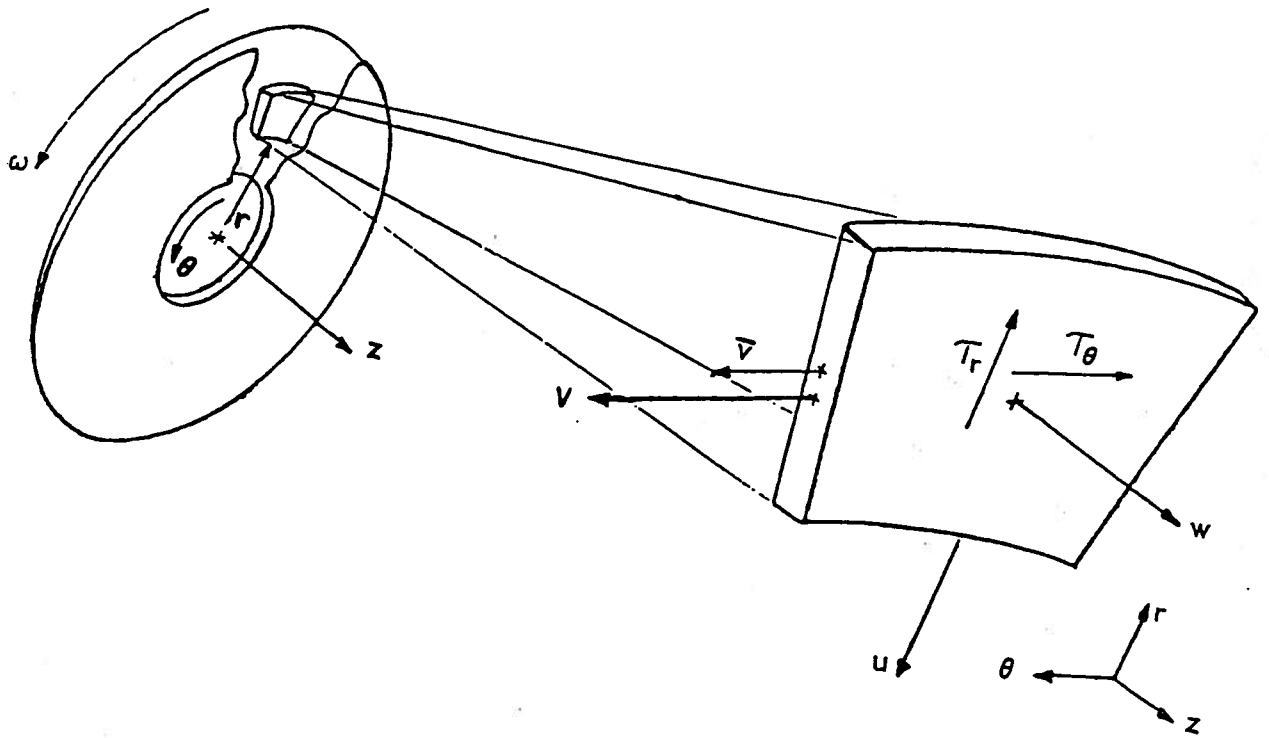


Figure 1.3: Fluid Element: Orientation, Forces, and Velocities

the original interest in this system was in analyzing the Tesla turbine. However, the model developed is as valid for pump analysis as it is for turbine analysis. The only changes necessary are in the boundary conditions.

Chapter 2

ANALYTICAL MODEL

This chapter highlights the model development detailed in Appendix A through D and discusses various properties of the model and the behavior of specific terms contained within the model equations. The analytical model will be developed from general conservation principles; i.e. mass, momentum, and energy. The purpose of this model is to predict fluid velocity components and pressures for various fluid properties, rotor configurations, and operating conditions. In other words, given a description of the system the analytical model will describe the behavior of the fluid within the system. Once the velocity components are known the performance of the system, either as a pump or turbine, can be determined.

The complete development of the analytical model is contained in Appendix A through Appendix D. Appendix A describes the reduction of the continuity equation and the solution for the radial velocity component of the fluid. Appendix B describes the reduction of the momentum equations. In Appendix C the θ -momentum equation is solved for the relative tangential velocity component, \bar{V} . The pressure is found by solving the r -momentum equation and is shown in Appendix D.

2.1 Differential Equations of Motion

Several approximations are imposed upon the general conservation principles in the development of the fluid model. The first approximation is isentropic flow. Since the temperature is constant throughout the flow there is no exchange in thermal energy and the conservation of energy principle need not be used. Therefore, the fluid model may be described by the differential forms of the conservation of mass and the conservation of momentum principles only. Expressed vectorially these principles are:

Conservation of Mass:

$$\dot{\rho} + \vec{\nabla} \cdot (\rho \vec{u}) = 0 \quad (2.1)$$

Conservation of Momentum:

$$\dot{\vec{u}} + (\vec{u} \cdot \vec{\nabla}) \vec{u} = \frac{-1}{\rho} \vec{\nabla} P + \vec{g} + \nu \nabla^2 \vec{u}. \quad (2.2)$$

Further approximations are applied to the mass and momentum conservation principles; such as incompressibility of the fluid which, with the assumption of isentropic flow, uncouples the governing Equations 2.1 and 2.2. Also, the flow is assumed to be steady-state, and body forces are ignored. Another assumption is that of fully-developed boundary layer flow existing throughout the rotor. This is the worst assumption of the model and the appropriateness of this assumption will be discussed later. Assuming fully-developed flow does, however, eliminate axial flow between the disks. That is, the axial component, w , of the fluid velocity is zero. Therefore, the characteristics of the fluid velocity field, \vec{u} , may be modelled using a velocity profile normal to the boundary layer; i.e., in the axial direction. Using a velocity profile for the flow effectively makes the field one-dimensional; however, the conservation equations are two dimensional in the coordinate system defined for the model shown in Figure 1.2. With these assumptions the conservation equations may now be used to solve for two components of the velocity and pressure (r and θ) at the centerline ($z = 0$)

of the model.

The velocity profile exists only for those components of the velocity relative to the rotating disk face. But the conservation equations are only valid for velocities relative to a non-rotating frame of reference. Therefore, to use the velocity profile in the conservation equations the absolute velocities are referenced to the rotating coordinate system. For the absolute radial velocity component, u , there is no change; the disk surface is not moving relative to r . However, the tangential velocity component, v , does change between rotating and stationary frames of reference. If we define v as the tangential velocity component of the fluid relative to a fixed frame of reference and \bar{v} as the tangential velocity component relative to a rotating frame of reference; i.e. the disk face, then the absolute tangential velocity, v , is a function of \bar{v} such that

$$v(r, \theta) = \bar{v}(r, \theta) + r\omega \quad (2.3)$$

where ω is the angular velocity of the rotor. The tangential velocity component relative to the disk face, \bar{v} , will be referred to as the *relative tangential velocity* throughout the rest of this study. By substituting Equation 2.3 into the conservation relations (Equations 2.1 and 2.2) for v we can use the velocity profile in modelling the flow field. This transformation also introduces Coriolis and centripetal forces into the convective term, $(\vec{u} \cdot \vec{\nabla})\vec{u}$, of the the conservation of momentum, Equation 2.2.

Now, assume that the flow characteristics are independent of the angular position. In other words, the velocity and pressure components are constant with respect to θ . This assumption will have repercussions in defining the boundary conditions, later. For nozzle directed flow in a turbine this assumption is not very precise. However, for a pump this is generally an accurate estimate of the flow conditions. The velocity components can now be expressed as the product of a radially dependent function at $z = 0$ and a velocity profile function.

Applying these approximations to the conservation principles we can reduce Equa-

tions 2.1 and 2.2 to the following forms:

continuity:

$$\frac{1}{r} \frac{\partial(ru)}{\partial r} = 0, \quad (2.4)$$

r -momentum:

$$\left(u \frac{\partial u}{\partial r} - \frac{\bar{v}^2}{r} \right) - (2\bar{v}\omega) - (r\omega^2) = -\frac{1}{\rho} \frac{dP}{dr} + \nu \left(\frac{\partial^2 u}{\partial r^2} + \frac{1}{r} \frac{\partial u}{\partial r} - \frac{u}{r^2} \right) + \nu \left(\frac{\partial^2 u}{\partial z^2} \right), \quad (2.5)$$

θ -momentum:

$$\left(u \frac{\partial \bar{v}}{\partial r} + \frac{u\bar{v}}{r} \right) + (2u\omega) = \nu \left(\frac{\partial^2 \bar{v}}{\partial r^2} + \frac{1}{r} \frac{\partial \bar{v}}{\partial r} - \frac{\bar{v}}{r^2} \right) + \nu \left(\frac{\partial^2 \bar{v}}{\partial z^2} \right). \quad (2.6)$$

2.2 Velocity Profile

If we define $\eta = z/\delta$ and the velocity profile function as $\mathcal{F}(\eta)$ then the velocity components of Equations 2.5 and 2.6 become

$$u(r, \theta) = U(r)\mathcal{F}(\eta) \quad (2.7)$$

and

$$\bar{v}(r, \theta) = \bar{V}(r)\mathcal{F}(\eta) \quad (2.8)$$

where $U(r)$ and $\bar{V}(r)$ are the centerline values ($z = 0$) of u and \bar{v} , respectively. The separation of variables for the velocities, u and \bar{v} , is possible through the assumption of fully-developed boundary layer flow. Substituting the product function form of the velocity components, Equations 2.7 and 2.8, into Equations 2.4, 2.5, and 2.6 produces the following form of the differential equations of motion:

continuity:

$$\frac{1}{r} \frac{d(rU)}{dr} = 0, \quad (2.9)$$

r -momentum:

$$\begin{aligned} \mathcal{F}^2(\eta) \left(U \frac{dU}{dr} - \frac{\bar{V}^2}{r} \right) - \mathcal{F}(\eta) (2\bar{V}\omega) - (r\omega^2) = \\ \frac{-1}{\rho} \frac{dP}{dr} + \nu \mathcal{F}(\eta) \left(\frac{d^2U}{dr^2} + \frac{1}{r} \frac{dU}{dr} - \frac{U}{r^2} \right) + \frac{\nu U}{\delta^2} \frac{d^2 \mathcal{F}(\eta)}{d\eta^2}, \end{aligned} \quad (2.10)$$

θ -momentum:

$$\begin{aligned} \mathcal{F}^2(\eta) \left(U \frac{d\bar{V}}{dr} + \frac{U\bar{V}}{r} \right) + \mathcal{F}(\eta) (2U\omega) = \\ \nu \mathcal{F}(\eta) \left(\frac{d^2\bar{V}}{dr^2} + \frac{1}{r} \frac{d\bar{V}}{dr} - \frac{\bar{V}}{r^2} \right) + \frac{\nu \bar{V}}{\delta^2} \frac{d^2 \mathcal{F}(\eta)}{d\eta^2}. \end{aligned} \quad (2.11)$$

Note that Equations 2.9, 2.10, and 2.11 are functions of total differentials of the velocity components as opposed to Equations 2.4, 2.5, and 2.6 which were functions of partial differentials of the velocity components.

If we integrate across the disk spacing, $-1 \leq \eta \leq 1$, the velocity profile functions, $\mathcal{F}(\eta)$, of Equations 2.9, 2.10, and 2.11 may be treated as constants. Define these constants as λ -coefficients, where

$$\lambda_1 = \int_0^1 \mathcal{F}^2(\eta) d\eta, \quad (2.12)$$

$$\lambda_2 = \int_0^1 \mathcal{F}(\eta) d\eta, \quad (2.13)$$

$$\lambda_3 = \int_0^1 \left[\frac{d^2 \mathcal{F}(\eta)}{d\eta^2} \right] d\eta, \quad (2.14)$$

$$\lambda_4 = \int_0^1 d\eta. \quad (2.15)$$

Because the velocity profile, $\mathcal{F}(\eta)$, is symmetric a factor of 2δ can be cancelled from each term in Equations 2.10 and 2.11. The λ -coefficients are constants with respect to

Table 2.1: λ -Coefficient Values

	Laminar	Turbulent
λ_1	8/15	7/9
λ_2	2/3	7/8
λ_3	-2	1/0 : undefined

r ; therefore, the characteristics of Equations 2.9, 2.10, and 2.11 remain unchanged for different flow regimes. The behavior of these equations for a laminar velocity profile is the same as for a turbulent velocity profile; only the value of the λ -coefficients vary.

Let us examine the λ -coefficients for two profiles. A power law is used to approximate a turbulent velocity profile:

$$\mathcal{F}(\eta) = (1 - \eta)^{1/7} \quad (2.16)$$

and a laminar velocity profile is approximated as parabolic:

$$\mathcal{F}(\eta) = 1 - \eta^2 . \quad (2.17)$$

By substituting Equations 2.16 and 2.17 into Equations 2.12, 2.13, and 2.14 we can compute the values of λ_1 , λ_2 , and λ_3 . The comparison is shown in Table 2.1

In Table 2.1 we see that the convective coefficients, λ_1 and λ_2 , approach 1 as the flow becomes turbulent. This is due to λ_1 and λ_2 being the averages of the convective effects in the velocity field. For instance, in slug flow both λ_1 and λ_2 would equal 1. The λ_3 -coefficient acts on the viscous dissipation terms and is a measure of the strain rate of the fluid at the wall. Unfortunately, the derivative of the turbulent power law approximation, Equation 2.16, breaks down at the wall ($\eta = \pm 1$) and results in an undefined λ_3 -coefficient. Therefore, some other measure of the strain rate at the disk face, such as a Blasius relation, must be used to determine λ_3 . The power law approximation is, however, still valid for λ_1 and λ_2 .

This study concentrates on the general behavior of fluid flow in parallel co-rotating annular disks; subsequently, the exact values of the λ -coefficients are not crucial. For the purposes of this study the λ -coefficients corresponding to a parabolic velocity profile (laminar flow), Equation 2.17, will be used.

Now, substitute the λ -coefficients into Equations 2.9, 2.10, and 2.11. A factor of 2δ is cancelled from each term. The equations of motion become:

continuity:

$$\frac{dU}{dr} + \frac{U}{r} = 0 \quad (2.18)$$

r -momentum:

$$\lambda_1 \left(U \frac{dU}{dr} - \frac{\bar{V}^2}{r} \right) - \lambda_2 (2\bar{V}\omega) - (r\omega^2) = \frac{-1}{\rho} \frac{dP}{dr} + \lambda_2 \nu \left(\frac{d^2 U}{dr^2} + \frac{1}{r} \frac{dU}{dr} - \frac{U}{r^2} \right) + \lambda_3 \frac{\nu U}{\delta^2} \quad (2.19)$$

θ -momentum:

$$\lambda_1 \left(U \frac{d\bar{V}}{dr} + \frac{u\bar{V}}{r} \right) + \lambda_2 (2U\omega) = \lambda_2 \nu \left(\frac{d^2 \bar{V}}{dr^2} + \frac{1}{r} \frac{d\bar{V}}{dr} - \frac{\bar{V}}{r^2} \right) + \lambda_3 \frac{\nu \bar{V}}{\delta^2} \quad (2.20)$$

2.3 Solution to Continuity

Examining Equation 2.18 we find that the radial velocity component at the centerline, $U(r)$, is independent of the flow regime since there is no dependency upon the λ -coefficients. Thus, the radial velocity relationship is identical for laminar and turbulent flows. Solving Equation 2.18 (See Appendix A) for the radial velocity component results in:

$$U(r) = \frac{a}{r}, \quad (2.21)$$

where a is an undetermined constant dependent upon the boundary conditions. In Equation 2.21 we see that the radial velocity component is directly proportional to the inverse of radial position; as the radius decreases the radial velocity increases.

If the solution for the radial velocity, Equation 2.21, is substituted into the r -momentum equation (2.19) we find that the dilation viscous term,

$$\frac{d}{dr} \left[\frac{1}{r} \frac{d}{dr} (rU) \right],$$

is zero. Likewise, the dilation viscous terms in Equation 2.20 can also be neglected. The reader is referred to Appendix B for details. Using Equation 2.21, the conservation of momentum (Equations 2.19 and 2.20), become

r -momentum:

$$\lambda_1 \left(\frac{U^2 + \bar{V}^2}{r} \right) + \lambda_2 (2\bar{V}\omega) + (r\omega^2) = \frac{1}{\rho} \frac{dP}{dr} - \lambda_3 \frac{\nu U}{\delta^2}, \quad (2.22)$$

θ -momentum:

$$\lambda_1 \left(U \frac{d\bar{V}}{dr} + \frac{U\bar{V}}{r} \right) + \lambda_2 (2U\omega) = \lambda_3 \frac{\nu \bar{V}}{\delta^2}. \quad (2.23)$$

In Equation 2.22 we can see the convective forces¹ (left side of equation) now include linear momentum effects, $(U^2 + \bar{V}^2)/r$, Coriolis effects, $2\bar{V}\omega$, and centripetal effects, $r\omega^2$. The convective forces are balanced by viscous dissipation, $\nu U/\delta^2$, and the pressure gradient, dP/dr . Equation 2.23 represents a force balance in the tangential direction and shows no centripetal or pressure effects. Therefore, the viscous effects are balanced by momentum and Coriolis effects.

2.4 The R -Constant

We can simplify the solutions of Equations 2.22 and 2.23 through the introduction of a term, R , defined as

$$R = -\frac{\lambda_3 \nu}{2\lambda_1 \delta^2 r U}. \quad (2.24)$$

¹These terms are actually accelerations. Multiplying through by the density will make Equations 2.22 and 2.23 force balances.

Note that the units for Equation 2.24 are $[1/\text{length}^2]$. Therefore, we can define a dimensionless term, R^* , such that

$$R^* = Rr^2. \quad (2.25)$$

Now, if we define the aspect ratio of the rotor, r/δ , as γ , Equation 2.25 can be rearranged as

$$R^* = -\frac{\lambda_3}{2\lambda_1} \frac{\gamma^2}{Re_r} \quad (2.26)$$

or

$$R^* = -\frac{\lambda_3}{2\lambda_1} \frac{\gamma}{Re_\delta}, \quad (2.27)$$

where Re_r is the radial Reynold's number:

$$Re_r = \frac{Ur}{\nu} = \frac{a}{\nu} \quad (2.28)$$

and Re_δ is the Reynold's number based upon disk spacing:

$$Re_\delta = \frac{U\delta}{\nu}. \quad (2.29)$$

Therefore, R^* is a ratio of the rotor configuration to the viscous/momentum force balance. Also, the radial Reynold's number, Re_r , is a constant for the system while Re_δ is dependent upon radial position.

Using the definition of R , Equation 2.24, we can rearrange the momentum equations, 2.22 and 2.23, to

r -momentum:

$$\frac{1}{\rho} \frac{dP}{dr} = \lambda_1 \left(\frac{U^2 + \bar{V}^2}{r} \right) + \lambda_2 (2\bar{V}\omega) + (r\omega^2) + \lambda_3 \left(\frac{\nu U}{\delta^2} \right), \quad (2.30)$$

θ -momentum:

$$\frac{d\bar{V}}{dr} + (1 + 2Rr^2) \frac{\bar{V}}{r} + 2 \frac{\lambda_2}{\lambda_1} \omega = 0. \quad (2.31)$$

We found that the radial velocity component, U , could be solved explicitly from continuity, Equation 2.18. From Equations 2.30 and 2.31 we see that the relative tangential velocity, \bar{V} , can be explicitly solved from the conservation of θ -momentum, Equation 2.31, and the pressure can be explicitly solved for from Equation 2.30.

2.5 Solution to Momentum Equations

The solution for Equation 2.31 (See Appendix C) results in a power series expression for the relative tangential velocity:

$$\bar{V}(r) = \frac{bS_m(R^*) - c}{r} \quad (2.32)$$

where $S_m(r)$ is a power series function of r ,

$$S_m(R^*) = \sum_{m=0}^{\infty} \frac{(-R^*)^m}{m!}. \quad (2.33)$$

In Equation 2.32 the constant, b , is dependent upon the boundary conditions. The second constant, c , is a function of angular velocity, ω , and R :

$$c = \frac{\lambda_2}{\lambda_1} \left(\frac{\omega}{R} \right). \quad (2.34)$$

The solution for the pressure is obtained by substituting the expressions for the radial and relative tangential velocities, Equations 2.21 and 2.32, into the r -momentum relation, Equation 2.30, and integrating with respect to r (See Appendix D). The solution for the pressure was simplified through the introduction of a convention for factorial functions:

$$F_m = \frac{1}{m!}, \quad (2.35)$$

and

$$G_m = \sum_{n=0}^m \frac{1}{n!} \frac{1}{(m-n)!} = \sum_{n=0}^m F_n F_{m-n}. \quad (2.36)$$

Using these conventions the solution for the pressure becomes:

$$\begin{aligned}
\frac{1}{\rho}P(r) &= -\lambda_1 \left\{ [a^2 + (b-c)^2] \frac{1}{2r^2} \right\} \Leftarrow \text{I} \\
&\quad -\lambda_1 \left\{ (b^2 - 2bc) R \ln r^2 \right\} \Leftarrow \text{II} \\
&\quad -\lambda_1 \left\{ bR \sum_{m=0}^{\infty} \frac{(-R^*)^{m+1}}{2(m+1)} [bG_{m+2} - 2cF_{m+2}] \right\} \Leftarrow \text{III} \\
&\quad -\lambda_1 \left\{ (c^2 - bc) R \ln r^2 \right\} \Leftarrow \text{IV} \\
&\quad -\lambda_1 \left\{ bR \sum_{m=0}^{\infty} \frac{(-R^*)^{m+1}}{2(m+1)} [-2cF_{m+1}] \right\} \Leftarrow \text{V} \\
&\quad + \left\{ [\omega^2] \frac{r^2}{2} \right\} \Leftarrow \text{VI} \\
&\quad -\lambda_1 \left\{ (a^2) R \ln r^2 \right\} \Leftarrow \text{VII} \\
&\quad + d \tag{2.37}
\end{aligned}$$

The terms on the right side of Equation 2.37 are separated with respect to the type of force effect from which each term evolved. For example, the integration of the convective term in Equation 2.30 results in terms I, II, and III. Summarizing the grouping:

- I, II, and III are from convective effects, $(U^2 + \bar{V}^2)/r$
- IV and V are from Coriolis effects, $2\bar{V}\omega$
- VI is from centripetal effects, $r\omega^2$
- VII is from viscous effects, $(\nu U)/\delta^2$
- d is an unknown constant of integration.

If we rearrange Equation 2.37 so as to group the terms by like powers of r a simpler solution form is obtained.

$$\begin{aligned} \frac{1}{\rho}P(r) = & -\lambda_1 \left\{ [a^2 + (b-c)^2] \left[\frac{1}{2r^2} + R \ln r^2 \right] \right\} \\ & -\lambda_1 \left\{ \left[bR \sum_{m=0}^{\infty} \frac{(-R^*)^{m+1}}{2(m+1)} [bG_{m+2} - 2c(m+3)F_{m+2}] \right] \right\} \\ & + [\omega^2] \frac{r^2}{2} + d \end{aligned} \quad (2.38)$$

2.6 Summary

In this chapter the conservation equations are solved to find expressions for U , \bar{V} , and P for fluid flow between parallel co-rotating annular disks. Equations 2.21, 2.32, and 2.38 describe a model for fluid flow within a system configured either as a pump or as a turbine. The constants in this set of equations (a , b , c , R , and d) vary with the operating conditions; i.e. boundary conditions. These constants will change depending upon the configuration of the system, but the characteristic behavior of the system is still described by the model.

Chapter 3

BOUNDARY CONDITIONS

In each of the solutions for U , \bar{V} , and P there are constants which must be specified in order to completely solve the system. These constants a , b , c , R , and d are dependent upon the boundary conditions. The constants determine the type of system; i.e. pump or turbine, but the solutions for the velocity and pressure, Equations 2.21, 2.32, and 2.38, are always the same.

3.1 Mass Flow Rate and Angular Velocity

From Equation 2.21 we see that the radial velocity constant, a , will change sign upon a change in the direction of the radial flow. If the flow is radially outward, as in a pump configuration, the radial velocity is positive, hence a must be positive. In a turbine configuration the flow is radially inward and a must be negative in order to have a negative radial velocity. This sign change is illustrated in Figure 3.1. The value of a can be determined by specifying the mass flow rate. By definition, the mass flow rate is

$$\dot{m} = \int_{\partial V} \rho \vec{v} \cdot d\vec{A}. \quad (3.1)$$

For both the pump and turbine configurations Equation 3.1 reduces to

$$\dot{m} = \rho A \bar{V} \cdot \hat{n}, \quad (3.2)$$

where A is a cross-sectional area at given radius and \hat{n} is the unit normal to the area. This area is equal to the circumference multiplied by the disk spacing and by the number of disk spaces. From this the mass flow rate can be written as

$$\dot{m} = \rho [(2\pi r)(2\delta)(N + 1)] (U\hat{e}_r + V\hat{e}_\theta) \cdot \hat{e}_r . \quad (3.3)$$

The term N in Equation 3.3, as defined earlier in Section 1.1.2, is equal to zero for a single pair of disks. Substituting the solution for the radial velocity, U , (Equation 2.21) into Equation 3.3 and rearranging we have

$$a = \pm \frac{\dot{m}}{4\pi(N + 1)\rho\delta} . \quad (3.4)$$

Therefore, given the rotor configuration, fluid density, and the mass flow rate the radial velocity component, U , of the fluid velocity can be determined for any radial position. Note that the correct sign must be assigned to a . For a turbine configuration a is negative and for a pump configuration a is positive.

If we examine the definition of R given in Equation 2.24 we find that the rU factor in the denominator may be replaced with the solution for the radial velocity (Equation 2.21). Subsequently, the term R is a constant such that

$$R = -\frac{\lambda_3}{2\lambda_1} \frac{\nu}{\delta^2 a} . \quad (3.5)$$

Now, by specifying the rotor dimensions, the fluid density and viscosity, and the mass flow rate, both the constant a and the constant R may be determined. With the constant R known, the determination of the constant c (Equation 2.34) in the solution of the relative tangential velocity, (Equation 2.32) can be accomplished by specifying the angular velocity, ω . Both R and c have a direct dependence upon a ; therefore, R and c will also vary in sign between a pump and a turbine configuration.

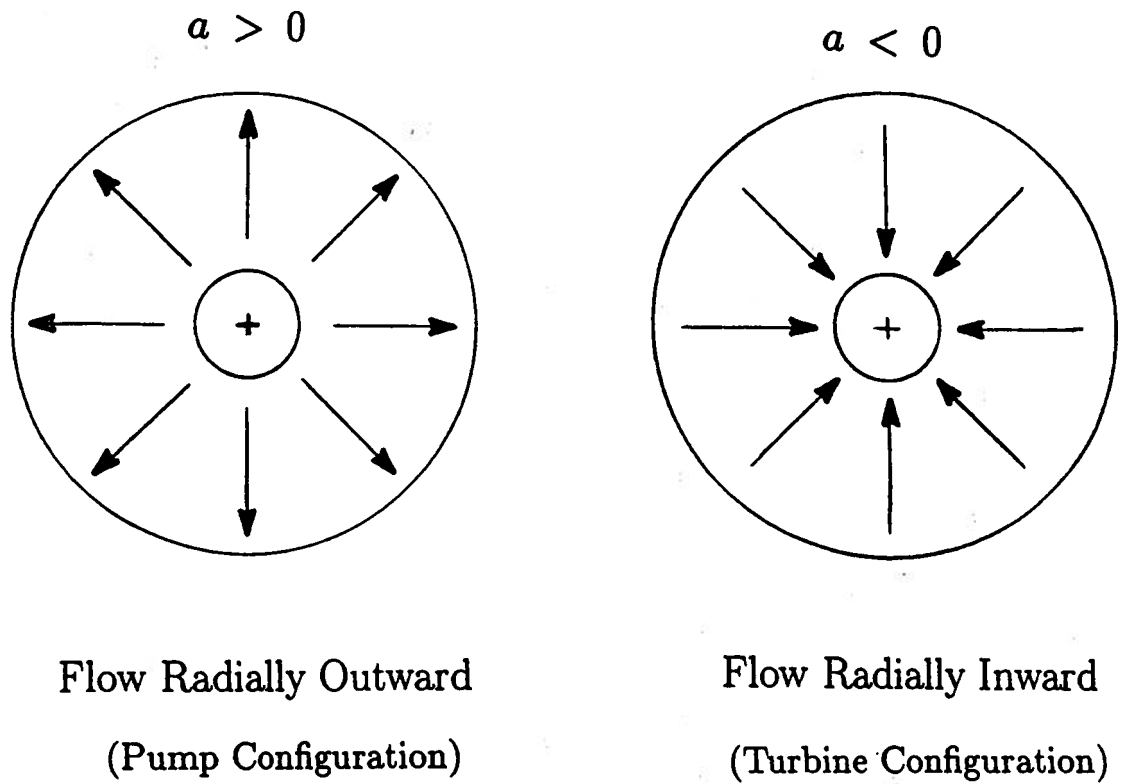


Figure 3.1: Directions of the Radial Velocity Component

3.2 Tangential Velocity and Angle of Tangency

The last two unknown constants, b of the relative tangential velocity solution (Equation 2.32) and d of the pressure solution (Equation 2.38) can be specified by two methods. The first method is to specify a static pressure at some radius and iterate on the pressure solution (Equation 2.38) while varying b and d until the correct pressure and angular velocity are found. The second method is to specify a pressure and a tangential velocity to solve for b and d separately. The first method appears to be the more desirable because there are fewer restrictions upon the system and because of the difficulty in specifying an accurate tangential velocity. Unfortunately, in the turbine configuration, the pressure drop across the disk has been found to be small experimentally [8] and analytically. Also the solution for the pressure (Equation 2.38) is only weakly dependent upon b . Therefore, the first method for determining b and d may not be accurate.

The second technique requires that the value of b is known in order to determine the value of d . To find b some tangential velocity at a fixed radius (i.e. outer) must be specified. Given that a relative tangential velocity, \bar{V} , is known for some radius then we can rearrange the solution for \bar{V} (Equation 2.32) in terms of b :

$$b = \frac{r\bar{V} + c}{S_m(R^*)}, \quad (3.6)$$

where $S_m(r)$ is defined in Equation 2.33.

For a pump configuration we can assume that the absolute tangential velocity at the inner radius is zero. This results in a relative tangential velocity at the inner radius equal to $-r_i\omega$. Therefore, Equation 3.6 becomes:

$$b = \frac{c - r_i^2\omega}{S_m(R^*_i)}. \quad (3.7)$$

For a turbine configuration the specification of a relative tangential velocity for Equation 3.6 is not as simple. In the specification of this \bar{V} we must remember

that any dependence upon angular position has been eliminated. Any locally known (θ -dependent) tangential velocity must be distributed over the entire circumference at the given radius. For example, in a turbine configuration we can experimentally determine the tangential velocity of the fluid as it exhausts from the nozzle and enters the rotor; however, using this value in Equation 3.6 will result in a value of b that is too large. This problem can be overcome by coupling the tangential velocity to the angle of incidence of the nozzle upon the rotor. This, in effect, relates the tangential velocity at the outer radius to the mass flow rate which is a constant; i.e. independent of θ . Figure 3.2 illustrates the angle, α , which is defined as the *angle of tangency*. Given α , then the absolute tangential velocity at the outer radius can be specified in terms of α and U_o ; the radial velocity at the outer radius:

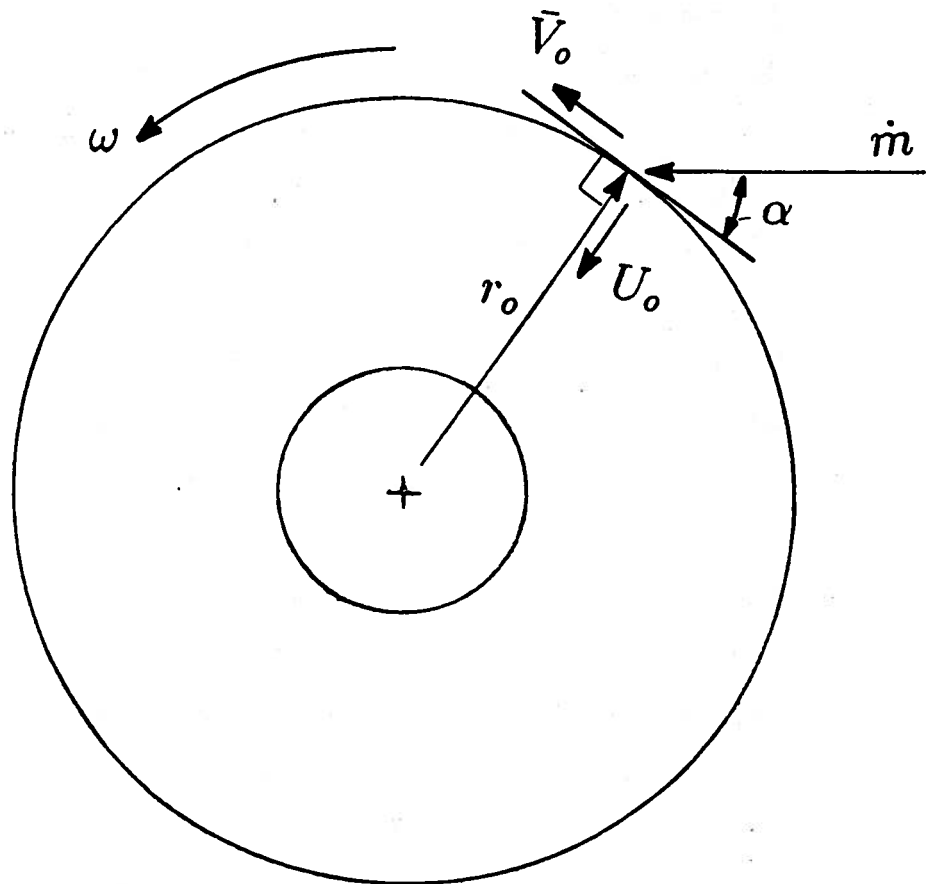
$$V_o = \frac{U_o}{\tan \alpha}. \quad (3.8)$$

The radial velocity, U_o , can be determined from the mass flow rate and Equations 2.21 and 3.4. Subtracting the surface velocity of the disk at the outer radius from Equation 3.8 will give the relative tangential velocity at the outer radius. Substituting this relative tangential velocity and the solution for U_o into Equation 3.6 gives a solution for b in the turbine configuration:

$$b = \frac{c - r_o^2 \omega + a / \tan \alpha}{S_m(R_o^*)}. \quad (3.9)$$

Equation 3.9 must be used cautiously! Because of the nature of the tangent function a small change in α can produce very large changes in b . As α approaches $\pi/2$ the tangent of α goes to zero which forces b to infinity. Subsequently, the relative tangential velocity and, ultimately, the output torque of the turbine are strongly effected by small variations in α .

The pressure constant, d , is now determined by specifying a static pressure at some radius and solving for d in Equation 2.38. In a pump configuration the specified



Turbine Configuration

Figure 3.2: Angle of Tangency

Table 3.1: Determination of System Constants

Constant	Pump	Turbine
a	$\frac{+\dot{m}}{4\pi(N+1)\rho\delta}$	$\frac{-\dot{m}}{4\pi(N+1)\rho\delta}$
b	$\frac{c - r_i^2\omega}{S_m(R^*_o)}$	$\frac{c - r_o^2\omega + a/\tan\alpha}{S_m(R^*_o)}$
c	$\frac{\lambda_2\omega}{\lambda_1 R}$	$\frac{\lambda_2\omega}{\lambda_1 R}$
R	$-\frac{\lambda_3\nu}{2\lambda_1\delta^2a}$	$-\frac{\lambda_3\nu}{2\lambda_1\delta^2a}$
d	$P_i - P(r_i)$	$P - P(r)$

pressure is most likely at the inner radius. For a turbine configuration the specified pressure could easily be at either the outer or inner radius.

Table 3.1 summarizes the specification of the system constants. With the specification of the system constants the velocity and pressure can be calculated at any position between the disks. The explicit relations for velocity and pressure allow for very quick computations; even with the presence of a power series in the momentum equations.

Chapter 4

CHARACTERISTICS PARAMETERS

In developing the model in Chapters 2 and 3 several characteristic parameters appeared. These are:

- the λ -coefficients ,
- the aspect ratio, γ ,
- the boundary layer Reynold's number, Re_δ ,
- the dimensionless R -constant, R^* , and
- the angular velocity constant, c .

All of the above parameters are dimensionless with exception of c . The following discussion of these parameters will focus on the relation between various types of forces, or effects, that each parameter describes. The actual trends or values that these parameters exhibit for specific systems will be discussed in Chapter 7. The λ -coefficients will not be discussed here since these parameters do not greatly effect the behavior of the model. A thorough treatment of the λ -coefficients is given in Section 2 of Chapter 2.

4.1 Dimensionless Parameters γ and Re_δ

The local aspect ratio is defined as

$$\gamma = \frac{r}{\delta}. \quad (4.1)$$

For the type of system described in Chapter 1 the radius, r , is nearly always much greater than the half-disk spacing, δ . In general, $\gamma \gg 1$. In the development of the model, fully-developed boundary layer flow is assumed. Therefore, δ is equivalent to the boundary layer thickness and the aspect ratio, γ , is a measure of the size of the rotor relative to the size of the fluid boundary layer. Therefore, γ is a scale of the flow passage.

The Reynold's number based upon the boundary layer thickness is defined as

$$Re_\delta = \frac{\delta U}{\nu}. \quad (4.2)$$

There is a second Reynold's number, Re_r , which also occurs naturally in the model development. However, this Reynold's number is based upon the radius and is not as indicative of the flow regime as Re_δ .

Individually, these two parameters can only characterize a portion of the system. The aspect ratio can describe the device, but not the flow. Similarly, the Reynold's number, Re_δ , can describe the flow but not the device. A combination of these two parameters is needed.

4.2 R^*

In Chapter 2 the conservation of momentum relation (Equation 2.6) is reduced to a force balance between momentum, Coriolis, and viscous effects. This force balance (Equation 2.23) is repeated here for convenience;

$$\lambda_1 U \left(\frac{d\bar{V}}{dr} + \frac{\bar{V}}{r} \right) + \lambda_2 U (2\omega) - \lambda_3 \frac{\nu r}{\delta^2} \left(\frac{\bar{V}}{r} \right) = 0. \quad (4.3)$$

The first term is a momentum element, the second is a Coriolis element, and the third is a viscous element. In order to solve for the relative tangential velocity, \bar{V} , the term R is introduced in Chapter 2 as;

$$R = -\frac{\lambda_3}{2\lambda_1} \frac{\nu}{\delta^2 r U}. \quad (4.4)$$

Comparing the definition of R to Equation 4.3 we find that R is the ratio of the viscous coefficient to the momentum coefficient. Using R transforms Equation 4.3 to

$$\frac{d\bar{V}}{dr} + (1 + Rr^2) + 2\frac{\lambda_2}{\lambda_1}\omega = 0. \quad (4.5)$$

Since R has units of $1/\text{length}^2$ a natural dimensionless form of R is

$$R^* = Rr^2 = -\frac{\lambda_3}{2\lambda_1} \frac{r\nu}{\delta^2 U}. \quad (4.6)$$

Therefore, R^* is a dimensionless measure of viscous and momentum effects.

If the definitions of γ and Re_δ (Equations 4.1 and 4.2) are substituted into Equation 4.6, then R^* becomes

$$R^* = -\frac{\lambda_3}{2\lambda_1} \frac{\gamma}{Re_\delta}. \quad (4.7)$$

Using Equations 4.6 and 4.7 we find that R^* is a relativistic measure of the system and of the momentum forces:

$$R^* \sim \frac{\text{flow passage}}{\text{flow regime}} \sim \frac{\text{viscous effects}}{\text{momentum effects}} \quad (4.8)$$

The magnitude of R^* dictates the importance of the momentum and viscous effects on the relative tangential velocity. If $R^* \ll 1$ then viscous effects are negligible¹. If $R^* \gg 1$ then viscous effects are dominant. In Appendix B, both viscous and momentum effects are found to be important for a typical turbine configuration; resulting in an R^* on the order of 1.

¹The model is also negligible since fully-developed boundary layer flow is meaningless in an inviscid flow.

The effect that variations in the system has upon R^* can be examined in Equation 4.6 by substituting the solution for the radial velocity (Equation 2.21) in for U :

$$R^* = -\frac{\lambda_3}{2\lambda_1} \frac{r^2 \nu}{\delta^2 a}. \quad (4.9)$$

Now, if the mass flow rate boundary condition (Equation 3.4) is applied to Equation 4.9 the R^* becomes

$$R^* = -2\pi \frac{\lambda_3}{\lambda_1} \left(\frac{\mu r}{\dot{m}} \right) \frac{r}{\delta}. \quad (4.10)$$

Equation 4.10 shows that R^* increases quadratically with r and decreases reciprocally as δ increases. In general, the radius of the system will be less than a foot (for a system specified in English units of measure) while the half-disk spacing, δ , will be much less than a foot (up to four orders of magnitude less). Therefore, R^* is more affected by disk spacing than radius. The relative effects between mass flow rate, \dot{m} , and viscosity, μ , are less clear since these boundary conditions can vary greatly.

4.3 Angular Velocity Constant, c

The solution for \bar{V} from Equation 4.5 in Chapter 2 is

$$\bar{V} = \frac{bS_m(R^*)}{r} - \frac{c}{r}, \quad (4.11)$$

where the constant, c is defined as

$$c = -\frac{\lambda_2}{\lambda_1} \frac{\omega}{R}. \quad (4.12)$$

This constant relates the angular velocity of the rotor, ω , to the relative tangential velocity, \bar{V} . In addition, c has units of $length^2/time$ which indicates that c is a diffusivity coefficient. Thus, c can be interpreted as the ratio of rotational (or kinetic) energy to viscous dissipation. Equation 4.12 can be rewritten in terms of R^* resulting in

$$c = \frac{\lambda_3}{\lambda_1} \frac{r^2 \omega}{R^*}. \quad (4.13)$$

Therefore, c describes a balance between the three effects present in Equation 4.3, momentum, Coriolis, and viscous.

From Equation 4.11 the relative tangential velocity, \bar{V} , can be shown to be proportional to c such that

$$\bar{V} \sim \frac{c}{r} \sim \frac{r\omega}{R^*}. \quad (4.14)$$

Divide through by the local relative tangential velocity;

$$1 \sim \frac{1}{R^*} \frac{r\omega}{\bar{V}}. \quad (4.15)$$

The dimensionless angular velocity term is defined as

$$\omega^* = \frac{r\omega}{\bar{V}}. \quad (4.16)$$

Equation 4.16 is actually a dimensionless form of the Coriolis effect upon the relative tangential velocity, \bar{V} . If Equation 4.11 is non-dimensionalized by the local relative tangential velocity, the result is

$$1 = b^* S_m(R^*) - c^*, \quad (4.17)$$

where b^* is equal to $b/r\bar{V}$ and

$$c^* = -\frac{\lambda_2}{\lambda_1} \frac{c}{r\bar{V}} = -\frac{\lambda_2}{\lambda_1} \frac{\omega^*}{R^*}. \quad (4.18)$$

4.4 Rossby Number

The dimensionless Coriolis term, ω^* , defined in Equation 4.16 is equivalent to the reciprocal of the Rossby number², R_s ;

$$\omega^* = \frac{1}{R_s}. \quad (4.19)$$

The Rossby number is by definition a measure of the importance of Coriolis forces. A description of the Rossby number is presented here from Batchelor[6]:

²Named in recognition of the Swedish meteorologist.

The extent to which the restoring effect of Coriolis forces restricts the displacement of fluid evidently depends on the relative magnitudes of Coriolis forces and other forces acting on the fluid; ... If $[V]$ is a representative velocity magnitude (relative to rotating axis) and L is a measure of the distance over which u varies appreciably, the ratio of the magnitudes of the terms $u \cdot \nabla u$ and $2\Omega \times u$... is of order

$$V/L\Omega .$$

When $V/L\Omega \gg 1$, Coriolis forces are likely to cause only a slight modification of the flow pattern; but when $V/L\Omega \ll 1$, the tendency for Coriolis forces to oppose any expansion in a lateral plane is likely to be dominant. And in the intermediate case when $V/L\Omega$ is of the order of unity, an interesting mixture of effects is to be expected, ...

Therefore, when $\omega^* \ll 1$ ($R_s \gg 1$), Coriolis forces are negligible and when $\omega^* \gg 1$ ($R_s \ll 1$), Coriolis forces are dominant.

Examining Equation 4.18 in the context of Batchelor's description and through the relationship expressed in 4.8 we find that c^* relates the three forces balanced by Equation 4.3:

$$c^* \sim \frac{(\text{momentum})(\text{Coriolis})}{(\text{viscous})} . \quad (4.20)$$

4.5 Summary

The momentum force balance in the tangential direction between momentum, Coriolis, and viscous forces is expressed in Equation 4.3. The relations between these three forces are characterized through several unique parameters. The flow passage, or device size, is described by the aspect ratio, γ . The flow regime within that passage is described by the boundary layer Reynold's number, Re_δ . The relation between the

strength of the momentum forces and the strength of the viscous forces is described by R^* . And finally, the strength of the Coriolis forces is described by the Rossby number, R_s , or the dimensionless angular velocity, ω^* . The constant c relates the three forces in terms of R^* and R_s .

Chapter 5

PATHLINES

5.1 Change In Angular Position of Fluid

From Equations 2.21 and 2.32 the velocity components of the fluid relative to the rotor, U and \bar{V} , can be calculated for any radius. With the relative velocities known the change in the position of a fluid particle can be determined.

In Figure 5.1 a fluid particle trajectory is shown for a portion of a rotor disk. The radial positions for points P_1 and P_4 are the same; likewise for P_3 and P_2 . Assuming the fluid particle position is known at point P_1 , we wish to find the point P_2 that lies on the fluid particle trajectory. Since the radial position is a specified parameter in the model, the velocity components, U and \bar{V} , are known for the radial positions P_1 and P_3 . However, the fluid does not travel from P_1 to P_3 , rather, it travels from P_1 to P_2 . Therefore, the change in angular position, $\Delta\theta$, has to be determined. We can find the time required for the fluid to move from P_1 to P_2 by examining the radial change in velocity from P_1 to P_3 . The average radial velocity between P_1 and P_3 is defined as

$$U_{avg} = \frac{\Delta r}{\Delta t}; \quad (5.1)$$

therefore, the time difference between P_1 and P_3 is

$$\Delta t = \frac{r_1 - r_3}{\frac{1}{2}(U_1 + U_3)}. \quad (5.2)$$

Since the velocity components and radial position are the same at P_3 and P_2 , Equation 5.2 expresses the time required for the fluid particle to travel from P_1 to P_2 in terms of P_1 to P_3 .

The relative angular velocity *of the fluid*, Ω , is determined by dividing the relative tangential velocity, \bar{V} , by the radius;

$$\Omega = \frac{\bar{V}}{r}. \quad (5.3)$$

Analogous to the average radial velocity, but working in the tangential direction, the average angular velocity of the fluid between P_1 and P_4 is defined as

$$\Omega_{avg} = \frac{\Delta\theta}{\Delta t}. \quad (5.4)$$

Thus, the change in angular position between P_1 and P_4 is

$$\Delta\theta = \Omega_{avg} \Delta t. \quad (5.5)$$

As was the case with radial time differences, the $\Delta\theta$ between P_1 and P_4 is the same as the $\Delta\theta$ between P_1 and P_2 .

The incremental change in angular position, $\Delta\theta$, can be expressed in terms of known velocities and radial positions by substituting Equation 5.2 in for Δt and rewriting Ω_{avg} in terms of \bar{V} and r . The resulting expression for $\Delta\theta$ is

$$\Delta\theta = \left(\frac{r_1 - r_2}{r_1 r_2} \right) \left(\frac{r_2 \bar{V}_1 + r_1 \bar{V}_2}{U_1 + U_2} \right). \quad (5.6)$$

Now, if the radial and angular positions of the initial point, P_1 , are known, the new angular position, θ_2 , for a specified r_2 can be calculated from Equation 5.6.

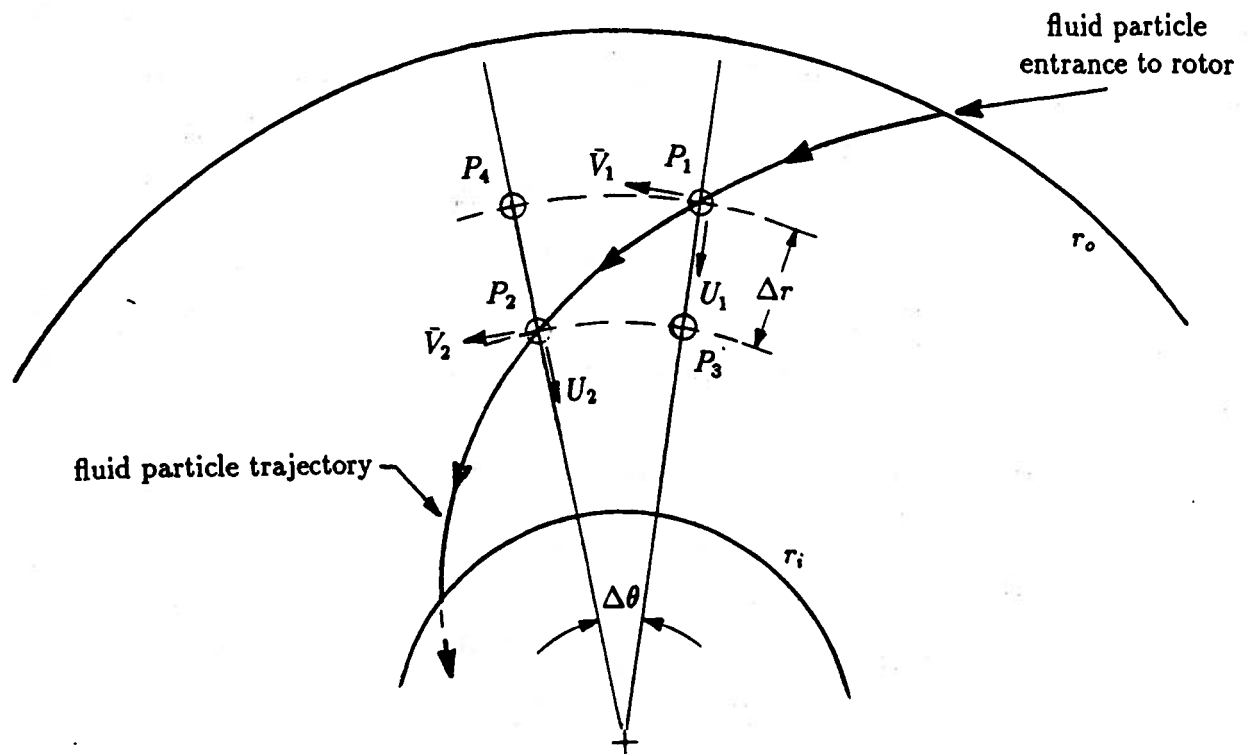


Figure 5.1: Incremental Change in Fluid Particle Position

5.2 Pathlines And Relative Velocities

Given an initial angular position (say, 0°), then if the incremental radius is small enough, a smooth succession of fluid element positions can be obtained resulting in a *pathline* of a fluid particle. Figure 5.2 illustrates a typical pathline for a turbine configuration. The disk is rotating at an angular velocity, ω , in the direction shown. Note that near the outer radius the fluid particle is moving in a tangential direction opposite that of the rotation of the disk. In this situation the rotor velocity, $r\omega$ is greater than the tangential velocity of the fluid, V . Therefore, the relative tangential velocity, \bar{V} , is less than zero. In Figure 5.2, as the fluid travels radially inward, the relative tangential velocity becomes less negative until a *peak* forms in the pathline. At this position the relative tangential velocity is zero. Below this peak the relative tangential velocity becomes positive.

Figure 5.2 is unique to the turbine configuration. In the outer radial region where \bar{V} is negative the system is acting as a pump; i.e. the rotor is imparting energy to the fluid. Another way to look at this region is that the fluid is exacting a torque from the rotor. In the inner radial region the rotor is exacting a torque from the fluid; the system is acting as a turbine. Overall, the torque created by the fluid in the inner region is greater than the torque absorbed by the fluid in the outer region. Thus, the system as a whole performs like a turbine. This type of situation is unlikely for the pump configuration. The initial relative tangential velocity, \bar{V} , is generally less than the speed of rotor at the entrance (inner radius) with the relative velocity becoming less negative as the radial position increases and the fluid absorbs energy from the rotor. Since there is no other source of energy than the rotating disks, the relative velocity of the fluid can never be greater than the speed of the disk. Therefore, there will be no peak in the pathline.

In addition to illustrating the fluid trajectory, the pathline gives an indication of

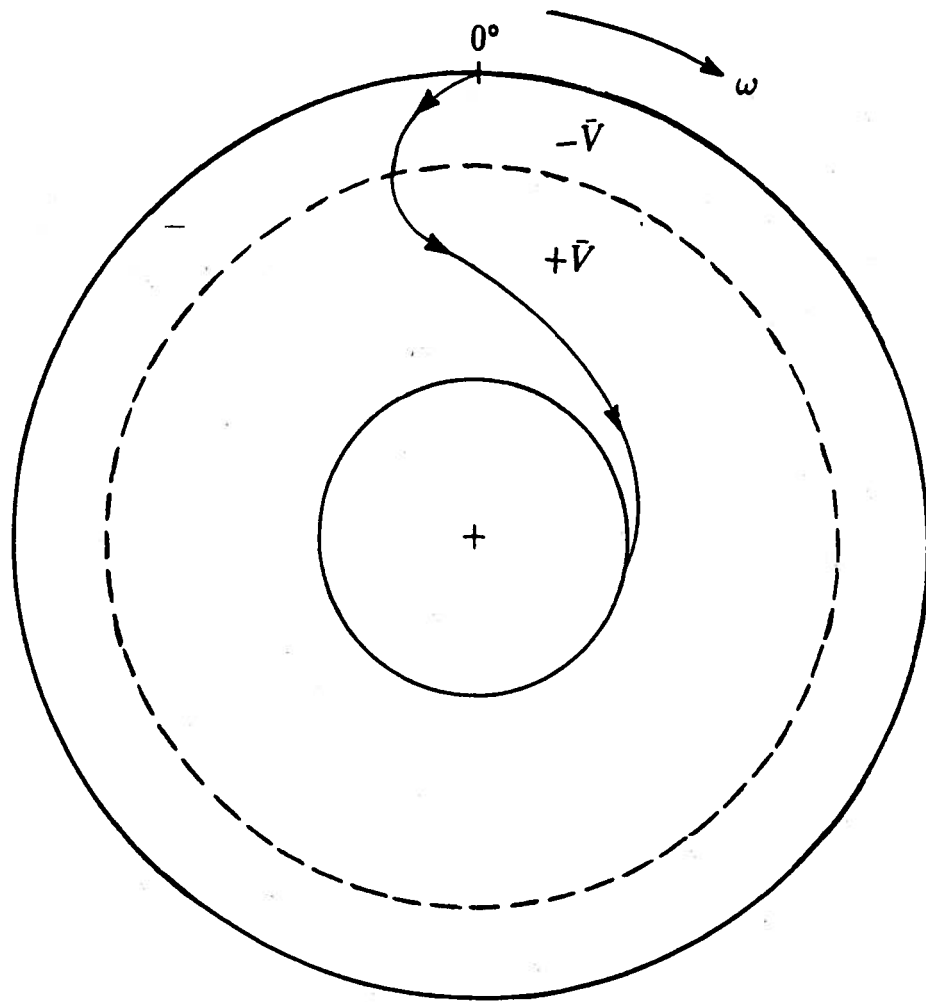


Figure 5.2: Typical Pathline For Turbine Configuration

the energy transfer occurring between the fluid and the rotor. The latter concept of a pathline is more appropriate since the boundary conditions and fluid velocities are not dependent upon the angular position, θ . The fluid is defined to be entering the disk simultaneously at all points on the circumference, this results in a pathline for every point on the circumference. The single pathline shown in Figure 5.2 is actually one of infinitely many, parallel pathlines on that disk.

Chapter 6

TORQUE AND POWER

This chapter utilizes the solution for fluid velocities and pressures within the system determined in Chapter 2 and Chapter 3 for calculating the performance of the system. In the pump configuration the performance is a work input, whereas in a turbine configuration the performance is work gained. To determine the work for either case both the angular velocity and the torque must be known. The angular velocity is specified as a boundary condition (See Chapter 3). The torque may be determined from the conservation of angular momentum.

6.1 Conservation of Angular Momentum

There are two approaches to determining the torque of this system. One is to define the system as a control volume and apply conservation of angular momentum to that control volume. The second is to sum the forces acting on a differential fluid element (Figure 1.3) and integrate that sum over the volume of the system. For this study the control volume approach will be used.

The control volume to which the conservation principle is applied is shown in Figure 6.1. The control volume incloses the fluid located within the rotor, but does not include the disks. Thus, the control volume has four sides; one side is the inner radius of the rotor, another is the outer radius, and the remaining two sides are along

the disk face at $\eta = \pm 1$. Also, the control volume rotates such that the relative velocity between the control volume and the rotor is zero.

The general conservation principles are only valid for inertial systems. Since a rotating control volume is non-inertial, the conservation of angular momentum must be modified. In Appendix E the conservation of angular momentum for a rotating system is shown to be

$$\begin{aligned} \vec{T}_{shaft_{C.V.}} + \vec{T}_{surface_{C.V.}} &= \frac{\partial}{\partial t} \int_{C.V.} (\vec{r} \times \vec{v}) \rho dV + \int_{\partial C.V.} (\vec{r} \times \vec{v}) \rho \vec{v} \cdot d\vec{A} \\ &+ \int_{C.V.} \vec{r} \times [\vec{\omega} \times \vec{r} + 2\vec{\omega} \times \vec{v} + \vec{\omega} \times (\vec{\omega} \times \vec{r})] \rho dV. \end{aligned} \quad (6.1)$$

In Equation 6.1, \vec{r} is a position vector of a particle within the control volume, \vec{v} is the velocity of that particle, and \mathcal{T} is torque. Both \vec{r} and \vec{v} are relative to the rotating control volume. The rotation of the control volume is described by $\vec{\omega}$. In Equation 6.1 the first two terms on the right are in the form for the general conservation of an intensive property within an inertial control volume. In this instance the quantity being conserved is angular momentum, $\rho (\vec{r} \times \vec{v})$. However, the control volume is not inertial so a *correction* in the form of the third term on the right of Equation 6.1 is required. This term contains a rate of change in angular momentum, $\rho (\vec{\omega} \times \vec{r})$, a Coriolis force, $\rho (2\vec{\omega} \times \vec{v})$, and a centripetal force, $\rho [\vec{\omega} \times (\vec{\omega} \times \vec{r})]$.

In applying Equation 6.1 to the control volume defined in Figure 6.1 the following assumptions are made:

- steady, incompressible flow,
- no variations with respect to θ ; $\frac{\partial}{\partial \theta} (-) = 0$,
- fully-developed boundary layer flow.

For the control volume defined there is no shaft work since no shaft crosses any surface

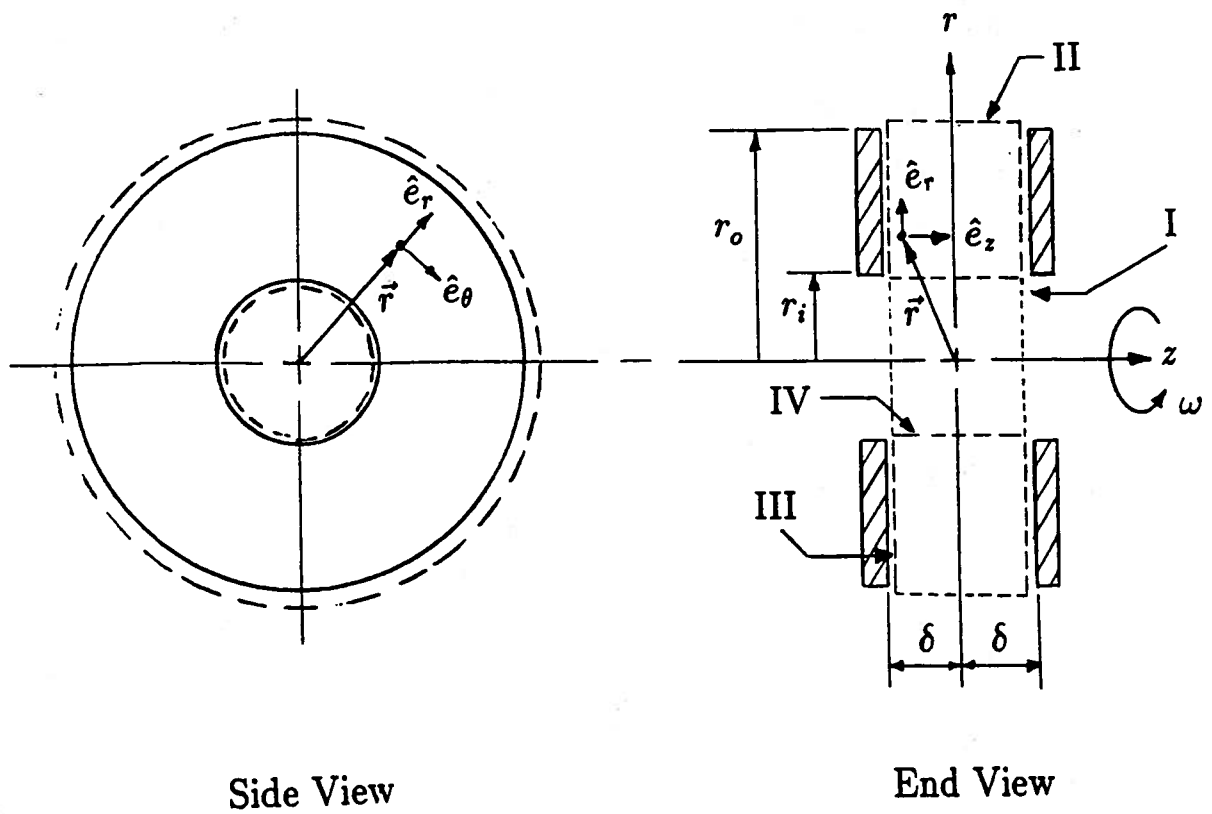


Figure 6.1: Control Volume Definition for System Model ($N = 0$)

of the control volume. With these assumptions Equation 6.1 becomes

$$\begin{aligned} \vec{T}_{surfaceC.V.} &= \int_{\partial C.V.} (\vec{r} \times \vec{v}) \rho \vec{v} \cdot d\vec{A} \\ &+ \int_{C.V.} \vec{r} \times [\vec{\omega} \times \vec{r} + 2\vec{\omega} \times \vec{v} + \vec{\omega} \times (\vec{\omega} \times \vec{r})] \rho dV. \end{aligned} \quad (6.2)$$

6.2 Torque

The torque of the rotor shaft can be shown to be equal the torque on the surface of the control volume. Therefore, the torque into or out of the system (as opposed to into or out of the control volume) can be written in terms of Equation 6.2:

$$\begin{aligned} \vec{T}_{shaft} &= \int_{\partial C.V.} (\vec{r} \times \vec{v}) \rho \vec{v} \cdot d\vec{A} \\ &+ \int_{C.V.} \vec{r} \times [\vec{\omega} \times \vec{r} + 2\vec{\omega} \times \vec{v} + \vec{\omega} \times (\vec{\omega} \times \vec{r})] \rho dV. \end{aligned} \quad (6.3)$$

The position vector, \vec{r} , for the control volume is defined as

$$\vec{r} = r\hat{e}_r + z\hat{e}_z, \quad (6.4)$$

and the velocity vector as

$$\vec{v} = u(r, z)\hat{e}_r + \bar{v}(r, z)\hat{e}_\theta. \quad (6.5)$$

Recalling the coordinate system defined in Chapter 1 (See Figure 1.2) the rotation of the control volume, $\vec{\omega}$, is described as

$$\vec{\omega} = \omega\hat{e}_z. \quad (6.6)$$

From the assumption of fully-developed boundary layer flow the velocity components may be written as the product of a centerline velocity ($\eta = 0$) and a velocity profile function, $\mathcal{F}(\eta)$. The velocity vector, \vec{v} , expressed in this manner is

$$\vec{v} = [U(r)\hat{e}_r + \bar{V}(r)\hat{e}_\theta] \mathcal{F}(\eta). \quad (6.7)$$

Using Equations 6.4, 6.6, and 6.7 let us examine the surface integral of the moment of momentum relation (Equation 6.3). The area vectors, $d\vec{A}$, for each surface of the control volume are

- $d\vec{A}_1 = dA_1\hat{e}_z$
- $d\vec{A}_2 = dA_2\hat{e}_r$
- $d\vec{A}_3 = -dA_3\hat{e}_z$
- $d\vec{A}_4 = -dA_4\hat{e}_r$

Since there are no axial components for the velocity the dot product in the surface integral becomes

$$\vec{v} \cdot d\vec{A} = \mathcal{F}(\eta) [U_2 dA_2 - U_4 dA_4]. \quad (6.8)$$

Evaluating the cross product, $\vec{r} \times \vec{v}$, results in

$$\vec{r} \times \vec{v} = \mathcal{F}(\eta) [r\bar{V}\hat{e}_z + \delta\eta (U\hat{e}_\theta - \bar{V}\hat{e}_z)]. \quad (6.9)$$

Substitute Equations 6.8 and 6.9 into the surface integral of Equation 6.3 and evaluate the integral of surface areas 2 and 4 as shown in Figure 6.1:

$$\int_{\partial C.V.} (\vec{r} \times \vec{v}) \rho \vec{v} \cdot d\vec{A} = \rho \left\{ 4\pi\delta [(r_o U_o) (r_o \bar{V}_o) - (r_i U_i) (r_i \bar{V}_i)] \int_0^1 \mathcal{F}^2(\eta) \right\} \hat{e}_z \quad (6.10)$$

In Chapter 2 the solution for the radial velocity, U , (Equation 2.21) results in a constant, a , such that

$$a = Ur = U_o r_o = U_i r_i \quad (6.11)$$

Also in Chapter 2, the integral of the square of the velocity profile, $\mathcal{F}^2(\eta)$, is defined as λ_1 (Equation 2.12). Therefore, the surface integral (Equation 6.10) becomes

$$\int_{\partial C.V.} (\vec{r} \times \vec{v}) \rho \vec{v} \cdot d\vec{A} = \lambda_1 (4\pi\rho\delta a) (r_o \bar{V}_o - r_i \bar{V}_i) \quad (6.12)$$

Now, examine the volume integral of the angular momentum in Equation 6.3. First evaluate the cross product terms using Equations 6.4, 6.6, and 6.7:

$$\vec{r} \times [\vec{\omega} \times (\vec{\omega} \times \vec{r})] = \delta\eta (-\omega^2 r) \hat{e}_\theta, \quad (6.13)$$

and

$$\vec{r} \times (2\vec{\omega} \times \vec{v}) = 2\omega [(rU) \hat{e}_z + \delta\eta (\bar{V} \hat{e}_\theta - U \hat{e}_r)] \mathcal{F}(\eta). \quad (6.14)$$

Substitute Equations 6.13 and 6.14 into volume integral and integrating over θ and z :

$$\int_{C.V.} \vec{r} \times [\vec{\omega} \times \vec{r} + 2\vec{\omega} \times \vec{v} + \vec{\omega} \times (\vec{\omega} \times \vec{r})] \rho dV = \int_{r_i}^{r_o} dr [\lambda_2 (4\pi\rho\delta a) (2r\omega)] \hat{e}_z. \quad (6.15)$$

Equation 6.15 can be integrated over the radius to give

$$\int_{C.V.} \vec{r} \times [\vec{\omega} \times \vec{r} + 2\vec{\omega} \times \vec{v} + \vec{\omega} \times (\vec{\omega} \times \vec{r})] \rho dV = \lambda_2 (4\pi\rho\delta a) \omega (r_o^2 - r_i^2) \hat{e}_z. \quad (6.16)$$

Subsequently, the conservation of angular momentum becomes

$$\vec{T}_{shaft} = (4\pi\rho\delta a) \{ \lambda_1 (r_o \bar{V}_o - r_i \bar{V}_i) + \lambda_2 \omega (r_o^2 - r_i^2) \} \hat{e}_z. \quad (6.17)$$

In Chapter 3 the mass flow rate for the model ($N = 0$) is found to be

$$\dot{m} = 4\pi\rho\delta a. \quad (6.18)$$

The sign on the constant a depends upon the system configuration (pump or turbine). For multiple pairs of disks Equation 6.18 is corrected by N

$$\dot{m} = 4\pi(N+1)\rho\delta a. \quad (6.19)$$

Thus, the coefficient $N + 1$ also transforms the shaft torque of the model to a shaft torque of a system.

In Chapter 1 the axis of rotation is defined to lie on the z -axis. Therefore,

$$\vec{T}_{shaft} = -\mathcal{T}_{shaft} \hat{e}_z. \quad (6.20)$$

From the definition of c (Equation 2.34) the coefficient $\lambda_2\omega$ is found to equal λ_1cR . The magnitude of the torque is now

$$\mathcal{T} = -\lambda_1\dot{m} \left[(r_o\bar{V}_o - r_i\bar{V}_i) + cR(r_o^2 - r_i^2) \right] ; \quad (6.21)$$

where a negative \mathcal{T} indicates work gained (turbine) and a positive \mathcal{T} indicates work required (pump).

6.3 Power

Note that \bar{V} and c are the only functions of angular velocity, ω , in Equation 6.21 and both are first order functions. Therefore, the torque is a function of ω such that as the angular velocity increases the torque decreases linearly.

If the system is operating as a turbine then the torque is work out of the system. In the pump configuration torque is work input. The power of the system is defined as

$$\mathcal{P} = \mathcal{T}\omega . \quad (6.22)$$

In terms of horsepower,

$$\mathcal{P}_{hp} = \frac{\mathcal{T}\omega}{63025} . \quad (6.23)$$

In Equation 6.23 the torque is specified in *in-lb_f* and the angular velocity is specified in terms of *rpm*. Torque is a linear function of angular velocity and power (or work) is a function of torque multiplied by angular velocity. Therefore, work is a quadratic function of angular velocity. Through Equations 6.21 and 6.22 the overall performance of the system can be studied.

Chapter 7

RESULTS AND DISCUSSION

The fluid-disk system introduced in Chapter 1 has been mathematically specified. A model for fluid flow between co-rotating disks based upon conservation principles is complete and from this model the work into or out of the system can be calculated from conservation of angular momentum relationships. In addition, several characteristic parameters have developed within the model. Now, the fluid-disk system can be studied through performance (torque and power) and/or fluid flow behavior (pathlines and characteristic parameters). The analysis in this chapter will be limited to a turbine configuration of the system.

7.1 Model Verification

The most critical assumption made in developing this model is that of fully-developed boundary layer flow. In actual fluid flow through a rotor the velocity profile will not be constant, but will develop over some distance from the entrance point. If this distance, or *entrance length*, is significant compared to the total length the fluid traverses, then the fluid model calculations will be inaccurate. The total length the fluid travels can be determined by the pathline. However, if the model is inaccurate, so to the pathline. The transverse length the fluid travels can still be approximated by the radial distance the fluid travels, $r_o - r_i$; understanding that this distance will

always be less than the actual transverse length.

The entrance length is not so easily approximated. In studying turbulent source flow between parallel, co-rotating disks Bakke, Kreider, and Kreith [7] determined experimentally that the friction factor of their system approached that of a square duct for relatively small disk spacings. Their analysis was for a pump configuration with relatively large disk spacings relative to this study. The correlation of a friction factor to that of a square duct occurs in systems with parameters closer to this study (i.e. R^* approaching 1). Although this correlation is for a pump configuration, it is used in this study with the understanding that this is a rough estimate for the entrance length calculation.

Now, assuming the flow develops similarly to that of flow in a square duct, the Reynold's number based on the hydraulic diameter of the duct is equivalent to the boundary layer Reynold's number, Re_δ . The expression for entrance length in a duct given in White [8] is

$$\frac{x_l}{\delta} \approx 0.04Re_\delta + 0.5 . \quad (7.1)$$

Substituting some typical values in for Re_δ results in a range of possible entrance lengths:

$$8\delta \leq x_l \leq 200\delta . \quad (7.2)$$

An entrance length of 8δ corresponds to an R^* on the order of 1 or greater. An entrance length of 200δ corresponds to an R^* on the order of 10^{-2} . Using an outer radius of 3 inches results in

$$.25 \text{ inches} \leq x_l \leq 9 \text{ inches} . \quad (7.3)$$

For very small R^* fully-developed flow may never develop. Therefore, the assumption of fully-developed boundary layer flow is improper for systems having small R^* . This supports the conclusion made in Chapter 2 on the limitations of this model at small R^* due to the domination of momentum effects.

Table 7.1: System Specification for Figures 7.1 and 7.2

curve	δ in	Re_δ	γ	R^*
1	.015	382	200	-.9806
2	.0095	382	315.8	-1.5482
3	.0085	382	352.9	-1.7304
4	.0075	382	400	-1.9611
5	.0065	382	461.5	-2.2628

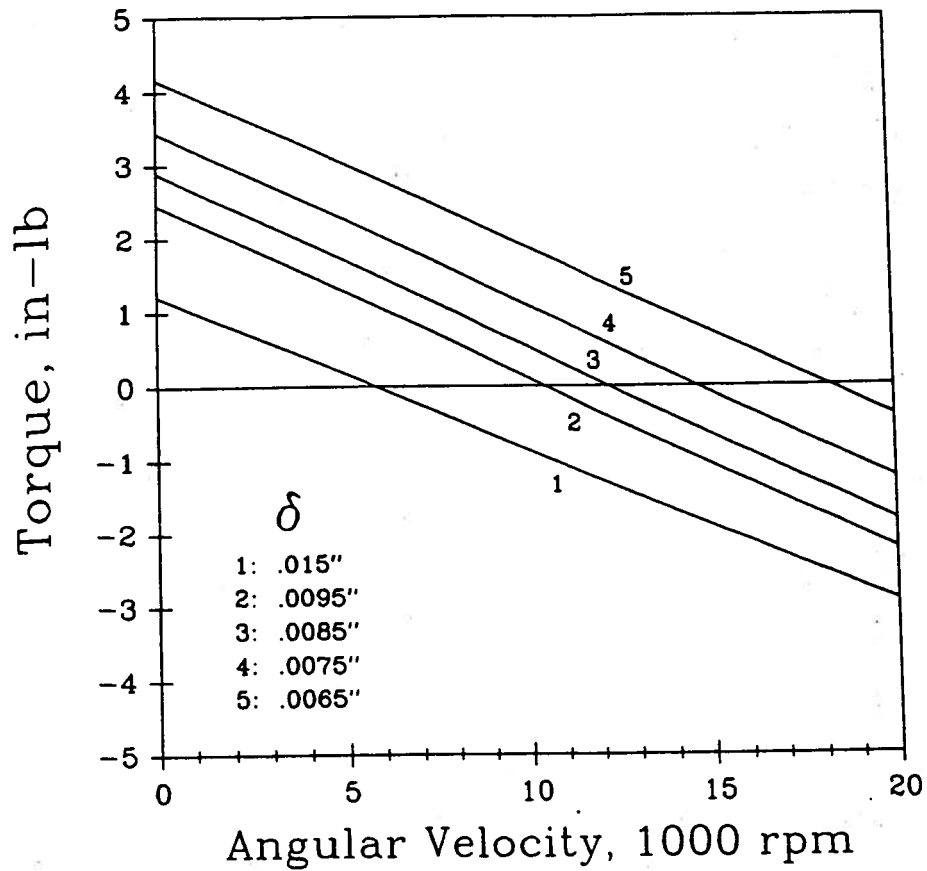
ρ :	.25 lb/ft ³	r_o :	3 in	\dot{m} :	-.75 lb/s
μ :	.1224 · 10 ⁻⁴ lb/ft · s	r_i :	1 in	α :	15 deg
		N :	50		

For R^* on the order of 1 the viscous effects are important and the model appears to be well suited. Since the flow is nearly tangential at the outer radius an entrance length of even 50δ is negligible when flow along the pathline is considered.

7.2 System Performance

In Chapter 6 the conservation of momentum principle was applied to the system using the model for fluid flow developed in Chapters 2 and 3. Since only the turbine configuration is being analyzed, the sign convention for torque and power has been reversed from that of Chapter 6 for easier analysis in this chapter. Work gained from the fluid will be signified by a positive torque and power while work lost from the fluid will be signified by a negative torque and power.

Figure 7.1 illustrates torque as a function of angular velocity for various half-disk spacings, δ . The five numbered curves represent the same system with five different half-disk spacings. As the δ decreases the torque curve shifts upward, becoming positive over a greater range of ω . The corresponding variations in Re_δ , γ , and R^*

Figure 7.1: Torque versus Angular Velocity for Various δ

for same δ 's in Figure 7.1 are shown in Table 7.1. In Figure 7.1 the torque for a given system is at a maximum when the rotor is stationary. As the angular velocity increases the torque decreases linearly until a maximum ω is obtained at zero torque. If the angular velocity is increased further a torque must be supplied to the system; i.e. a negative torque. The negative torques of Figure 7.1 result from specifying boundary conditions that are infeasible for the system. Since both the angular velocity and the mass flow rate are fixed, it is possible to specify an angular velocity which can not be reached with the mass flow rate given. Therefore, torque must be supplied in order to reach the specified ω . The slope of the torque curve is dependent upon the mass flow rate. As mass flow rate increases the slope of the torque also increases.

For a fixed mass flow rate the relation in Figure 7.1 moves upward into the positive torque region at an increasing rate for a constant increase in the aspect ratio, γ . For example, the change in γ from lines 4 to 3 is same as that from lines 2 to 1, but the torque line shift from 1 to 2 is greater than that from 4 to 3. This upward acceleration of the torque line is due to the increase in relative velocities that occurs as γ increases. As shown in Equation 6.21 the torque is a function of velocity squared. Therefore, a linear increase in γ produces a linear increase in the relative tangential velocity which in turn produces a quadratic increase in the torque for any given ω . This increasing torque pattern continues until the model fails. As γ continues to increase the given mass flow rate is forced through a reduced area; subsequently, the velocities will eventually increase to supersonic at which point the model is no longer valid. An interesting aspect of this velocity change is that although the aspect ratio increases to where the velocities are supersonic, the boundary layer Reynold's number, Re_δ , remains constant (See Table 7.1).

Figure 7.2 illustrates the power curves for the same set of systems as Figure 7.1. Since power, P is the product of torque and angular velocity the same type of patterns illustrated in Figure 7.1 are seen in Figure 7.2. In addition to an increase in the

maximum obtainable angular velocity with an increase in γ , the ω associated with the peak power also increases.

7.3 Model Behavior

The variation in pressure across the disk has been virtually ignored to this point. Although an expression for the pressure as a function of radius is developed in Chapter 2 (Equation 2.38), it has not yet been used. Analytically, the radial pressure drop calculated for various turbine configurations has been very small (on the order of a few p.s.i.) for all but a few extreme system configurations (such as supersonic velocities). The small radial pressure drop has also been found experimentally by Armstrong[9].

Figure 7.3 illustrates normalized pressure drop curves for various R^* . When the magnitude of R^* is equal to 1 the normalized pressure has a downward curvature (albeit slight) in the vicinity of the outer radius and an upward curvature in the vicinity of the inner radius. For an R^* of 1 viscous effects are slightly more important than momentum effects at the outer radius. As the radius decreases the local R^* also decreases and the momentum effects become slightly more important than viscous effects. Thus, a change occurs in the curvature of the normalized pressure. As R^* decreases the curvature becomes more pronounced and the inflection point on the curve moves towards the outer radius. This indicates that the momentum effects are becoming more and more dominant. The inflection point very quickly becomes attached to the outer radius as R^* decreases. If R^* were to become greater than 1 the inflection point would move towards the inner radius and the normalized pressure would have a pronounced downward curvature. Unfortunately, the data which illustrated the effects of viscous domination for Figure 7.3 was lost and could not be recovered in time for this thesis. If R^* becomes very large or very small the curvature

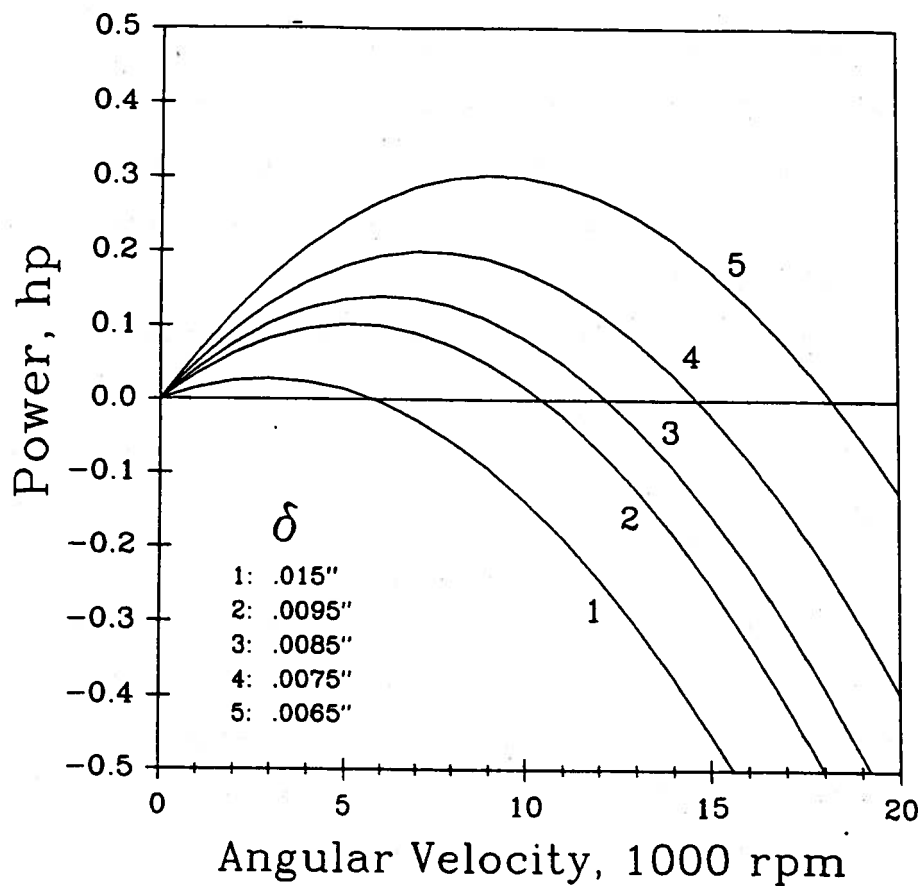


Figure 7.2: Power versus Angular Velocity for Various δ

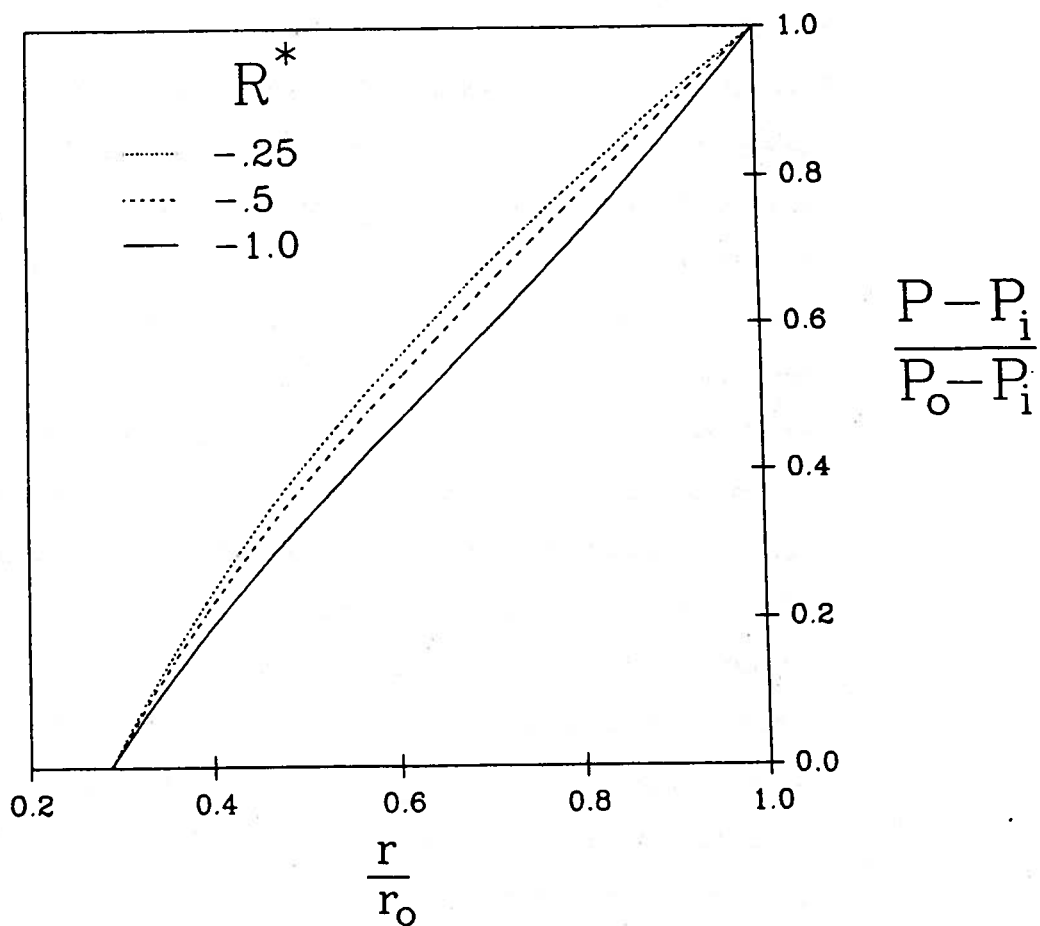


Figure 7.3: Normalized Pressure for Various R^*

will become greater. A better depiction of viscous-momentum effects in the pressure relation for R^* on the order of 1 would possibly be a normalized pressure gradient in which the inflection point would become a change in sign for the curve.

Figure 7.4 illustrates how the pathline is effected by a change in R^* . At relatively large R^* there is little or no negative relative velocity at the outer radius. The negative relative tangential velocity, \bar{V} , occurs in the region where the pathline is opposite the direction of rotation (See Figure 5.2). As R^* decreases the *dip* of negative \bar{V} becomes more pronounced and the point of zero relative tangential velocity move radially inward. Another way to examine the effects of R^* is with a parameter whose variation will decrease R^* . For example, if the half-disk spacing, δ , is increased, R^* will decrease. In relation to pathlines, if the disk spacing is increased while maintaining all other system parameters, then the mass flow rate has a larger area to flow through; hence, the absolute velocities at the outer radius will decrease. Since the outer edge velocity of the disks $r\omega$, is unchanged, the pathline will begin to move backwards relative to the rotation as the relative tangential velocity of the fluid, \bar{V} , becomes negative. An interesting feature of Figure 7.4 is that although R^* varies, the fluid pathlines all exit the rotor at the same angular position on the inner radius. This indicates that the final change in angular position is a function of ω and not of R^* .

Since R^* is a dimensionless function of r , it will vary over the radius of the disk. Figure 7.5 illustrates the contours of R^* over the radius of the disk. The negative values of R^* indicate a turbine configuration of the system. For a pump configuration the contours are identical in magnitude, but the sign of R^* is positive.

Figure 7.6 illustrates the variation in the relative tangential velocity, \bar{V} , over the radius of the disk for an increasing angular velocity, ω . R^* is a constant for this figure. The interesting feature is the point of coalescence at approximately $r/r_o = .45$. This point is apparently a function only of R^* , but the exact relationship is still undetermined.

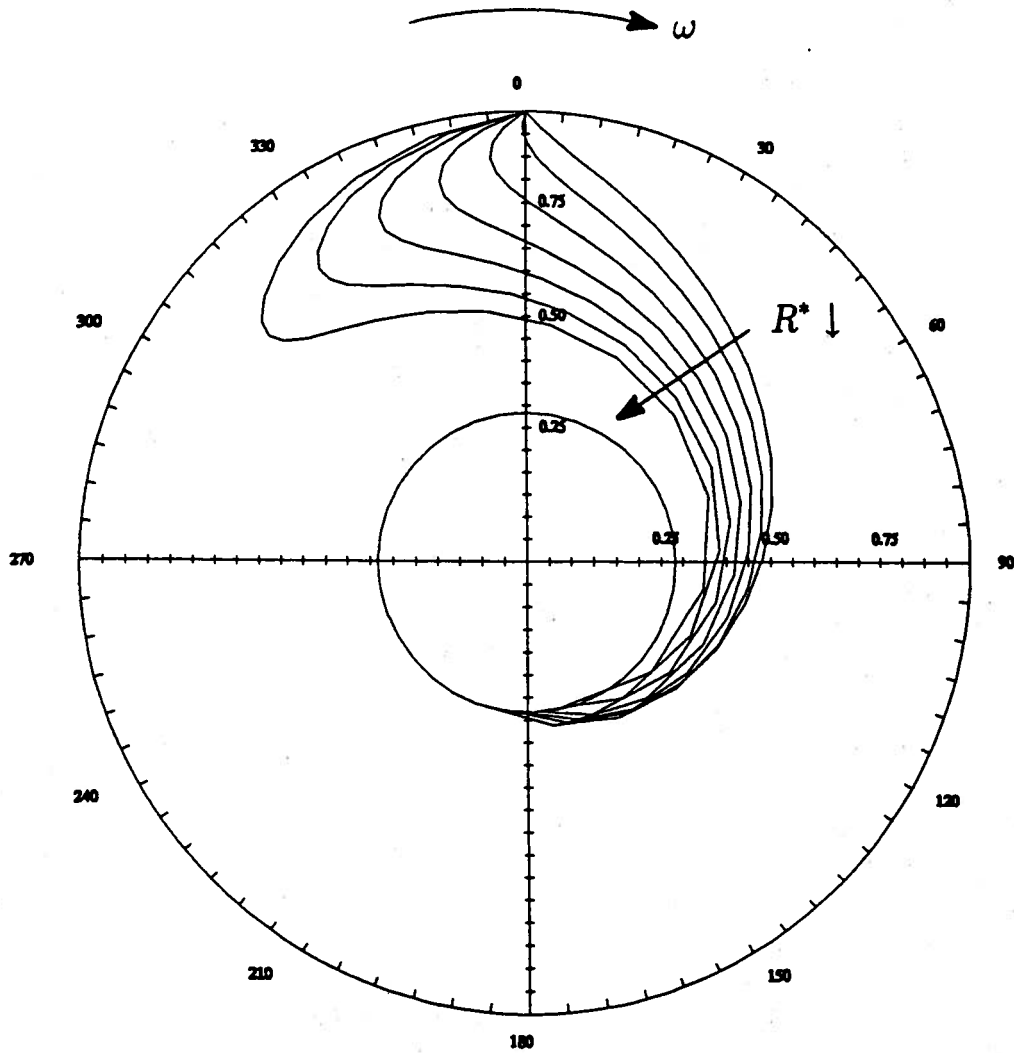
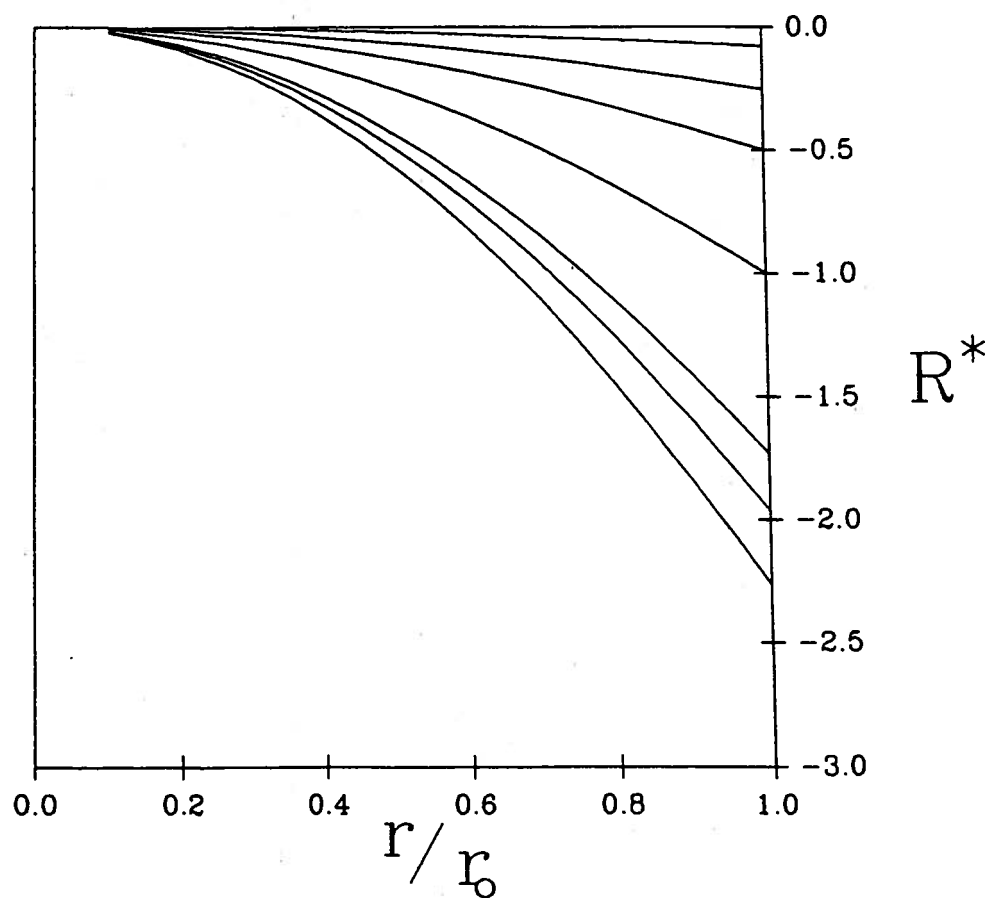


Figure 7.4: Pathlines for Various R^*

Figure 7.5: R^* versus r^*

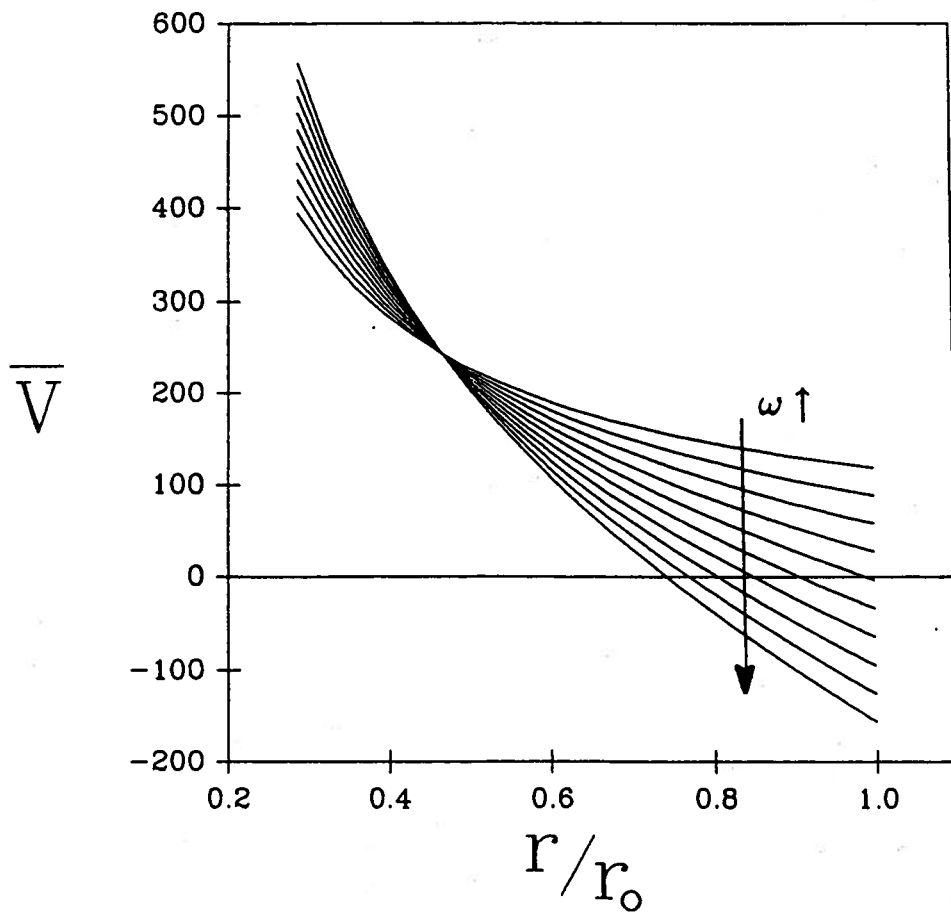


Figure 7.6: \bar{V} versus r^*

7.4 Summary

In conclusion, this chapter offers a brief overview of the use of the analytical model in studying various systems. Much more work is required to fully understand the behavior of this model. This is readily apparent in Figure 7.6.

Chapter 8

CONCLUSION

8.1 Summary of Model

For the two disk system described in Chapter 1 the fluid velocity components at the centerline ($\eta = 0$) and the pressure are determined through conservation of mass and conservation of momentum principles to be:

$$U(r) = \frac{a}{r}; \quad (8.1)$$

$$\bar{V}(r) = \frac{bS_m(R^*) - c}{r}; \quad (8.2)$$

$$\begin{aligned} \frac{1}{\rho}P(r) = & -\lambda_1 \left\{ [a^2 + (b-c)^2] \left[\frac{1}{2r^2} + R \ln r^2 \right] \right\} \\ & -\lambda_1 \left\{ \left[bR \sum_{m=0}^{\infty} \frac{(-R^*)^{m+1}}{2(m+1)} [bG_{m+2} - 2c(m+3)F_{m+2}] \right] \right\} \\ & + [\omega^2] \frac{r^2}{2} + d; \end{aligned} \quad (8.3)$$

where

$$S_m(R^*) = \sum_{m=0}^{\infty} \frac{(-R^*)^m}{m!}$$

and

$$R^* = Rr^2 = \frac{-\lambda_3\gamma}{2\lambda_1 Re_\delta} \quad (8.4)$$

$$R = \frac{-\lambda_3\nu}{2\lambda_1\delta^2 a} \quad (8.5)$$

$$\gamma = \frac{r}{\delta} \quad (8.6)$$

$$Re_\delta = \frac{\delta U}{\nu} \quad (8.7)$$

$$c = \frac{\lambda_2\omega}{\lambda_1 R} \quad (8.8)$$

The performance of the system can be described by torque which is determined from the conservation of angular momentum:

$$\mathcal{T} = -\dot{m}\lambda_1 \left[(r_o \bar{V}_o - r_i \bar{V}_i) + cR (r_o^2 - r_i^2) \right]. \quad (8.9)$$

This set of equations can be applied to fluid flow within the system described in either a pump configuration or a turbine configuration; only the boundary conditions vary. Several dimensionless parameters appear in the development of the model and these parameters describe the force balance relationships between various effects.

8.2 Recommendations

For an R^* on the order of or greater than 1 (viscous flows) the model appears to be an appropriate solution. At this point it is premature to discuss the validity of the model in detail since no experimental data is readily available for comparison and a great deal of literature has yet to be reviewed. However, preliminary results are promising and an experimental turbine has been built. This turbine will be made operational

in order to gather experimental data. In addition, an in depth data base on available literature in this area has been in progress and the information from other researchers will be examined with respect to this model.

There are several areas which require immediate investigation. The first is an examination of how stable a velocity profile is across the radius of the rotor. In other words, when the velocity profile develops in the outer radial region, does it remain the same shape for the duration of the flow? Also, the analysis on the dimensionless parameters needs to be continued; particularly on ω^* and c^* and the relationship that these two have with R^* . The performance of the system (as a turbine or a pump) can be examined in greater detail by applying the first and second laws of thermodynamics to the control volume defined in Chapter 6. This should give some insight into the efficiency of various system configurations and the relationship between the viscous losses and energy transfer between fluid and disks. An optimization study on the torque with respect to the rotor parameters r_o , r_i , and δ has been initiated and appears to offer additional information on the nature of the relationship between performance and the dimensionless parameters.

In general, this thesis concentrates on the development of the model. Analysis with the model is far from complete and a great deal more work is needed both analytically and experimentally.

Bibliography

- [1] O'Neill, John, *Prodigal Genius: The Life of Nikola Tesla*, Ives, Washburn, Inc. 1944, pp 218-228.
- [2] Cheney, Margaret, *TESLA: Man Out of Time*, Dell Publishing Co., Inc., NY 1981, pp 188-192, 198-200.
- [3] Tesla, Nikola, Patent No. 1,061,142, *Fluid Power*, May 6, 1913.
- [4] Tesla, Nikola, Patent No. 1,061,206, *Turbine*, May 6, 1913.
- [5] Gottfredson, R.K., Torpedo Propulsion Systems, *ASME Transactions: Journal of Engineering for Industry*, Vol. 102, Feb. 1980, pp 85-90.
- [6] Batchelor, G.K., *An Introduction to Fluid Mechanics*, Cambridge University Press, 1967.
- [7] Bakke, E., Kreider, J.F., Kreith, F. , Turbulent Source Flow Between Parallel Stationary and Co-Rotating Disks, *J. Fluid Mech.* Vol. 58, part 2, (1973) pp 209-231.
- [8] White, Frank., *Viscous Fluid Flow*, McGraw-Hill, Inc., 1974.
- [9] Armstrong, James H. *An Investigation of the Performance of a Modified Tesla Turbine*, M.S. Thesis, Georgia Institute of Technology, June 1952.
- [10] Fox, Robert W., McDonald, Alan T., *Introduction to Fluid Mechanics*, 3rd Ed., John Wiley and Sons, NY 1985.
- [11] Speigal, Murray R., *Vector Analysis*, Schaum's Outline Series, McGraw-Hill Book Company, 1959.

Appendix A

Conservation of Mass

A.1 Reduction of Continuity

The conservation of mass, or continuity, is expressed vectorially as

$$\dot{\rho} + \vec{\nabla} \cdot (\rho \vec{u}) = 0. \quad (\text{A.1})$$

For the system described in Chapter 1 the continuity expression is reduced through the following assumptions:

- steady, incompressible flow,
- constant flow characteristics with respect to θ , $\frac{\partial(-)}{\partial\theta}$, and
- fully-developed boundary layer flow.

The first assumption eliminates density from the continuity relation (Equation A.1); leaving

$$\text{div } \vec{u} = 0. \quad (\text{A.2})$$

In cylindrical coordinates Equation A.2 appears as

$$\frac{1}{r} \frac{\partial(ru)}{\partial r} + \frac{1}{r} \frac{\partial v}{\partial \theta} + \frac{\partial w}{\partial z} = 0. \quad (\text{A.3})$$

The tangential velocity term in Equation A.3 is eliminated by the second assumption of no θ dependence and the axial velocity term is eliminated by the assumption of fully-developed boundary layer flow ($w = 0$). Thus, the continuity relation becomes solely a function of the radial velocity component, u , and radial position, r ,

$$\frac{1}{r} \frac{\partial(ru)}{\partial r} = 0. \quad (\text{A.4})$$

A.2 Solution for the Radial Velocity Component

Also from the assumption of fully-developed boundary layer flow, the velocity characteristics of the boundary layer (i.e., those velocity components relative to the disk faces) can be approximated as a product function of a radially dependent function and a velocity profile function normal to the flow direction. If we define $\eta = z/\delta$ and the velocity profile as $\mathcal{F}(\eta)$, the velocity component u can be expressed as

$$u(r, \eta) = U(r)\mathcal{F}(\eta). \quad (\text{A.5})$$

The radially dependent function, $U(r)$, is the magnitude of the velocity, u , at the centerline ($\eta = 0$) of the velocity profile function, $\mathcal{F}(\eta)$.

Substituting Equation A.5 into the continuity relation of Equation A.4,

$$\frac{1}{r} \frac{\partial[rU(r)\mathcal{F}(\eta)]}{\partial r} = 0, \quad (\text{A.6})$$

we find that the velocity profile function, $\mathcal{F}(\eta)$, can be eliminated since it is not a function of radius. Equation A.6 then becomes a first order differential equation

$$\frac{dU}{dr} + \frac{U}{r} = 0, \quad (\text{A.7})$$

which is easily solved. The result is a solution for the radial component of the fluid velocity

$$U(r) = \frac{a}{r}, \quad (\text{A.8})$$

where a is a constant dependent upon the boundary conditions. Equation A.8 is the same for any assumed velocity profile, $\mathcal{F}(\eta)$. Thus, the radial velocity is independent of the flow regime; be it laminar or turbulent.

Appendix B

Conservation of Momentum

B.1 Reduction of the Navier-Stokes Equations

If we begin with the incompressible form of the Navier-Stokes equations for a Newtonian fluid,

$$\dot{\vec{u}} + (\vec{u} \cdot \vec{\nabla}) \vec{u} = \vec{g} - \frac{1}{\rho} \vec{\nabla} P + \nu \nabla^2 \vec{u}, \quad (\text{B.1})$$

and apply this relation to the system described in Chapter 1, then the following approximations can be used to reduce Equation B.1:

1. steady, incompressible flow,
2. velocity and pressure independent of θ ; $\frac{\partial(-)}{\partial\theta} = 0$,
3. fully-developed boundary layer flow, and
4. no body forces.

The first assumption eliminates the time dependence of the velocities. The second assumption states that the characteristics of the flow are constant with respect to θ . The velocity and pressure are, therefore, only functions of radial and axial positions. The assumption of fully-developed boundary layer flow restricts these results to relatively thin disk spacings. If δ becomes too large then the boundary layers grow;

off each disk face will not meet. This assumption eliminates axial flow between the disks ($w = 0$); subsequently, the axial dependence of the velocity components can be modelled as a velocity profile. Neglecting body forces in the fourth assumption eliminates the inertial body forces; that is, the body forces due to gravity or other events which are relative to an inertial frame of reference. Note that body forces relative to the rotating frame of reference, such as Coriolis and Centripetal forces, are not addressed by this assumption.

Applying these assumptions to Equation B.1 and expanding this equation in the cylindrical coordinate system defined in Chapter 1 we find that the conservation of momentum becomes

$$r : \quad u \frac{\partial u}{\partial r} - \frac{v^2}{r} = -\frac{1}{\rho} \frac{\partial P}{\partial r} + \nu \left(\frac{\partial^2 u}{\partial r^2} + \frac{1}{r} \frac{\partial u}{\partial r} - \frac{u}{r^2} \right) + \nu \frac{\partial^2 u}{\partial z^2} \quad (\text{B.2})$$

$$\theta : \quad u \frac{\partial v}{\partial r} + \frac{uv}{r} = \nu \left(\frac{\partial^2 v}{\partial r^2} + \frac{1}{r} \frac{\partial v}{\partial r} - \frac{v}{r^2} \right) + \nu \frac{\partial^2 v}{\partial z^2} \quad (\text{B.3})$$

$$z : \quad 0 = -\frac{1}{\rho} \frac{\partial P}{\partial z} \quad (\text{B.4})$$

From this reduction we find that the pressure is only a function of radial position. Therefore, with the solution for the radial velocity component, u , known (Appendix A), the solutions for the tangential velocity component, v , and the pressure, P , can be found independently. The tangential velocity component is found by substituting the solution for the radial velocity component, u (Equation A.8), into the θ -momentum equation (Equation B.3) and solving this differential relation for v . The solution for the pressure is then calculated by substituting the solutions for u and v into the r -momentum equation (Equation B.2).

The assumption of fully-developed boundary layer flow is valid only for those velocity components relative to the solid boundary, which in this case is the rotating disk

face. However, the conservation of momentum relation expressed in Equation B.1 is valid only for velocity components relative to an inertial frame of reference. Therefore, the velocity components in Equations B.2 and B.3 must be expressed as functions of a velocity relative to the disk face so that assumption 3 may be used effectively. The radial velocity component does not change with the change of reference frames; u is the same if measured against a fixed frame of reference or if measured against the disk face. However, the tangential velocity component, v , does vary with the change in reference frames. If we define the tangential velocity relative to an inertial frame of reference as v and the tangential velocity relative to the rotating frame of reference, or disk face, as \bar{v} , then

$$v = \bar{v} + r\omega, \quad (\text{B.5})$$

where ω is the angular velocity of the rotor. The tangential velocity component relative to the rotor, \bar{v} , will be referred to as the *relative tangential velocity* and v will be referred to as the *absolute tangential velocity*.

Substituting Equation B.5 into the momentum equations for the absolute tangential velocity and expanding the velocity components results in

r :

$$u \frac{\partial u}{\partial r} - \frac{\bar{v}^2}{r} - 2\bar{v}\omega - r\omega^2 = -\frac{1}{\rho} \frac{dP}{dr} + \nu \left(\frac{\partial^2 u}{\partial r^2} + \frac{1}{r} \frac{\partial u}{\partial r} - \frac{u}{r^2} \right) + \nu \frac{\partial^2 u}{\partial z^2}, \quad (\text{B.6})$$

and

θ :

$$u \frac{\partial \bar{v}}{\partial r} + \frac{u\bar{v}}{r} + 2u\omega = \nu \left(\frac{\partial^2 \bar{v}}{\partial r^2} + \frac{1}{r} \frac{\partial \bar{v}}{\partial r} - \frac{\bar{v}}{r^2} \right) + \nu \frac{\partial^2 \bar{v}}{\partial z^2}. \quad (\text{B.7})$$

Coriolis accelerations, $2u\omega$ and $2\bar{v}\omega$, appear in both the radial and tangential directions. In addition, the radial direction also exhibits a centripetal acceleration, $r\omega^2$. There is no centripetal effects in the tangential direction.

B.2 Velocity Profile Function

From the assumption of fully-developed flow, the velocity components relative to the disk face, u and \bar{v} , can be expressed as the product of a radially dependent function and a velocity profile function normal to the boundary layer. Defining η to be equal to z/δ and the velocity profile function to be $\mathcal{F}(\eta)$, the velocity components become

$$u(r, \eta) = U(r)\mathcal{F}(\eta), \quad (\text{B.8})$$

$$\bar{v}(r, \eta) = \bar{V}(r)\mathcal{F}(\eta). \quad (\text{B.9})$$

Substituting Equations B.8 and B.9 into Equations B.6 and B.7 for the velocity components transforms the momentum equations to ordinary differential equations:

r :

$$\begin{aligned} & \left(U \frac{dU}{dr} - \frac{\bar{V}^2}{r} \right) \mathcal{F}^2(\eta) - (2\bar{V}\omega) \mathcal{F}(\eta) - (r\omega^2) = \\ & -\frac{1}{\rho} \frac{dP}{dr} + \nu \left(\frac{dU}{dr} + \frac{1}{r} \frac{dU}{dr} - \frac{U}{r^2} \right) \mathcal{F}(\eta) + \frac{\nu U}{\delta^2} \frac{d^2 \mathcal{F}(\eta)}{d\eta^2}, \end{aligned} \quad (\text{B.10})$$

θ :

$$\begin{aligned} & \left(U \frac{d\bar{V}}{dr} + \frac{U\bar{V}}{r} \right) \mathcal{F}^2(\eta) + (2U\omega) \mathcal{F}(\eta) = \\ & \nu \left(\frac{d\bar{V}}{dr} + \frac{1}{r} \frac{d\bar{V}}{dr} - \frac{\bar{V}}{r^2} \right) \mathcal{F}(\eta) + \nu \frac{\bar{V}}{\delta^2} \frac{d^2 \mathcal{F}(\eta)}{d\eta^2}. \end{aligned} \quad (\text{B.11})$$

Integrating Equations B.10 and B.11 over the disk spacing ($-1 \leq \eta \leq 1$) results in the velocity profile functions, $\mathcal{F}(\eta)$, becoming constants.

Define those constant coefficients as

$$\lambda_1 = \int_0^1 \mathcal{F}^2(\eta) d\eta, \quad (\text{B.12})$$

$$\lambda_2 = \int_0^1 \mathcal{F}(\eta) d\eta, \quad (\text{B.13})$$

$$\lambda_3 = \int_0^1 \left[\frac{\partial^2 \mathcal{F}(\eta)}{\partial \eta^2} \right] d\eta, \text{ and} \quad (\text{B.14})$$

$$\lambda_4 = \int_0^1 d\eta = 1. \quad (\text{B.15})$$

Approximating a laminar boundary layer with a parabolic velocity profile,

$$\mathcal{F}(\eta) = 1 - \eta^2, \quad (\text{B.16})$$

results in λ -coefficients of $\lambda_1 = 8/15$, $\lambda_2 = 2/3$, and $\lambda_3 = -2$.

Substituting the λ -coefficients into the integrated momentum equations and dividing out a 2δ factor common to each term:

r :

$$\begin{aligned} \lambda_1 \left(U \frac{dU}{dr} - \frac{\bar{V}^2}{r} \right) - \lambda_2 (2\bar{V}\omega) - (r\omega^2) &= -\frac{1}{\rho} \frac{dP}{dr} \\ &+ \nu \lambda_2 \left(\frac{dU}{dr} + \frac{1}{r} \frac{dU}{dr} - \frac{U}{r^2} \right) + \lambda_3 \frac{\nu U}{\delta^2}, \end{aligned} \quad (\text{B.17})$$

θ :

$$\lambda_1 \left(U \frac{d\bar{V}}{dr} + \frac{U\bar{V}}{r} \right) + \lambda_2 (2U\omega) = \nu \lambda_2 \left(\frac{d\bar{V}}{dr} + \frac{1}{r} \frac{d\bar{V}}{dr} - \frac{\bar{V}}{r^2} \right) + \lambda_3 \frac{\nu \bar{V}}{\delta^2}. \quad (\text{B.18})$$

B.3 Incorporating Continuity

From the conservation of mass (See Appendix A) the radial velocity can be expressed in differential form as Equation A.7;

$$\frac{dU}{dr} = -\frac{U}{r}, \quad (\text{B.19})$$

or in the final form as Equation A.8;

$$U(r) = \frac{a}{r}. \quad (\text{B.20})$$

B.3.1 r -momentum

Substitute Equations B.19 and B.20 into the viscous dilation terms of the r -momentum equation (Equation B.17) to obtain

$$\frac{d^2 U}{dr^2} + \frac{1}{r} \frac{dU}{dr} - \frac{U}{r^2} = 0. \quad (\text{B.21})$$

Also, replace the derivative of U in the convective term of Equation B.17 with Equation B.19 and multiply through by a -1 . This leaves the r -momentum equation as a derivative of pressure only:

r :

$$\lambda_1 \left(\frac{U^2 + \bar{V}^2}{r} \right) + \lambda_2 (2\bar{V}\omega) + (r\omega^2) = \frac{1}{\rho} \frac{dP}{dr} - \lambda_3 \left(\frac{\nu U}{\delta^2} \right). \quad (\text{B.22})$$

B.3.2 θ -momentum

Now examine the θ -momentum equation (Equation B.18) with the solution for the radial velocity (Equation B.20) substituted in for U ,

$$\lambda_1 \frac{a}{r} \left(\frac{d\bar{V}}{dr} + \frac{\bar{V}}{r} \right) + \lambda_2 \left(2\frac{a}{r}\omega \right) = \nu \lambda_2 \left(\frac{d^2 \bar{V}}{dr^2} + \frac{1}{r} \frac{d\bar{V}}{dr} - \frac{\bar{V}}{r^2} \right) + \lambda_3 \left(\frac{\nu \bar{V}}{\delta^2} \right). \quad (\text{B.23})$$

Dividing through Equation B.23 by $\nu \lambda_2$:

$$\frac{\lambda_1 a}{\lambda_2 \nu} \left(\frac{1}{r} \frac{d\bar{V}}{dr} + \frac{\bar{V}}{r^2} \right) + \frac{a}{\nu} \left(\frac{2\omega}{r} \right) = \left(\frac{d^2 \bar{V}}{dr^2} + \frac{1}{r} \frac{d\bar{V}}{dr} - \frac{\bar{V}}{r^2} \right) + \frac{\lambda_3 r^2}{\lambda_2 \delta^2} \left(\frac{\bar{V}}{r^2} \right). \quad (\text{B.24})$$

Examining the a/ν coefficient we find that this is equivalent to the Reynold's number based on disk radius;

$$\frac{a}{\nu} = \frac{rU}{\nu} = Re_r, \quad (\text{B.25})$$

and if we define the aspect ratio of the rotor (r/δ) as γ then Equation B.24 becomes

$$\frac{\lambda_1}{\lambda_2} Re_r \left(\frac{1}{r} \frac{d\bar{V}}{dr} + \frac{\bar{V}}{r^2} \right) + Re_r \left(\frac{2\omega}{r} \right) = \left(\frac{d^2\bar{V}}{dr^2} + \frac{1}{r} \frac{d\bar{V}}{dr} - \frac{\bar{V}}{r^2} \right) - \frac{\lambda_3}{\lambda_2} \gamma^2 \left(\frac{\bar{V}}{r^2} \right). \quad (\text{B.26})$$

Equation B.26 can be rearranged to a standard form of a Bessel's equation. However, for this system, both Re_r and γ are generally much greater than one. Assuming that

$$\frac{d^2\bar{V}}{dr^2} \sim \frac{d\bar{V}}{dr},$$

then by an order of magnitude reduction we can neglect the viscous dilation terms for the conservation of θ -momentum. Equation B.26 now becomes

$$\begin{array}{ccc} \text{I} & \text{II} & \text{III} \\ \frac{\lambda_1}{\lambda_2} Re_r \left(\frac{1}{r} \frac{d\bar{V}}{dr} + \frac{\bar{V}}{r^2} \right) & + Re_r \left(\frac{2\omega}{r} \right) & - \frac{\lambda_3}{\lambda_2} \gamma^2 \left(\frac{\bar{V}}{r^2} \right) = 0. \end{array} \quad (\text{B.27})$$

The three terms of Equation B.27 are descended from

I. momentum flux, $\frac{u}{r} \left[\frac{\partial}{\partial r} (r\bar{v}) \right],$

II. Coriolis force, $2u\omega,$ and

III. viscous dissipation, $\nu \frac{\partial^2 \bar{v}}{\partial z^2}.$

Now divide through Equation B.27 by $(\lambda_1 Re_r)/(\lambda_2 r)$. This results in a conservation of θ -momentum expressed in terms of an ordinary differential equation for \bar{V} :

$$\frac{d\bar{V}}{dr} + \left(1 - \frac{\lambda_3}{\lambda_1} \frac{\gamma^2}{Re_r} \right) \frac{\bar{V}}{r^2} + 2 \frac{\lambda_2}{\lambda_1} \omega = 0 \quad (\text{B.28})$$

The γ^2/Re_r term can be rewritten in terms of another Reynold's number:

$$\frac{\gamma^2}{Re_r} = \frac{r^2}{\delta^2} \left(\frac{\nu}{rU} \right) = \frac{r}{\delta} \left(\frac{\nu}{\delta U} \right) = \frac{\gamma}{Re_\delta}, \quad (\text{B.29})$$

where Re_δ is the Reynold's number based on disk spacing. If the term γ/Re_δ is much greater than the λ -coefficients or much less than the λ -coefficients then Equation B.28 becomes much easier to solve. The λ -coefficients are all on the order of one; however, the order of γ/Re_δ is not known.

B.4 γ vs. Re_δ

In evaluating the order of magnitude of the γ/Re_δ coefficient there are three possibilities with regard to Equation B.28:

1. $\frac{\gamma}{Re_\delta} \ll 1$,
2. $\frac{\gamma}{Re_\delta} \sim 1$, and
3. $\frac{\gamma}{Re_\delta} \gg 1$.

The first case ($\gamma/Re_\delta \ll 1$) is unlikely for this system since case 1 would indicate that viscous effects are negligible. The second and third cases are viable, though.

The magnitude of γ/Re_δ can be determined by applying the boundary conditions using general values of fluid and rotor parameters. The mass flow rate boundary condition is

$$\dot{m} = 4\pi(N+1)\rho\delta rU \quad (\text{B.30})$$

which leads to an expression for Re_δ ,

$$Re_\delta = \frac{1}{4\pi(N+1)} \left(\frac{\dot{m}}{\mu r} \right). \quad (\text{B.31})$$

The radial Reynold's number can also be expressed in this fashion:

$$Re_r = \frac{1}{4\pi(N+1)} \left(\frac{\dot{m}}{\mu\delta} \right). \quad (\text{B.32})$$

Table B.1: Typical Rotor and Fluid Parameters for Turbine Configuration

Rotor	Fluid (air)
$r \sim 10^{-1} \text{ ft}$	$\rho \sim 10^{-1} \text{ to } 10^{-2} \text{ lb}_m/\text{ft}^3$
$\delta \sim 10^{-3} \text{ to } 10^{-4} \text{ ft}$	$\mu \sim 10^{-5} \text{ lb}_m/\text{ft} - \text{sec}$
$N \sim 10^0 \text{ to } 10^{-1}$	

Using Equations B.31 and B.32 the three cases become

$$1. 4\pi(N+1)\gamma \ll \frac{\dot{m}}{\mu r}, \text{ or, } 4\pi(N+1)\gamma^2 \ll \frac{\dot{m}}{\mu \delta},$$

$$2. 4\pi(N+1)\gamma \sim \frac{\dot{m}}{\mu r}, \text{ or, } 4\pi(N+1)\gamma^2 \sim \frac{\dot{m}}{\mu \delta},$$

$$3. 4\pi(N+1)\gamma \gg \frac{\dot{m}}{\mu r}, \text{ or, } 4\pi(N+1)\gamma^2 \gg \frac{\dot{m}}{\mu \delta}$$

The values for the rotor and fluid parameters in the turbine configuration are shown in Table B.1. Substituting these values into the three cases will yield limitations on the mass flow rate:

$$1. \dot{m} \ll 10^{-3} \text{ lb}_m/\text{sec},$$

$$2. \dot{m} \sim 10^{-3} \text{ lb}_m/\text{sec}, \text{ and}$$

$$3. \dot{m} \gg 10^{-3} \text{ lb}_m/\text{sec}.$$

Let N equal 0 and study the three order of magnitude cases for the model instead of the system. For this model the velocities must remain subsonic; therefore, the radial velocity, U , is on the order of 10^2 ft/sec . Now, by examining Equation B.30 again we find

$$\dot{m} \sim (4\pi) \cdot 10^{-2} \cdot 10^{-3} \cdot 10^{-1} \cdot 10^2 \sim 10^{-3}. \quad (\text{B.33})$$

This result corresponds to case 2, which is the most general of the three cases.

B.5 The R Constant

Returning to Equation B.28 we can rearrange the Reynold's number term using the relations described in B.29:

$$-\frac{\gamma}{Re_\delta} = 2 \left(\frac{-\lambda_3}{2\lambda_1} \frac{\nu}{\delta^2 a} \right) r^2. \quad (\text{B.34})$$

Now define a term R such that

$$R = \left(\frac{-\lambda_3}{2\lambda_1} \right) \frac{\nu}{\delta^2 a}. \quad (\text{B.35})$$

This term, R , is a constant for the system and has units of $[1/\text{length}^2]$; subsequently, we can define a dimensionless quantity, R^* , by

$$R^* = R r^2. \quad (\text{B.36})$$

The dimensionless quantity R^* , can also be written in terms of the aspect ratio, γ , and Reynold;s numbers, Re_δ and Re_r :

$$R^* = \left(\frac{-\lambda_3}{2\lambda_1} \right) \frac{\gamma}{Re_\delta} = \left(\frac{-\lambda_3}{2\lambda_1} \right) \frac{\gamma^2}{Re_r}. \quad (\text{B.37})$$

Thus, when viscous effects are dominant $R^* \gg 1$ and when both viscous and momentum effects are important $R^* \sim 1$.

B.6 Summary

The conservation of momentum equations have been reduced to two ordinary differential equation in terms of the relative tangential velocity and pressure. Using the definition of R stated in B.35 the θ -momentum equation can be written as

$$\frac{d\bar{V}}{dr} + \left(\frac{1}{r} + 2Rr \right) \bar{V} + 2 \frac{\lambda_2}{\lambda_1} \omega = 0. \quad (\text{B.38})$$

The r -momentum equation (Equation B.22) can be rearranged to the form

$$\frac{1}{\rho} \frac{dP}{dr} = \lambda_1 \left(\frac{U^2 + \bar{V}^2}{r} \right) + \lambda_2 (2\bar{V}\omega) + (r\omega^2) - \lambda_3 \left(\frac{\nu U}{\delta^2} \right). \quad (\text{B.39})$$

These two relations can be solved separately. Thus, with continuity and Equations B.38 and B.39 the velocity and pressure of the fluid can be determined for any point within the model.

Appendix C

Solution to θ -Momentum

From Appendix B we found that the behavior of the relative tangential velocity component of the fluid is described by the conservation of momentum in the θ -direction (Equation B.38). The results of Appendix B pertinent to the solution for the relative tangential velocity, \bar{V} , are repeated.

The resulting differential equation is

$$\frac{d\bar{V}}{dr} + (1 + 2Rr^2) \frac{\bar{V}}{r} + 2 \frac{\lambda_2}{\lambda_1} \omega = 0. \quad (\text{C.1})$$

The constant R is defined as

$$R = -\frac{\lambda_3}{2\lambda_1} \frac{\nu}{\delta^2 a}, \quad (\text{C.2})$$

and the term Rr^2 as a dimensionless quantity, R^* , which can be written in terms of two different Reynold's numbers:

$$R^* = \left(\frac{-\lambda_3}{2\lambda_1} \right) \frac{\gamma}{Re_\delta} = \left(\frac{-\lambda_3}{2\lambda_1} \right) \frac{\gamma^2}{Re_r}. \quad (\text{C.3})$$

C.1 Homogeneous Solution

Finding the solution for \bar{V} begins with the homogeneous form of Equation C.1;

$$\frac{d\bar{V}_h}{dr} + \left(\frac{1}{r} + 2Rr \right) \bar{V}_h = 0. \quad (\text{C.4})$$

Let the solution for the relative tangential velocity, \bar{V} , take the form of an infinite power series:

$$\bar{V}_h = r^s \sum_{m=0}^{\infty} b_m r^m, \quad (\text{C.5})$$

where s is an undetermined exponent and the b_m are constant coefficients. Differentiating Equation C.5 and substituting into Equation C.4 results in

$$\left[\sum_{m=0}^{\infty} (s+m)b_m r^{s+m-1} \right] + \left(\frac{1}{r} + 2Rr \right) \left[\sum_{m=0}^{\infty} b_m r^{s+m} \right] = 0. \quad (\text{C.6})$$

Using term-wise addition Equation C.6 can be combined into a single series of the form

$$\sum_{m=0}^{\infty} b_m \left[(s+m+1)r^{s+m-1} + 2Rr^{s+m+1} \right] = 0. \quad (\text{C.7})$$

Now, expand the series several terms and collect like powers of r :

$$\begin{aligned} 0 &= r^{s-1} [b_0(s+1)] \\ &+ r^s [b_1(s+2)] \\ &+ r^{s+1} [b_0(2R) + b_2(s+3)] \\ &+ r^{s+2} [b_1(2R) + b_3(s+4)] \\ &+ r^{s+3} [b_2(2R) + b_4(s+5)] + \dots \end{aligned} \quad (\text{C.8})$$

For the series to equal zero, each term in r from Equation C.8 must equal zero. Since the radius, r , can vary, the coefficient for each power of r must equal zero:

$$\begin{aligned}
 r^{s-1} : b_0(s+1) &= 0 & \rightarrow & \text{if } b_0 \neq 0, \text{ then } s = -1 \\
 r^s : b_1(s+2) &= 0 & \rightarrow & \text{if } s = -1, \text{ then } b_1 = 0 \\
 r^{s+1} : b_0(2R) + b_2(s+3) &= 0 & \rightarrow & b_2 = (-2Rb_0)/(s+3) \\
 r^{s+2} : b_1(2R) + b_3(s+4) &= 0 & \rightarrow & \text{if } b_1 = 0, \text{ then } b_3 = 0 \\
 r^{s+3} : b_2(2R) + b_4(s+5) &= 0 & \rightarrow & b_4 = (-2Rb_2)/(s+5) \\
 r^{s+4} : b_3(2R) + b_5(s+6) &= 0 & \rightarrow & \text{if } b_3 = 0, \text{ then } b_5 = 0 \\
 r^{s+5} : b_4(2R) + b_6(s+7) &= 0 & \rightarrow & b_6 = (-2Rb_4)/(s+7) \\
 & \vdots & &
 \end{aligned}$$

The odd coefficients in the power series solution of \bar{V} are zero. Substituting the value of s into the even coefficients results in:

$$\left. \begin{aligned}
 b_2 &= \frac{(-2R)}{2} b_0 \\
 b_4 &= \frac{(-2R)}{4} b_2 = \frac{(-2R)^2}{4 \cdot 2} b_0 \\
 b_6 &= \frac{(-2R)}{6} b_4 = \frac{(-2R)^3}{6 \cdot 4 \cdot 2} b_0 \\
 & \vdots
 \end{aligned} \right\} b_{2m} = \frac{(-2R)^m}{2^m (m)!}; \quad m = 0, 1, 2, 3, \dots$$

Therefore, the recursion formula for the b_m coefficients is:

$$b_{2m} = \frac{(-R)^m}{m!} b_0; \quad m = 0, 1, 2, 3, \dots \quad (\text{C.9})$$

Now, redefine the unknown coefficient, b_0 , as just b and define a function F_m such that

$$F_m = \frac{1}{m!}. \quad (\text{C.10})$$

The homogeneous solution for Equation C.4 is now

$$\bar{V}_h = \frac{b}{r} \sum_{m=0}^{\infty} (-Rr^2)^m F_m. \quad (\text{C.11})$$

Recalling the definition of R^* , now define a series function, S_m , as

$$S_m = \sum_{m=0}^{\infty} (-R^*)^m F_m. \quad (\text{C.12})$$

Therefore,

$$\bar{V}_h = \frac{bS_m(R^*)}{r}. \quad (\text{C.13})$$

C.2 Particular Solution

The particular form of Equation C.1 includes the angular velocity term, $2\lambda_2\omega/\lambda_1$, which is a constant with respect to r ;

$$\frac{d\bar{V}_p}{dr} + \left(\frac{1}{r} + 2Rr\right) \bar{V}_p = -2\frac{\lambda_2}{\lambda_1}\omega. \quad (\text{C.14})$$

Assume the solution to Equation C.14 is of the form of a Laurent series:

$$\bar{V}_p = c_1 r^{-1} + c_2 r^0 + c_3 r^1, \quad (\text{C.15})$$

where the c -coefficients are unknown.

Similar to the homogeneous solution, differentiate Equation C.15 and substitute into Equation C.14 for \bar{V}_p and $d\bar{V}_p/dr$;

$$\left[-c_1 r^{-2} + c_3\right] + \left(\frac{1}{r} + 2Rr\right) \left[c_1 r^{-1} + c_2 + c_3 r^1\right] = -2\frac{\lambda_2}{\lambda_1}\omega. \quad (\text{C.16})$$

Expanding Equation C.16 and collecting like powers of r :

$$\begin{aligned}
& (2Rc_3)r^{+2} + (2Rc_2)r^{+1} \\
& \quad + (2c_3 + 2Rc_1)r^0 \\
& + (c_2)r^{-1} + (-c_1 + c_1)r^{+1} = \left(-2\frac{\lambda_2}{\lambda_1}\omega\right)r^0.
\end{aligned} \tag{C.17}$$

Equating the coefficients of like powers of r results in:

$$\begin{aligned}
r^{+2}: 2Rc_3 &= 0 & \rightarrow & c_3 = 0 \\
r^{+1}: 2Rc_2 &= 0 & \rightarrow & c_2 = 0 \\
r^0: 2c_3 + 2Rc_1 &= -2\frac{\lambda_2}{\lambda_1}\omega & \rightarrow & c_1 = -\frac{\lambda_2\omega}{\lambda_1 R} \\
r^{-1}: c_2 &= 0 \\
r^{-2}: -c_1 + c_1 &= 0
\end{aligned}$$

Therefore, the particular solution depends only upon the c_1 term;

$$\bar{V}_p = \left(-\frac{\lambda_2\omega}{\lambda_1 R}\right)r^{-1}. \tag{C.18}$$

Now, define a constant c such that

$$c = \frac{\lambda_2\omega}{\lambda_1 R}. \tag{C.19}$$

The particular solution becomes

$$\bar{V}_p = \frac{c}{r}. \tag{C.20}$$

C.3 Total Solution

The total solution for the relative tangential velocity, \bar{V} , is the sum of the homogeneous solution (Equation C.13) and the particular solution (Equation C.20). The final result is:

$$\bar{V}(r) = \frac{b S_m(R^*) - c}{r}. \quad (\text{C.21})$$

Appendix D

Solution to r -Momentum

In Appendix B the r -momentum relation (Equation B.2) is reduced to

$$\begin{array}{cccccc} \text{I} & & \text{II} & & \text{III} & & \text{IV} & & \text{V} \\ \frac{1}{\rho} \frac{dP}{dr} & = & \lambda_1 \left(\frac{U^2 + \bar{V}^2}{r} \right) & + & \lambda_2 (2\bar{V}\omega) & + & (r\omega^2) & + & \lambda_3 \left(\frac{\nu U}{\delta^2} \right), \end{array} \quad (\text{D.1})$$

where the five terms are accelerations resulting from the following forces:

- I. pressure,
- II. momentum,
- III. Coriolis,
- IV. centripetal, and
- V. viscous.

The solutions for the radial and relative tangential velocity components are developed in Appendix A and Appendix C, respectively. The results are repeated here for convenience;

$$U(r) = \frac{a}{r}, \quad (\text{D.2})$$

and

$$\bar{V}(r) = \frac{bS_m(R^*) - c}{r}, \quad (\text{D.3})$$

where a and b are unknown constants. The constant c is defined as

$$c = \frac{\lambda_2 \omega}{\lambda_1 R}. \quad (\text{D.4})$$

Other definitions from Appendix B are:

$$R = -\frac{\lambda_3 \nu}{2\lambda_1 \delta^2 a}, \quad (\text{D.5})$$

$$R^* = Rr^2, \quad (\text{D.6})$$

$$F_m = \frac{1}{m!}, \quad (\text{D.7})$$

$$S_m(R^*) = \sum_{m=0}^{\infty} (-R^*)^m F_m. \quad (\text{D.8})$$

D.1 Integrations

To solve for the pressure, P , substitute Equations D.2 and D.3 for the velocity components and integrate Equation D.1 with respect to r . Thus, Equation D.1 becomes

$$\frac{1}{\rho} P(r) = \int \{\text{II}\} dr + \int \{\text{III}\} dr + \int \{\text{IV}\} dr + \int \{\text{V}\} dr. \quad (\text{D.9})$$

Integrating the viscous term $\{\text{V}\}$ first:

$$\begin{aligned} \int \{\text{V}\} dr &= \int \lambda_3 \left(\frac{\nu U}{\delta^2} \right) dr \\ &= \int \lambda_3 \left(\frac{\nu a}{\delta^2 r} \right) dr \\ &= \frac{\lambda_3 \nu a}{\delta^2} \int \frac{1}{r} dr \\ &= \frac{\lambda_3 \nu a}{\delta^2} \ln r. \end{aligned} \quad (\text{D.10})$$

The coefficient, $\lambda_3 \nu a / \delta^2$, can be shown to be equivalent to $-2\lambda_1 a^2 R$. Therefore, the integral of the viscous term {V} is

$$\int \{V\} dr = (-\lambda_1 a^2) R \ln r^2. \quad (D.11)$$

Next, integrate the centripetal term {IV}:

$$\int \{IV\} dr = \int (r\omega^2) dr = (\omega^2) \frac{r^2}{2}. \quad (D.12)$$

The Coriolis term {III} contains an infinite series, $S_m(R^*)$, which must be handled through term-wise integration. Thus,

$$\begin{aligned} \int \{III\} dr &= \int \lambda_2 (2\bar{V}\omega) dr \\ &= \int \lambda_2 (2\omega) \left[\frac{b}{r} \sum_{m=0}^{\infty} (-Rr^2)^m F_m - \frac{c}{r} \right] dr \\ &= \lambda_2 (2\omega) \left[b \sum_{m=0}^{\infty} (-R)^m F_m \int r^{2m-1} dr - c \int \frac{1}{r} dr \right]. \quad (D.13) \end{aligned}$$

Since the integration of r^{2m-1} will result in a coefficient of $1/2m$, the series must be expanded by one term before integrating in order to allow for the first element of the series in which m equals zero. Equation D.13 now appears as

$$\int \{III\} dr = 2\omega\lambda_2 \left[b \left(\int \frac{1}{r} dr + \sum_{m=1}^{\infty} (-R)^m F_m \int r^{2m-1} dr \right) - c \int \frac{1}{r} dr \right]. \quad (D.14)$$

Completing the integrations and making a transformation on the series to bring the initial element back to zero results in Equation D.14 becoming

$$\begin{aligned} \int \{III\} dr &= 2\omega\lambda_2 \left[(b-c) \ln r + b \sum_{m=1}^{\infty} (-R)^m F_m \frac{r^{2m}}{2m} \right] \\ &= 2\omega\lambda_2 \left[(b-c) \ln r + b \sum_{m=1}^{\infty} (-R^*)^m F_m \frac{1}{2m} \right] \\ &= 2\omega\lambda_2 \left[(b-c) \ln r + b \sum_{m=0}^{\infty} (-R^*)^{m+1} F_{m+1} \frac{1}{2(m+1)} \right] \quad (D.15) \end{aligned}$$

From the definition of c (Equation D.4), the $\lambda_2\omega$ coefficient is found to equal $\lambda_1 cR$.

With this substitution the integration of the Coriolis term {III} is

$$\int \{\text{III}\} dr = -\lambda_1 \left\{ (c^2 - bc) R \ln r^2 - 2bcR \sum_{m=0}^{\infty} (-R^*)^{m+1} \frac{F_{m+1}}{2(m+1)} \right\}. \quad (\text{D.16})$$

The substitutions for the velocity components result in the momentum term {II} transforming to

$$\begin{aligned} \{\text{II}\} &= \lambda_1 \left(\frac{U^2 + \bar{V}^2}{r} \right) \\ &= \frac{\lambda_1}{r} \left[\frac{a^2}{r^2} + \left(\frac{bS_m(R^*) - c}{r} \right)^2 \right] \\ &= \frac{\lambda_1}{r^3} \left[(a^2 + c^2) + b^2 S_m(R^*) S_m(R^*) - 2bc S_m(R^*) \right]. \quad (\text{D.17}) \end{aligned}$$

Before integrating the momentum term {II}, the double series, $S_m(R^*)S_m(R^*)$, must be resolved. The double series,

$$S_m(R^*)S_m(R^*) = \left[\sum_{m=0}^{\infty} (-R^*)^m F_m \right] \left[\sum_{m=0}^{\infty} (-R^*)^m F_m \right], \quad (\text{D.18})$$

can be combined into a single series through term-wise multiplication. Thus,

$$\begin{aligned} S_m S_m &= \sum_{m=0}^{\infty} \left[\frac{(-R^*)^0 (-R^*)^m}{(0)!(m)!} + \frac{(-R^*)^{0+1} (-R^*)^{m-1}}{(0+1)!(m-1)!} + \frac{(-R^*)^{0+2} (-R^*)^{m-2}}{(0+2)!(m-2)!} \right. \\ &\quad \left. + \dots + \frac{(-R^*)^{0+m} (-R^*)^{m-m}}{(0+m)!(m-m)!} \right], \quad (\text{D.19}) \end{aligned}$$

which reduces to

$$S_m S_m = \sum_{m=0}^{\infty} (-R^*)^m \left[\frac{1}{(0)!(m)!} + \frac{1}{(0+1)!(m-1)!} + \frac{1}{(0+2)!(m-2)!} + \dots + \frac{1}{(0+m)!(m-m)!} \right]. \quad (\text{D.20})$$

Table D.1: Values of Functions F_m and G_m for Various m

m	F_m	G_m
0	1	1
1	1	2
2	1/2	2
3	1/6	4/3
4	1/24	2/3
5	1/120	4/15
6	1/720	4/45

In order to simplify the subsequent calculations define a factorial function G_m such that

$$G_m = \frac{1}{(0)!(m)!} + \frac{1}{(0+1)!(m-1)!} + \frac{1}{(0+2)!(m-2)!} + \dots + \frac{1}{(0+m)!(m-m)!} . \quad (\text{D.21})$$

Equation D.21 can be reduced to the form of a finite series,

$$G_m = \sum_{n=0}^m \frac{1}{n!} \frac{1}{(m-n)!} = \sum_{n=0}^m F_n F_{m-n} . \quad (\text{D.22})$$

The values of the factorial functions, F_m and G_m , for several m is given in Table D.1. The function G_m decreases much less rapidly than F_m as the series progresses. Therefore, the infinite series containing G_m will require more summations than the infinite series containing F_m in order to meet the same convergence criterion.

The two series functions of the momentum term {II} as written in Equation D.17 have the same form;

$$S_m(R^*) = \sum_{m=0}^{\infty} (-R^*)^m F_m , \quad (\text{D.23})$$

and

$$S_m(R^*) S_m(R^*) = \sum_{m=0}^{\infty} (-R^*)^m G_m . \quad (\text{D.24})$$

Therefore, the momentum term {II} (Equation D.17) can be rewritten in terms of a single series.

$$\begin{aligned}
 \{\text{II}\} &= \frac{\lambda_1}{r^3} \left[(a^2 + c^2) + b^2 \sum_{m=0}^{\infty} (-R^*)^m F_m - 2bc \sum_{m=0}^{\infty} (-R^*)^m G_m \right] \\
 &= \frac{\lambda_1}{r^3} \left[(a^2 + c^2) + \sum_{m=0}^{\infty} (-R^*)^m [b^2 G_m - 2bc F_m] \right] \\
 &= \lambda_1 \left\{ (a^2 + c^2) \frac{1}{r^3} + \sum_{m=0}^{\infty} (-R)^m [b^2 G_m - 2bc F_m] (r^{2m-3}) \right\} \quad (\text{D.25})
 \end{aligned}$$

As is the case for the Coriolis term {III} the series for the momentum term {II} must be expanded before integration in order to avoid a singularity. In this case the singularity would occur at $m = 1$ so the series needs to be expanded by at least two terms. Equation D.25 becomes

$$\begin{aligned}
 \{\text{II}\} &= \lambda_1 \left\{ (a^2 + c^2) \frac{1}{r^3} + (b^2 - 2bc) \frac{1}{r^3} + 2(b^2 - bc) (-R) \frac{1}{r} \right\} \\
 &\quad + \lambda_1 \sum_{m=2}^{\infty} (-R)^m [b^2 G_m - 2bc F_m] (r^{2m-3}) \\
 &= \lambda_1 \left\{ [a^2 + (b - c)^2] \frac{1}{r^3} + 2(b^2 - bc) (-R) \frac{1}{r} \right\} \\
 &\quad + \lambda_1 \sum_{m=2}^{\infty} (-R)^m [b^2 G_m - 2bc F_m] (r^{2m-3}) . \quad (\text{D.26})
 \end{aligned}$$

Using term-wise integration, the momentum term {II} can be integrated as

$$\begin{aligned}
\int \{\text{II}\} dr &= \int \lambda_1 \left(\frac{U^2 + \bar{V}^2}{r} \right) dr \\
&\dots = \lambda_1 \left\{ \left[a^2 + (b-c)^2 \right] \int \frac{1}{r^3} dr + 2(b^2 - bc)(-R) \int \frac{1}{r} dr \right\} \\
&\quad + \lambda_1 \sum_{m=2}^{\infty} (-R)^m \left[b^2 G_m - 2bc F_m \right] \int r^{2m-3} dr \\
&\dots = \lambda_1 \left\{ \left[a^2 + (b-c)^2 \right] \frac{-1}{2r^2} + 2(b^2 - bc)(-R) \ln r \right\} \\
&\quad + \lambda_1 \sum_{m=2}^{\infty} (-R)^m \left[b^2 G_m - 2bc F_m \right] \frac{r^{2(m-1)}}{2(m-1)} \\
&\dots = \lambda_1 \left\{ \left[a^2 + (b-c)^2 \right] \frac{-1}{2r^2} - (b^2 - bc) R \ln r^2 \right\} \\
&\quad + \lambda_1 (-R) \sum_{m=2}^{\infty} (-R)^{m-1} \left[b^2 G_m - 2bc F_m \right] \frac{r^{2(m-1)}}{2(m-1)} \\
&\dots = -\lambda_1 \left\{ \left[a^2 + (b-c)^2 \right] \frac{1}{2r^2} + (b^2 - bc) R \ln r^2 \right\} \\
&\quad - \lambda_1 R \sum_{m=2}^{\infty} \frac{(-R^*)^{m-1}}{2(m-1)} \left[b^2 G_m - 2bc F_m \right]. \tag{D.27}
\end{aligned}$$

Now, transform the series so that the initial element, m , is zero.

$$\begin{aligned}
\int \{\text{II}\} dr &= -\lambda_1 \left\{ \left[a^2 + (b-c)^2 \right] \frac{1}{2r^2} + (b^2 - bc) R \ln r^2 \right\} \\
&\quad - \lambda_1 R \sum_{m=0}^{\infty} \frac{(-R^*)^{m+1}}{2(m+1)} \left[b^2 G_{m+2} - 2bc F_{m+2} \right]. \tag{D.28}
\end{aligned}$$

D.2 Solution

Combining the integration of the momentum term {II}, the Coriolis term {III}, the centripetal term {IV}, and the viscous term {V} results in a solution for the pressure:

$$\begin{aligned}
 \frac{1}{\rho}P(r) = & \left. \begin{aligned} & -\lambda_1 \left\{ \left[a^2 + (b-c)^2 \right] \frac{1}{2r^2} + (b^2 - bc) R \ln r^2 \right\} \\ & - \lambda_1 \left\{ bR \sum_{m=0}^{\infty} \frac{(-R^*)^{m+1}}{2(m+1)} [bG_{m+2} - 2cF_{m+2}] \right\} \end{aligned} \right\} \text{ {II}} \\
 & \left. \begin{aligned} & -\lambda_1 \left\{ (c^2 - bc) R \ln r^2 \right\} \\ & - \lambda_1 \left\{ bR \sum_{m=0}^{\infty} \frac{(-R^*)^{m+1}}{2(m+1)} [-2cF_{m+1}] \right\} \end{aligned} \right\} \text{ {III}} \\
 & + \left\{ [\omega^2] \frac{r^2}{2} \right\} \text{ {IV}} \\
 & -\lambda_1 \left\{ (a^2) R \ln r^2 \right\} \text{ {V}} \\
 & + d
 \end{aligned} \tag{D.29}$$

where d is a constant of integration. Equation D.29 can be simplified by collecting like powers of r . Also, the two series can be combined through term-wise addition.

The result is

$$\begin{aligned}
 \frac{1}{\rho}P(r) = & -\lambda_1 \left\{ \left[a^2 + (b-c)^2 \right] \left(\frac{1}{2r^2} + R \ln r^2 \right) \right\} \\
 & -\lambda_1 \left\{ bR \sum_{m=0}^{\infty} \frac{(-R^*)^{m+1}}{2(m+1)} [bG_{m+2} - 2c(F_{m+2} + F_{m+1})] \right\} \\
 & + [\omega^2] \frac{r^2}{2} + d.
 \end{aligned} \tag{D.30}$$

Finally, the factorial functions, F_m , can be combined such that

$$F_{m+2} + F_{m+1} = (m+3)F_{m+2}. \tag{D.31}$$

Therefore, the solution for the pressure from the r -momentum equation is:

$$\begin{aligned}
 \frac{1}{\rho}P(r) = & -\lambda_1 \left\{ [a^2 + (b-c)^2] \left(\frac{1}{2r^2} + R \ln r^2 \right) \right\} \\
 & -\lambda_1 \left\{ bR \sum_{m=0}^{\infty} \frac{(-R^*)^{m+1}}{2(m+1)} [bG_{m+2} - 2c(m+3)F_{m+2}] \right\} \\
 & + [\omega^2] \frac{r^2}{2} + d.
 \end{aligned} \tag{D.32}$$

Appendix E

Conservation of Angular Momentum

E.1 Rotating Control Volume

An inertial control volume is one which is stationary or moves with a constant velocity relative to a fixed frame of reference. The conservation principles are only valid for inertial systems. For the system described in Chapter 1, the most convenient control volume is defined as the fluid contained within the disks, but not the disks themselves, with the control volume rotating at the same angular velocity as the rotor. This control volume is non-inertial; therefore, the rotation must be accounted for in the conservation principles.

Figure E.1 illustrates how the non-inertial control volume, of the rotating disks, is related to an inertial frame of reference. The position vector \vec{R} is the position of the control volume relative to the inertial frame of reference. The position vector \vec{r} is the position of a fluid particle P relative to the rotating control volume. The position of P relative to the inertial frame of reference is \vec{x} :

$$\vec{x} = \vec{R} + \vec{r}. \quad (\text{E.1})$$

In order to clarify further development, a notation convention to distinguish be-

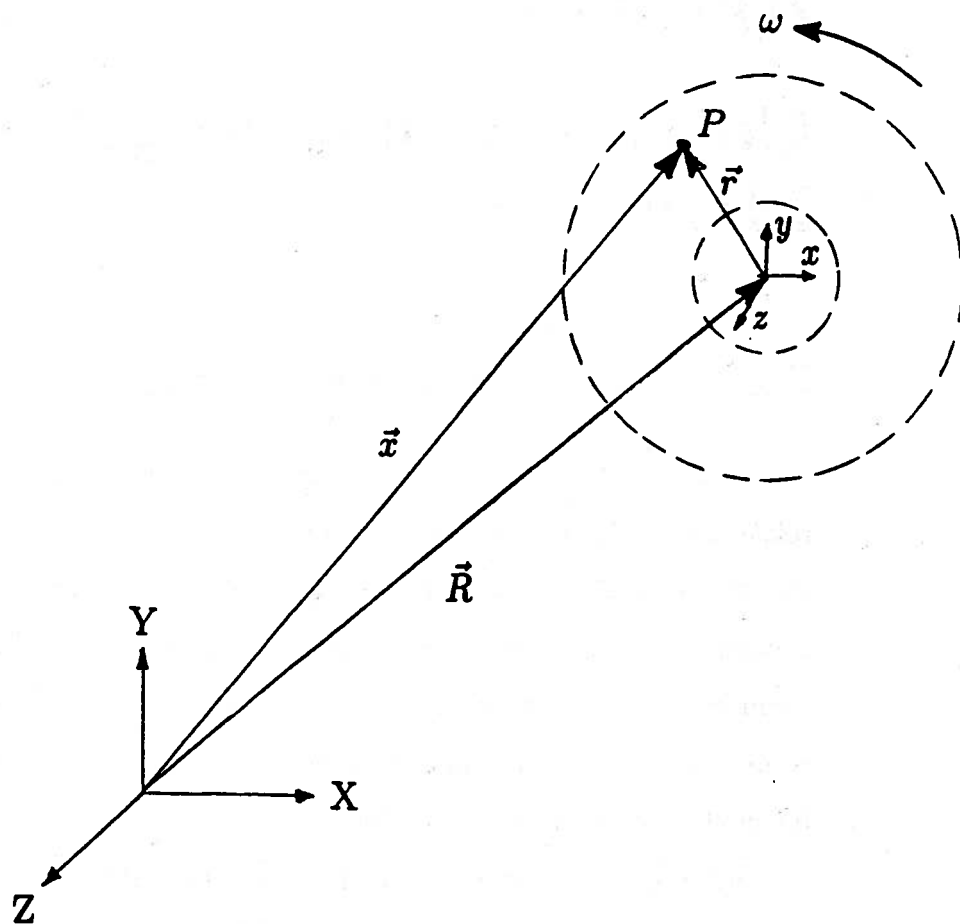


Figure E.1: Rotating Control Volume Relative to Inertial Frame of Reference

tween the time derivative of the inertial and non-inertial systems is defined:

$$\begin{aligned} \left(\dot{\quad} \right) &\equiv \frac{D}{Dt} \left(\quad \right) \equiv \text{Time Derivative Relative} \\ &\quad \text{to the Inertial System} \\ \frac{d}{dt} \left(\quad \right) &\equiv \text{Time Derivative Relative} \\ &\quad \text{to the Rotating System} \end{aligned} \quad (\text{E.2})$$

The velocity of particle P relative to the inertial coordinate system is the time derivative of the position vector \vec{x} ;

$$\frac{D(\vec{x})}{Dt} = \frac{D}{Dt} (\vec{R} + \vec{r}) = \frac{D(\vec{R})}{Dt} + \frac{D(\vec{r})}{Dt}, \quad (\text{E.3})$$

which becomes

$$\vec{V}_P = \vec{V}_{rel} + \frac{D(\vec{r})}{Dt}. \quad (\text{E.4})$$

\vec{V}_{rel} is the velocity of the rotating control volume relative to the inertial frame of reference. For the control volume described above the position vector \vec{R} and the relative velocity \vec{V}_{rel} are defined to be zero. In other words, the rotating frame of reference and the stationary frame of reference are attached to the same spatial location. Therefore, the position and velocity of particle P are

$$\vec{x}_P = \vec{r}. \quad (\text{E.5})$$

and

$$\vec{V}_P = \frac{D\vec{r}}{Dt}. \quad (\text{E.6})$$

In Equations E.5 and E.6 both the magnitude and the direction of the position vector \vec{r} are functions of time. For a cylindrical coordinate system \vec{r} is defined as

$$\vec{r} = r\hat{e}_r + \frac{\theta}{r}\hat{e}_\theta + z\hat{e}_z. \quad (\text{E.7})$$

Therefore, Equation E.6 is

$$\vec{V}_P = \frac{D}{Dt}(\vec{r}) = \frac{D}{Dt}(r_j\hat{e}_j) = \hat{e}_j \frac{Dr_j}{Dt} + r_j \frac{D\hat{e}_j}{Dt}. \quad (\text{E.8})$$

In Equation E.8 the i indice can be either the radial component r , the angular component θ , or the axial component z . The total derivative of r_i is the velocity of the fluid particle P with respect to the rotating coordinate system (or the control volume). The time derivative of the unit vectors can be shown to be the cross product of the axis of rotation. (See references [11] or [10].) The time derivative operator relative to the inertial frame of reference (Equation E.2) can be written with respect to the rotating control volume as

$$\frac{D}{Dt} \left(\quad \right) = \frac{d}{dt} \left(\quad \right) + \vec{\omega} \times \left(\quad \right), \quad (\text{E.9})$$

where $\vec{\omega}$ is the angular velocity of the control volume. Now, the absolute velocity of a particle P within the control volume can be expressed as

$$\vec{V}_P = \frac{D}{Dt}(\vec{x}) = \frac{D}{Dt}(\vec{r}) = \frac{d\vec{r}}{dt} + \vec{\omega} \times \vec{r}. \quad (\text{E.10})$$

Using these conventions a relationship for the conservation of angular momentum will be developed.

E.2 Conservation of Angular Momentum

The conservation of angular momentum states that for an inertial system the sum of the torques acting the system equals the rate of change of angular momentum:

$$\vec{T}_{system} = \frac{D}{Dt}(\vec{H}), \quad (\text{E.11})$$

where \vec{H} is the angular momentum of the system and is defined as

$$\vec{H} = \int_V (\vec{x} \times \vec{V}) \rho dV. \quad (\text{E.12})$$

In Equation E.12 \vec{x} is the position vector of the particle relative to the fixed frame of reference (See Figure E.1.) and \vec{V} is the velocity of that particle relative to the fixed

frame of reference. Using Equations E.5 and E.6 the conservation of momentum can be expressed as

$$\vec{T}_{system} = \frac{D}{Dt} \int_{C_V} (\vec{r} \times \vec{V}) \rho dV. \quad (E.13)$$

Since the integral is not time dependent Equation E.13 can be written as

$$\vec{T}_{system} = \int_{C_V} \left(\frac{D\vec{r}}{Dt} \times \vec{V} \right) \rho dV + \int_{C_V} \left(\vec{r} \times \frac{D\vec{V}}{Dt} \right) \rho dV. \quad (E.14)$$

From Equation E.6 the velocity \vec{V} is equal to $D\vec{r}/Dt$ which results in the first integral on the right side of Equation E.14 becoming zero:

$$\frac{D\vec{r}}{Dt} \times \frac{D\vec{r}}{Dt} = \vec{0}. \quad (E.15)$$

Also using Equation E.6 the cross product of the second integral on the right side of Equation E.13 may be rewritten as

$$\vec{r} \times \frac{D\vec{V}}{Dt} = \vec{r} \times \frac{D}{Dt} \left(\frac{D\vec{r}}{Dt} \right). \quad (E.16)$$

Now, using the differential operator defined in Equation E.9, Equation E.16 can be expressed as

$$\begin{aligned} \vec{r} \times \frac{D}{Dt} \left(\frac{D\vec{r}}{Dt} \right) &= \\ &= \vec{r} \times \frac{D}{Dt} \left(\frac{d\vec{r}}{dt} + \vec{\omega} \times \vec{r} \right) \\ &= \vec{r} \times \left[\frac{d}{dt} \left(\frac{d\vec{r}}{dt} + \vec{\omega} \times \vec{r} \right) + \vec{\omega} \times \left(\frac{d\vec{r}}{dt} + \vec{\omega} \times \vec{r} \right) \right] \\ &= \vec{r} \times \left[\frac{d}{dt} \left(\frac{d\vec{r}}{dt} \right) + \frac{d}{dt} (\vec{\omega} \times \vec{r}) + \left(\vec{\omega} \times \frac{d\vec{r}}{dt} \right) + \vec{\omega} \times (\vec{\omega} \times \vec{r}) \right] \\ &= \vec{r} \times \left[\frac{d}{dt} \left(\frac{d\vec{r}}{dt} \right) + \left(\frac{d\vec{\omega}}{dt} \times \vec{r} \right) + \left(\vec{\omega} \times \frac{d\vec{r}}{dt} \right) + \left(\vec{\omega} \times \frac{d\vec{r}}{dt} \right) + \vec{\omega} \times (\vec{\omega} \times \vec{r}) \right] \\ &= \vec{r} \times \left[\frac{d}{dt} \left(\frac{d\vec{r}}{dt} \right) + (\dot{\vec{\omega}} \times \vec{r}) + 2 \left(\vec{\omega} \times \frac{d\vec{r}}{dt} \right) + \vec{\omega} \times (\vec{\omega} \times \vec{r}) \right]. \end{aligned} \quad (E.17)$$

The velocity of a particle relative to the rotating control volume is $d\vec{r}/dt$ and is defined as \vec{v} . Using Equation E.17 the conservation of momentum relation (Equation E.14) becomes

$$\vec{T}_{system} = \int_{C_V} \vec{r} \times \left[\frac{d}{dt}(\vec{v}) + (\dot{\vec{\omega}} \times \vec{r}) + 2(\vec{\omega} \times \vec{v}) + \vec{\omega} \times (\vec{\omega} \times \vec{r}) \right] \rho dV, \quad (E.18)$$

which can be broken into two integrals

$$\begin{aligned} \vec{T}_{system} &= \int_{C_V} \left(\vec{r} \times \frac{d\vec{v}}{dt} \right) \rho dV \\ &+ \int_{C_V} \vec{r} \times \left[(\dot{\vec{\omega}} \times \vec{r}) + 2(\vec{\omega} \times \vec{v}) + \vec{\omega} \times (\vec{\omega} \times \vec{r}) \right] \rho dV. \end{aligned} \quad (E.19)$$

The first integral term on the right side of Equation E.19 can be simplified through use of the chain rule and Equation E.15;

$$\begin{aligned} \vec{r} \times \frac{d\vec{v}}{dt} &= \frac{d}{dt}(\vec{r} \times \vec{v}) - \frac{d\vec{r}}{dt} \times \vec{v} \\ &= \frac{d}{dt}(\vec{r} \times \vec{v}) - \frac{d\vec{r}}{dt} \times \frac{d\vec{r}}{dt} \\ &= \frac{d}{dt}(\vec{r} \times \vec{v}) - \vec{0}. \end{aligned} \quad (E.20)$$

Thus, Equation E.19 becomes

$$\begin{aligned} \vec{T}_{system} &= \frac{d}{dt} \int_{C_V} (\vec{r} \times \vec{v}) \rho dV \\ &+ \int_{C_V} \vec{r} \times \left[(\dot{\vec{\omega}} \times \vec{r}) + 2(\vec{\omega} \times \vec{v}) + \vec{\omega} \times (\vec{\omega} \times \vec{r}) \right] \rho dV. \end{aligned} \quad (E.21)$$

The first integral on the right side of Equation E.21 can be expanded again through the use of Reynold's Transport Theorem:

$$\frac{d}{dt} \int_{C_V} (\vec{r} \times \vec{v}) \rho dV = \frac{\partial}{\partial t} \int_{C_V} (\vec{r} \times \vec{v}) \rho dV + \int_{\partial C_V} (\vec{r} \times \vec{v}) \rho \vec{v} \cdot d\vec{A}. \quad (E.22)$$

The total torque acting on the control volume can now be expressed as

$$\begin{aligned} \vec{T}_{system} = & \frac{\partial}{\partial t} \int_{C_V} (\vec{r} \times \vec{v}) \rho dV + \int_{\partial C_V} (\vec{r} \times \vec{v}) \rho \vec{v} \cdot d\vec{A} \\ & + \int_{C_V} \vec{r} \times [(\dot{\vec{\omega}} \times \vec{r}) + 2(\vec{\omega} \times \vec{v}) + \vec{\omega} \times (\vec{\omega} \times \vec{r})] \rho dV. \end{aligned} \quad (E.23)$$

The sum of the torques acting on the system, \vec{T}_{system} , can be broken down into various types of effects;

$$\vec{T}_{system} = \vec{T}_{surfaceC_V} + \vec{T}_{bodyC_V} + \vec{T}_{shaftC_V}. \quad (E.24)$$

For the system under study there are no torques due to body forces.

Therefore, using Equations E.22, E.23, and E.24 the conservation of momentum for a rotating control volume can be expressed as

$$\begin{aligned} \vec{T}_{shaftC_V} + \vec{T}_{surfaceC_V} = & \frac{\partial}{\partial t} \int_{C_V} (\vec{r} \times \vec{v}) \rho dV + \int_{\partial C_V} (\vec{r} \times \vec{v}) \rho \vec{v} \cdot d\vec{A} \\ & + \int_{C_V} \vec{r} \times [(\dot{\vec{\omega}} \times \vec{r}) + 2(\vec{\omega} \times \vec{v}) + \vec{\omega} \times (\vec{\omega} \times \vec{r})] \rho dV. \end{aligned} \quad (E.25)$$

E.3 Solution to Moment of Momentum

Figure E.2 shows two views of the rotating control volume. The left view is the control volume looking at the face of one disk. The view on the right is an end view of the disks. There are four surfaces on the control volume. The first surface {I} is on the $z = \delta$ disk face, the second surface {II} is on the outer radial edge, the third surface {III} is on the $z = -\delta$ disk face, and the fourth surface {IV} is on the inner radial edge. The control volume contains the fluid for a single pair of disks; thus, the results of analyzing this control volume are valid for the model described in Chapter 1.

In analyzing the control volume the following assumptions are applied:

- steady-state flow,
- steady rotation, $\dot{\omega} = 0$, and
- no variations with respect to θ .

With these assumptions the conservation of momentum relation (Equation E.25) can be simplified to

$$\begin{aligned} \vec{T}_{shaft_{CV}} + \vec{T}_{surface_{CV}} &= \int_{\partial CV} (\vec{r} \times \vec{v}) \rho \vec{v} \cdot d\vec{A} \\ &+ \int_{CV} \vec{r} \times [2(\vec{\omega} \times \vec{v}) + \vec{\omega} \times (\vec{\omega} \times \vec{r})] \rho dV. \end{aligned} \quad (E.26)$$

The vector quantities of Equation E.26 are defined from Figure E.2 as

$$\vec{r} = r\hat{e}_r + z\hat{e}_z, \quad (E.27)$$

$$\vec{\omega} = \omega\hat{e}_z, \text{ and} \quad (E.28)$$

$$\vec{v} = u(r, z)\hat{e}_r + \bar{v}(r, z)\hat{e}_\theta + w(r, z)\hat{e}_z. \quad (E.29)$$

Also, fully-developed boundary layer flow is assumed. Therefore, w goes to zero and the remaining velocity components may be separated into a radial dependent function and an axial dependent function. If η is defined as z/δ and the axial function as $\mathcal{F}(\eta)$ then the velocity (Equation E.29) can be expressed as

$$\begin{aligned} \vec{v} &= U(r)\mathcal{F}(\eta)\hat{e}_r + \bar{V}(r)\mathcal{F}(\eta)\hat{e}_\theta \\ &= (U(r)\hat{e}_r + \bar{V}(r)\hat{e}_\theta) \mathcal{F}(\eta). \end{aligned} \quad (E.30)$$

In Equation E.30 the radial functions U and \bar{V} are the fluid velocity components at $\eta = 0$ and the axial function $\mathcal{F}(\eta)$ is a velocity profile function.

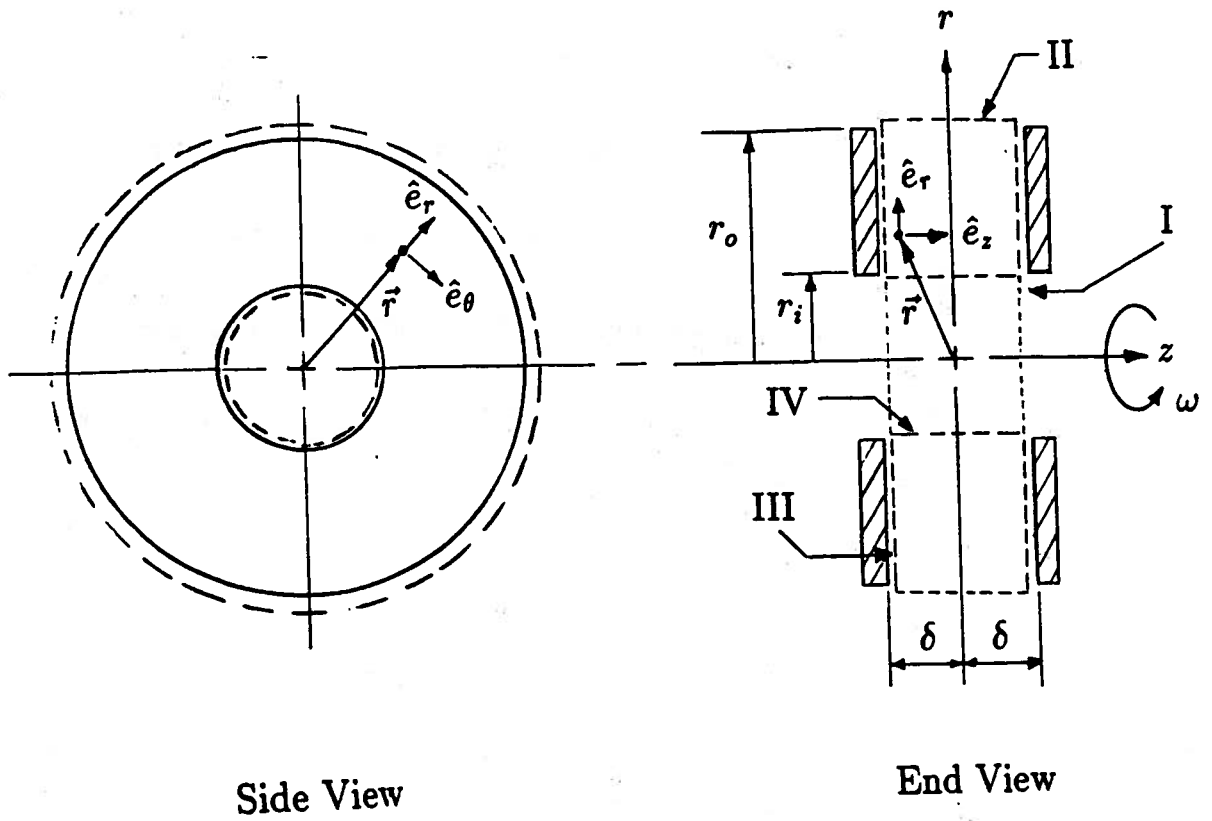


Figure E.2: Control Volume Definition

E.3.1 Surface Integral Evaluation

With Equations E.27, E.28, and E.30 the cross product terms of Equation E.26 can be evaluated. Examining the cross product quantity of the surface integral first:

$$\begin{aligned}
 (\vec{r} \times \vec{v}) &= (r\hat{e}_r + z\hat{e}_z) \times (U\hat{e}_r + \bar{V}\hat{e}_\theta) \mathcal{F}(\eta) \\
 &= (r\hat{e}_r + \delta\eta\hat{e}_z) \times (U\hat{e}_r + \bar{V}\hat{e}_\theta) \mathcal{F}(\eta) \\
 &= (r\bar{V}\hat{e}_z + \delta\eta U\hat{e}_\theta - \delta\eta\bar{V}\hat{e}_r) \mathcal{F}(\eta) \\
 &= (r\bar{V}\hat{e}_z) \mathcal{F}(\eta) + \delta(U\hat{e}_z - \bar{V}\hat{e}_r) \eta \mathcal{F}(\eta). \quad (\text{E.31})
 \end{aligned}$$

Now, the infinitesimal area vectors, $d\vec{A}$, for the four sides of the control volume in Figure E.2 are defined as

$$d\vec{A}_1 = dA_1\hat{e}_z, \quad (\text{E.32})$$

$$d\vec{A}_2 = dA_2\hat{e}_r, \quad (\text{E.33})$$

$$d\vec{A}_3 = -dA_3\hat{e}_z, \quad (\text{E.34})$$

$$d\vec{A}_4 = -dA_4\hat{e}_r. \quad (\text{E.35})$$

Subsequently, the dot product of the surface integral becomes

$$\begin{aligned}
 \vec{v} \cdot d\vec{A} &= (U\hat{e}_r + \bar{V}\hat{e}_\theta) \mathcal{F}(\eta) \cdot d\vec{A} \\
 &= (U_2dA_2 - U_4dA_4) \mathcal{F}(\eta). \quad (\text{E.36})
 \end{aligned}$$

Equation E.36 shows that the surface integral of Equation E.26 can be separated into the integral over the outer radial surface and the integral over the inner radial surface.

Thus,

$$\begin{aligned}
 & \int_{\partial C_V} (\vec{r} \times \vec{v}) \rho \vec{v} \cdot d\vec{A} = \tag{E.37} \\
 & = \rho \int_{\partial C_{V_2}} \left[(r_2 \bar{V}_2 \hat{e}_z) \mathcal{F}(\eta) + \delta (U_2 \hat{e}_\theta - \bar{V}_2 \hat{e}_r) \eta \mathcal{F}(\eta) \right] U_2 \mathcal{F}(\eta) dA_2 \\
 & \quad - \rho \int_{\partial C_{V_4}} \left[(r_4 \bar{V}_4 \hat{e}_z) \mathcal{F}(\eta) + \delta (U_4 \hat{e}_\theta - \bar{V}_4 \hat{e}_r) \eta \mathcal{F}(\eta) \right] U_4 \mathcal{F}(\eta) dA_4 \\
 & = \rho \left\{ \int_{A_2} \left[(r_2 U_2 \bar{V}_2 \hat{e}_z) \mathcal{F}^2(\eta) \right] dA_2 \right. \\
 & \quad \left. + \int_{A_2} \left[\delta (U_2^2 \hat{e}_\theta - U_2 \bar{V}_2 \hat{e}_r) \eta \mathcal{F}^2(\eta) \right] dA_2 \right\} \\
 & \quad - \rho \left\{ \int_{A_4} \left[(r_4 U_4 \bar{V}_4 \hat{e}_z) \mathcal{F}^2(\eta) \right] dA_4 \right. \\
 & \quad \left. - \int_{A_4} \left[\delta (U_4^2 \hat{e}_\theta - U_4 \bar{V}_4 \hat{e}_r) \eta \mathcal{F}^2(\eta) \right] dA_4 \right\}. \tag{E.38}
 \end{aligned}$$

Examining the first integral over A_2 :

$$\begin{aligned}
 \int_{A_2} \left[(r_2 U_2 \bar{V}_2 \hat{e}_z) \mathcal{F}^2(\eta) \right] dA_2 & = \int_{-\delta}^{\delta} dz \int_0^{2\pi} r_2 d\theta \left[(r_2 U_2 \bar{V}_2 \hat{e}_z) \mathcal{F}^2(\eta) \right] \\
 & = \delta \int_{-1}^1 d\eta \cdot 2\pi r_2 \left[(r_2 U_2 \bar{V}_2 \hat{e}_z) \mathcal{F}^2(\eta) \right] \\
 & = 2\pi \delta \left[r_2 (r_2 U_2 \bar{V}_2 \hat{e}_z) \right] \int_{-1}^1 \mathcal{F}^2(\eta) d\eta. \tag{E.39}
 \end{aligned}$$

In Appendix B the integral from 0 to 1 of the velocity profile squared is defined as λ_1 . Since $\mathcal{F}^2(\eta)$ is an even function,

$$\int_{-1}^1 \mathcal{F}^2(\eta) d\eta = 2 \int_0^1 \mathcal{F}^2(\eta) d\eta = 2\lambda_1. \tag{E.40}$$

Similarly, the function $\eta \mathcal{F}^2(\eta)$ is an odd function and

$$\int_{-1}^1 \eta \mathcal{F}^2(\eta) d\eta = 0. \tag{E.41}$$

Therefore, Equation E.39 will become

$$\int_{\partial C_V} (\vec{r} \times \vec{v}) \rho \vec{v} \cdot d\vec{A} = 4\pi\rho\delta\lambda_1 (r_2^2 U_2 \bar{V}_2 - r_4^2 U_4 \bar{V}_4) \hat{e}_z. \quad (\text{E.42})$$

From the continuity equation in Appendix A, $rU = a$;

$$\int_{\partial C_V} (\vec{r} \times \vec{v}) \rho \vec{v} \cdot d\vec{A} = 4\pi\rho\delta a\lambda_1 (r_2 \bar{V}_2 - r_4 \bar{V}_4) \hat{e}_z. \quad (\text{E.43})$$

After substituting Equation E.43 into the moment of momentum relation, Equation E.26 becomes

$$\begin{aligned} \vec{T}_{shaftC_V} + \vec{T}_{surfaceC_V} &= 4\pi\rho\delta a\lambda_1 (r_o \bar{V}_o - r_i \bar{V}_i) \hat{e}_z \\ &+ \int_{C_V} \vec{r} \times [2(\vec{\omega} \times \vec{v}) + \vec{\omega} \times (\vec{\omega} \times \vec{r})] \rho dV. \end{aligned} \quad (\text{E.44})$$

E.3.2 Volume Integral Evaluation

Begin the evaluation of the volume integral term of Equation E.44 by substituting Equations E.27, E.28, and E.30 into the cross product terms. The second cross product term becomes

$$\vec{\omega} \times \vec{r} = \omega \hat{e}_z \times (r \hat{e}_r + \delta\eta \hat{e}_z) = \omega r \hat{e}_\theta, \quad (\text{E.45})$$

$$\vec{\omega} \times (\vec{\omega} \times \vec{r}) = \omega \hat{e}_z \times (\omega r \hat{e}_\theta) = -\omega^2 r \hat{e}_r, \quad (\text{E.46})$$

$$\vec{r} \times [\vec{\omega} \times (\vec{\omega} \times \vec{r})] = (r \hat{e}_r + \delta\eta \hat{e}_z) \times [-\omega^2 r \hat{e}_r] = -\omega^2 r \delta\eta \hat{e}_\theta. \quad (\text{E.47})$$

And the first cross product term is

$$\vec{\omega} \times \vec{v} = \omega \hat{e}_z \times (U \hat{e}_r + \bar{V} \hat{e}_\theta) \mathcal{F}(\eta) = \omega (U \hat{e}_\theta - \bar{V} \hat{e}_r) \mathcal{F}(\eta), \quad (\text{E.48})$$

$$\begin{aligned} \vec{r} \times [2\vec{\omega} \times \vec{v}] &= (r \hat{e}_r + \delta\eta \hat{e}_z) \times [2\omega (U \hat{e}_\theta - \bar{V} \hat{e}_r) \mathcal{F}(\eta)] \\ &= 2r\omega U \mathcal{F}(\eta) \hat{e}_z - \delta\eta\omega U \mathcal{F}(\eta) \hat{e}_r + \delta\eta\omega \bar{V} \mathcal{F}(\eta) \hat{e}_\theta \\ &= 2\omega [rU \hat{e}_z + z (\bar{V} \hat{e}_\theta - U \hat{e}_r)] \mathcal{F}(\eta). \end{aligned} \quad (\text{E.49})$$

Substituting Equation E.47 and E.49 into the volume integral;

$$\begin{aligned}
 \int_{C_V} \vec{r} \times [2(\vec{\omega} \times \vec{v}) + \vec{\omega} \times (\vec{\omega} \times \vec{r})] \rho dV &= \\
 &= \int_{C_V} \{2\omega [rU\hat{e}_z + \delta\eta (\bar{V}\hat{e}_\theta - U\hat{e}_r)] \mathcal{F}(\eta) - \omega^2 r \delta\eta \hat{e}_z\} \rho dV \\
 &= \int_{C_V} 2\omega\rho(rU) \mathcal{F}(\eta) \hat{e}_z dV + \int_{C_V} 2\omega\rho\delta\eta (\bar{V}\hat{e}_\theta - U\hat{e}_r) \mathcal{F}(\eta) dV \\
 &\quad - \int_{C_V} \rho\omega^2 r \delta\eta \hat{e}_z dV. \tag{E.50}
 \end{aligned}$$

Now, evaluate the first volume integral on the right side of Equation E.50;

$$\begin{aligned}
 \int_{C_V} 2\omega\rho(rU) \mathcal{F}(\eta) \hat{e}_z dV &= \int_{r_i}^{r_o} dr \int_0^{2\pi} r d\theta \int_{-\delta}^{\delta} dz [2\omega\rho(rU) \mathcal{F}(\eta) \hat{e}_z] \\
 &= \int_{r_i}^{r_o} dr [2\pi r (2\omega\rho(rU)) \delta \int_{-1}^1 \mathcal{F}(\eta) d\eta \hat{e}_z]. \tag{E.51}
 \end{aligned}$$

Recall the definition of the integral of $\mathcal{F}(\eta)$ from Appendix B;

$$\int_{-1}^1 \mathcal{F}(\eta) d\eta = 2 \int_0^1 \mathcal{F}(\eta) d\eta = \lambda_2. \tag{E.52}$$

Substituting this into Equation E.51 results in

$$\begin{aligned}
 \int_{C_V} 2\omega\rho(rU) \mathcal{F}(\eta) \hat{e}_z dV &= \int_{r_i}^{r_o} [4\pi\rho\delta(rU)r\omega\lambda_2] dr \hat{e}_z \\
 &= 4\pi\rho\delta a\omega\lambda_2 \int_{r_i}^{r_o} r dr \hat{e}_z \\
 &= 4\pi\rho\delta a\omega\lambda_2 (r_o^2 - r_i^2) \hat{e}_z. \tag{E.53}
 \end{aligned}$$

With the use of the relationship described in Equation E.41 the second and third volume integrals of Equation E.50 can be shown to be equal to zero.

Appendix F

Program Listing

This FORTRAN-77 program solves for the angular position, radial velocity, relative tangential velocity, and pressure at fixed incremental radii for a given system in a turbine configuration. In addition, the resulting torque of the system operating at the specified angular velocity is given. The mass flow rate is entered in as negative for inward flow; therefore, a torque output by the system will also be negative. Note, if the angular velocity specified is greater than the system can support the torque will appear to be positive indicating that torque is required as input to rotate at that speed.

The program uses a parabolic velocity profile to model laminar flow. The resulting λ -coefficients are:

- $\lambda_1 = 8/15$,
- $\lambda_2 = 2/3$, and
- $\lambda_3 = -2$.

```
C -----
C   DISKFLOW1.FOR
C
C   Program for determining fluid velocities and rotor performance for
C   flow between corotating, parallel annular disks as found in a Tesla
C   turbine or pump. The model is a closed form solution of the
C   Navier-Stokes equations with the assumptions of fully-developed,
C   incompressible, isotropic, laminar flow. Also, the assumption is
C   made that radial Reynold's number  $[A/Nu]$  is much greater than unity.
C
C -----
C
C   Jeff Allen
C   University of Dayton
C   April 10, 1990
C
C -----
C   IMPLICIT DOUBLE PRECISION (A-H,O-Z)
C   EXTERNAL FACTRL,SFJ,SFK,SFV,SFP
C
C   COMMON / GLOBAL / PI,GC
C   COMMON / FLUID / RHO,VMU,VNU
C   COMMON / ROTOR / RO,RI,DEL,ND
C   COMMON / SYSTEM / VMFR,ARAD,ADEG,WRAD,WRPM,POUT
C   COMMON / OUTPUT / PRO,TORQ,POWER
C   COMMON / EQNCONST / A,B,C,D,RC
C
C   DOUBLE PRECISION FACTRL,SFK,SFJ,SFV,SFP
C   DOUBLE PRECISION RADVEL,TANVEL,PRESSURE
C   CHARACTER FILENAME*12
C -----
C   Define universal constants.
C
C   PI = 3.1415927464
C   GC = 32.174
C
C   Input rotor parameters, fluid properties, and turbine parameters.
C
CALL INPUT
C
C   Input data file name for output.
```

```
CALL FNAME(FILENAME)

C   Calculate rotor performance and model constants.

CALL PERFORMANCE

C   Print input data and velocity constants.

CALL SYSTEMPRT(FILENAME)

C   Calculate path lines, velocities, and pressures; then print.

CALL ROTORPRT(FILENAME)

C   End of program.

END
C
C ***** SUBROUTINES *****
C
C ===== INPUT =====
C
SUBROUTINE INPUT
C
C   Subroutine for input of rotor parameters, fluid properties, and
C   turbine operating parameters in specified dimensions.
C
C   For TURBINE operation the fluid flows radial inward so the mass flow
C   rate should be entered as a negative value. Subsequently, the torque
C   that is calculated is negative since it is counter to the direction
C   of rotation. The power is positive to indicate that work is gained
C   from the system for the parameters entered.
C
C   For PUMP operation the mass flow rate should be entered as a positive
C   value. Also, the torque will be positive because it is in the same
C   direction as the rotation. The power is negative to indicate that
C   work must be supplied to the system.
C
C -----
C
IMPLICIT DOUBLE PRECISION (A-H,O-Z)
```

APPENDIX F. PROGRAM LISTING

111

```
COMMON / GLOBAL / PI,GC
COMMON / FLUID / RHO,VMU,VNU
COMMON / ROTOR / RO,RI,DEL,ND
COMMON / SYSTEM / VMFR,ARAD,ADEG,WRAD,WRPM,POUT
```

```
C -----
C   Define the pressure at the inner radius - atmospheric [gauge or absolute].
```

```
POUT = 0.
```

```
C   Read in rotor parameters.
```

```
WRITE(6,600)
READ(5,500) RO
WRITE(6,601)
READ(5,501) RI
WRITE(6,602)
READ(5,502) DEL
WRITE(6,604)
READ(5,504) ND
```

```
RO = RO/12.
RI = RI/12.
DEL = DEL/12.
```

```
500 FORMAT(E12.0)
501 FORMAT(E12.0)
502 FORMAT(E12.0)
504 FORMAT(I12)
```

```
600 FORMAT('1',/,',',3X,'ROTOR PARAMETERS:',/,
           $      /,',',5X,'Enter the outer radius of the disk [in]: ',,$)
601 FORMAT(' ',5X,'Enter the inner radius of the disk [in]: ',,$)
602 FORMAT(' ',5X,'Enter the disk half-spacing [in]: ',,$)
604 FORMAT(' ',5X,'Enter the number of disks on the rotor: ',,$)
```

```
C   Read in the fluid properties.
```

```
WRITE(6,605)
READ(5,505) RHO
WRITE(6,606)
READ(5,506) VMU
```

VNU = VMU/RHO

505 FORMAT(E12.0)

506 FORMAT(E12.0)

605 FORMAT(/, ' ', 3X, 'FLUID PROPERTIES:', /,

& /, ' ', 5X, 'Enter fluid density [lbm/ft³]: ', \$)

606 FORMAT(' ', 5X, 'Enter fluid viscosity [lbm/ft-s]: ', \$)

C Read in the operating parameters.

WRITE(6,607)

READ(5,507) WRPM

WRITE(6,608)

READ(5,508) VMFR

WRITE(6,615)

READ(5,515) ADEG

WRAD = PI*WRPM/30.

ARAD = PI*ADEG/180.

507 FORMAT(E12.0)

508 FORMAT(E12.0)

515 FORMAT(E12.0)

607 FORMAT(/, ' ', 3X, 'OPERATING PARAMETERS:', /,

& /, ' ', 5X, 'Enter the angular velocity [rpm]: ', \$)

608 FORMAT(' ', 5X, 'Enter mass flow rate [lbm/s]: ', \$)

615 FORMAT(' ', 5X, 'Enter the angle of tangency [deg]: ', \$)

RETURN

END

C

C ===== FNAME =====

C

SUBROUTINE FNAME(FILENAME)

C This subroutine asks the user for the name of the data file for
C storing the output.

C

C -----

IMPLICIT DOUBLE PRECISION (A-H,O-Z)

```
CHARACTER USRINPT*80,NAME*8,EXT*4,FILENAME*12,ANSWER*1
```

```
LOGICAL CHECK
```

```
C -----
```

```
C   Input the file name.
```

```
1000 WRITE(6,620)
```

```
READ(5,'(A)') USRINPT
```

```
620 FORMAT(/,' ',3X,'FILE NAME: ',/,
```

```
      &          /,' ',5X,'Enter name of output file w/o extension: ',,$)
```

```
C   Find the end of the file name.
```

```
I = 1
```

```
J = 0
```

```
DO WHILE (I .LE. 8)
```

```
  IF (USRINPT(I:I) .NE. ' ') THEN
```

```
    J = J + 1
```

```
  END IF
```

```
  I = I + 1
```

```
END DO
```

```
C   Assign letters to FILENAME and add extension.
```

```
READ(USRINPT(1:8),'(A8)') NAME
```

```
EXT = '.DAT'
```

```
FILENAME = NAME(1:J)//EXT
```

```
C   Check to see if file already exists.
```

```
INQUIRE(FILE=FILENAME,EXIST=CHECK)
```

```
IF (CHECK) THEN
```

```
  WRITE(6,621)
```

```
  READ(5,'(A)') USRINPT
```

```
  READ(USRINPT(1:1),'(A1)') ANSWER
```

```
  IF ((ANSWER .NE. 'Y') .AND. (ANSWER .NE. 'y')) THEN
```

```
    GOTO 1000
```

```
  END IF
```

```
END IF
```

```
621 FORMAT(//,' ',5X,'The output file already exists.',
&      /,' ',5X,'Do you wish to write another version [y/n]: ', $)
```

```
RETURN
```

```
END
```

```
C
```

```
C ===== PERFORMANCE =====
```

```
C
```

```
SUBROUTINE PERFORMANCE
```

```
C This subroutine calculates the constants for the model as well as
C the torque and power for the system.
```

```
C
```

```
C -----
```

```
IMPLICIT DOUBLE PRECISION (A-H,O-Z)
```

```
EXTERNAL FACTRL,SFJ,SFK,SFV,SFP
```

```
COMMON / GLOBAL / PI,GC
```

```
COMMON / FLUID / RHO,VMU,VNU
```

```
COMMON / ROTOR / RO,RI,DEL,ND
```

```
COMMON / SYSTEM / VMFR,ARAD,ADEG,WRAD,WRPM,POUT
```

```
COMMON / OUTPUT / PRO,TORQ,POWER
```

```
COMMON / EQNCONST / A,B,C,D,RC
```

```
DOUBLE PRECISION FACTRL,SFK,SFJ,SFV,SFP
```

```
C -----
```

```
C Calculate the radial velocity integration constant, A.
```

```
A = VMFR/(4.*PI*(ND+1)*DEL*RHO)
```

```
C Calculate radial viscosity constant, RC, and the angular constant, C.
```

```
RC = (15./8.)*VNU/(DEL*DEL*A)
```

```
C = (5./4.)*(WRAD/RC)
```

```
C Calculate the tangential velocity integration constant, B.
```

```
VOA = DABS( (A/RO)/DTAN(ARAD) )
```

```
VO = VOA - RO*WRAD
```

```
BNUM = VO*RO + C
```

```

ICODE = 100
CALL SERIES(SFV,RO,BDEN,IERR,NSUMS)
IF (IERR .EQ. 1) THEN
    CALL ERRCODE(ICODE)
ENDIF

B = BNUM/BDEN

C   Calculate the pressure integration constant, D, at the inner radius.

PTRI = PRESSURE(RI)
D = POUT - PTRI

C   Calculate the torque [ft-lbf] and power output [hp].

CALL TORQUE(TORQ)

POWER = -WRAD*TORQ/550.

C
RETURN
END
C
C ===== SYSTEMPRT =====
C
SUBROUTINE SYSTEMPRT(OUTFILE)
C
C   This subroutine prints the system parameters (rotor and turbine)
C   used in the evaluation of the rotor design.
C
C -----
IMPLICIT DOUBLE PRECISION (A-H,O-Z)
EXTERNAL FACTRL,SFJ,SFK,SFV,SFP

COMMON / GLOBAL / PI,GC
COMMON / FLUID / RHO,VMU,VNU
COMMON / ROTOR / RO,RI,DEL,ND
COMMON / SYSTEM / VMFR,ARAD,ADEG,WRAD,WRPM,POUT
COMMON / OUTPUT / PRO,TORQ,POWER
COMMON / EQNCONST / A,B,C,D,RC

```

CHARACTER OUTFILE*12

C -----

C Open output file.

OPEN(UNIT=2,FILE=OUTFILE,STATUS='NEW')

C Print file name and origin.

WRITE(6,645) OUTFILE

WRITE(2,645) OUTFILE

C Print fluid properties.

WRITE(6,647)

WRITE(6,648) RHO,VMU,VNU

WRITE(2,647)

WRITE(2,648) RHO,VMU,VNU

C Print rotor parameters.

WRITE(6,649)

WRITE(6,650) RO*12.,RI*12.,DEL*12.,ND

WRITE(2,649)

WRITE(2,650) RO*12.,RI*12.,DEL*12.,ND

C Print turbine parameters.

ADEG = 180.*ARAD/PI

PO = PRESSURE(RO)+D

WRITE(6,654)

WRITE(6,655) ADEG,VMFR,PO/144.,POUT/144.

WRITE(2,654)

WRITE(2,655) ADEG,VMFR,PO/144.,POUT/144.

C Print performance characteristics.

WRITE(6,656)

WRITE(6,657) WRAD,WRPM,TORQ*12,POWER

```
WRITE(2,656)
WRITE(2,657) WRAD,WRPM,TORQ*12,POWER
```

C Print values of constants.

```
WRITE(6,658)
WRITE(6,659) A,B,C,RC,D/144.
```

```
WRITE(2,658)
WRITE(2,659) A,B,C,RC,D/144.
```

C FORMAT statements.

```
645 FORMAT('1',///,' ',9X,A12)
647 FORMAT(///,' ',9X,'===== FLUID ==',
&
& '=====')
648 FORMAT(' ',14X,' Density [lbm/ft^3]:',1X,E12.5/,
&
& 15X,' Viscosity [lbm/ft-s]:',1X,E12.5/,
&
& 15X,'Kin.Viscosity [ft^2/s]:',1X,E12.5,/)

649 FORMAT(///,' ',9X,'===== ROTOR ==',
&
& '=====')
650 FORMAT(' ',14X,' Outer Radius [in]:',1X,F12.5/,
&
& 15X,' Inner Radius [in]:',1X,F12.5/,
&
& 15X,' Disk Spacing [in]:',1X,F12.5/,
&
& 15X,' Number of Disks:',1X,I12,/)

654 FORMAT(///,' ',9X,'===== TURBINE ==',
&
& '=====')
655 FORMAT(' ',14X,' Tangency Angle [deg]:',1X,E12.5/,
&
& 15X,' Mass Flow Rate [lbm/s]:',1X,E12.5/,
&
& 15X,' Outer Pressure [psig]:',1X,E12.5/,
&
& 15X,' Inner Pressure [psig]:',1X,E12.5,/)

656 FORMAT(///,' ',9X,'===== PERFORMANCE',
&
& '=====')
657 FORMAT(' ',14X,' Angular Velocity [1/s]:',1X,E12.5/,
&
& 15X,' [rpm]:',1X,E12.5/,
&
& 15X,' Torque [in-lbf]:',1X,E12.5/,
&
& 15X,' Power [hp]:',1X,E12.5,/)

```

```

658 FORMAT(///,' ',9X,'===== CONSTANTS ',
&
& '=====',/)
659 FORMAT(' ',14X,'          A  [ft^2/s]:',1X,E12.5/,
&          15X,'          B  [ft^2/s]:',1X,E12.5/,
&          15X,'          C  [ft^2/s]:',1X,E12.5/,
&          15X,'          Rc [1/ft^2]:',1X,E12.5/,
&          15X,'          D   [psi]:',1X,E12.5,/)

```

C

RETURN

END

C

C ===== ROTORPRT =====

C

SUBROUTINE ROTORPRT(OUTFILE)

C

C This subroutine prints the fluid pathlines, velocities, and pressures
C at various radii.

C

C -----

IMPLICIT DOUBLE PRECISION (A-H,O-Z)

EXTERNAL FACTRL,SFJ,SFK,SFV,SFP

COMMON / GLOBAL / PI,GC

COMMON / FLUID / RHO,VMU,VNU

COMMON / ROTOR / RO,RI,DEL,ND

COMMON / SYSTEM / VMFR,ARAD,ADEG,WRAD,WRPM,POUT

COMMON / OUTPUT / PRO,TORQ,POWER

COMMON / EQNCONST / A,B,C,D,RC

DOUBLE PRECISION XR(100),XT(100),U(100),V(100),P(100)

DOUBLE PRECISION R1,R2,U1,U2,V1,V2,DXR,DT,DXT

INTEGER NINT

CHARACTER OUTFILE*12

C

WRITE(6,685) OUTFILE

WRITE(2,685) OUTFILE

NINT = 20

DXR = (RO - RI)/NINT

```

I = 1
R = RO
DO WHILE (I .LE. NINT+1)
  XR(I) = R
  U(I) = RADVEL(R)
  V(I) = TANVEL(R)
  P(I) = PRESSURE(R) + D
  R = R - DXR
  I = I + 1
END DO

```

```

XT(1) = 0.
I = 1
DO WHILE (I .LE. NINT)
  R1 = XR(I)
  R2 = XR(I+1)
  U1 = U(I)
  U2 = U(I+1)
  V1 = V(I)
  V2 = V(I+1)
  CALL THETA(R1,U1,V1,R2,U2,V2,DT,DXT)
  XT(I+1) = XT(I) - DXT
  I = I + 1
END DO

```

```

I = 1
DO WHILE (I .LE. NINT+1)
  WRITE(6,686) XR(I)*12.,XT(I)*180./PI,U(I),V(I),P(I)/144.
  WRITE(2,686) XR(I)*12.,XT(I)*180./PI,U(I),V(I),P(I)/144.
  I = I + 1
END DO

```

C Close the data file.

CLOSE (UNIT=2)

C FORMAT statements.

```

685 FORMAT('1', ' ',9X,A12,////,' ',
&          9X,'=====','=====',' INTERNAL CONDITIONS ',
&          '=====','=====','=====','//',
&          10X,' R (in) ',2X,' Theta (deg)',2X,' U (ft/s) ',

```

```

&          2X,' Vbar (ft/s)',2X,' P (psig) ',/,
&          10X,'-----',2X,'-----',2X,'-----',
&          2X,'-----',2X,'-----')

```

```
686 FORMAT(' ',9X,F12.5,2X,F12.3,2X,E12.5,2X,E12.5,2X,E12.5)
```

```
RETURN
```

```
END
```

```
C
```

```
C ===== SERIES =====
```

```
C
```

```
SUBROUTINE SERIES(SF,PAR,VAL,IERR,NSUM)
```

```
C
```

```
C This subroutine sums a function SF(PAR,M) from M = 0 to MMAX or until
C the convergence criterion is met.
```

```
C
```

```
C SF := Series Function being evaluated at each increment M.
```

```
C PAR := PARAMeter being passed to the function.
```

```
C VAL := VALue of the summed series.
```

```
C NSUM := Number of SUMmations made.
```

```
C IERR := Integer ERRor code set during the summation.
```

```
C IERR = 0 := Normal completion.
```

```
C IERR = 1 := The maximum number of additions was made
```

```
C without passing the convergence criterion.
```

```
C
```

```
C The convergence criterion is for the last term calculated to be less
C than current total, VAL, multiplied by some constant, EPSLON.
```

```
C
```

```
C -----
```

```
IMPLICIT DOUBLE PRECISION (A-H,O-Z)
```

```
INTEGER IERR,L,M,MMAX,NSUM,ITEST
```

```
DOUBLE PRECISION SF,PAR,VAL,EPSLON,TERM
```

```
C -----
```

```
C Set up limits.
```

```
EPSLON = .0001
```

```
MMAX = 50
```

```
IERR = 0
```

```
ITEST = 0
```

```
C Initialize variables.
```



```

&          15X,'*',/,
&          10X,'*',48X,'*',/,
&          10X,'*****','*****','*****',
&          '*****','*****',////)

RETURN

END
C
C ***** SERIES FUNCTIONS *****
C
C This part of the program contains the functional parts of the
C infinite series for the relative tangential velocity and the pressure.
C
C FACTRL(M) := M!
C SFJ := Series Function Jm      : 1/M!
C SFK := Series Function Km      : 1/N! * 1/(M-N)!
C SFV := Series Function for V : (-R)^M * Jm * r^2M
C SFP := Series Function for P : f(R,Jm,Km,r)
C
C ===== SFV FUNCTION =====
C
DOUBLE PRECISION FUNCTION SFV(R,M)
C
C This is a recurring function that is summed from 0 to infinity. It
C is used in the evaluation of the relative tangential velocity and the
C torque.
C
C R := Radius at which the function is being evaluated.
C M := Current summation point in series.
C
C -----
IMPLICIT DOUBLE PRECISION (A-H,O-Z)

COMMON / EQNCONST / A,B,C,D,RC

INTEGER M,N
C -----

N = 2*M

SFV = ((-RC)**M) * SFJ(M) * (R**N)

```

```

END
C
C ===== SFP FUNCTION =====
C
DOUBLE PRECISION FUNCTION SFP(R,M)
C
C   The infinite series portion of the pressure formulation.
C
C R  := Radius the function is being evaluated at.
C M  := Current summation point in series.
C
C -----
IMPLICIT DOUBLE PRECISION (A-H,O-Z)

COMMON / EQNCONST / A,B,C,D,RC

INTEGER M,N
C -----

L = M + 2
N = M + 1

SFP1 = ( (-RC*R*R)**N )/(2.*N)

SFP2 = B*SFK(L) - 2.*C*(M+3)*SFJ(L)

SFP = SFP1 * SFP2

END
C
C ===== SFJ FUNCTION =====
C
DOUBLE PRECISION FUNCTION SFJ(M)
C -----
IMPLICIT DOUBLE PRECISION (A-H,O-Z)

INTEGER M
C -----

SFJ = 1./FACTRL(M)

```

```

END
C
C ===== SFK FUNCTION =====
C
DOUBLE PRECISION FUNCTION SFK(M)
C -----
IMPLICIT DOUBLE PRECISION (A-H,O-Z)

INTEGER M,N
C -----

N = 0
SFK = 0
DO WHILE (N .LE. M)
    SFK = SFK + (1./FACTRL(N))*(1./FACTRL(M-N))
    N = N + 1
END DO

END
C
C ===== FACTRL FUNCTION =====
C
DOUBLE PRECISION FUNCTION FACTRL(I)
C -----
INTEGER I,J
C -----

FACTRL = 1
J = 1
DO WHILE (J .LE. I)
    FACTRL = FACTRL*J
    J = J + 1
END DO

END
C
C ***** FLUID MODEL *****
C
C ===== RADVEL =====
C
DOUBLE PRECISION FUNCTION RADVEL(R)
C

```

C This function evaluates the radial velocity at a given radius.

C

C -----
 IMPLICIT DOUBLE PRECISION (A-H,O-Z)

COMMON / EQNCONST / A,B,C,D,RC

C -----

RADVEL = A/R

END

C

C ===== TANVEL =====

C

DOUBLE PRECISION FUNCTION TANVEL(R)

C

C This function evaluates the tangential velocity relative to the
 C rotating disk at a given radius.

C

C -----

IMPLICIT DOUBLE PRECISION (A-H,O-Z)

EXTERNAL FACTRL,SFJ,SFK,SFV,SFP

COMMON / EQNCONST / A,B,C,D,RC

DOUBLE PRECISION VS

C -----

ICODE = 500

CALL SERIES(SFV,R,VS,IERR,NSUMS)

IF (ICODE .EQ. 1) THEN

CALL ERRCODE(ICODE)

ENDIF

TANVEL = (B*VS - C)/R

END

C

C ===== PRESSURE =====

C

DOUBLE PRECISION FUNCTION PRESSURE(R)

C

APPENDIX F. PROGRAM LISTING

C This function evaluates the pressure at a given radius.

C

C -----

IMPLICIT DOUBLE PRECISION (A-H,O-Z)

EXTERNAL FACTRL,SFJ,SFK,SFV,SFP

COMMON / GLOBAL / PI,GC

COMMON / FLUID / RHO,VMU,VNU

COMMON / SYSTEM / VMFR,ARAD,ADEG,WRAD,WRPM,POUT

COMMON / EQNCONST / A,B,C,D,RC

DOUBLE PRECISION P1,P2,P3,P4,P5,P6

C -----

P1 = RHO/GC

P2 = -(8./15.)

P3 = A*A + (B-C)*(B-C)

P4 = .5*R*R + RC*DLOG(R*R)

ICODE = 600

CALL SERIES(SFP,R,P5,IERR,NSUMS)

IF (IERR .EQ. 1) THEN

CALL ERRCODE(ICODE)

ENDIF

P6 = .5*(WRAD*R)*(WRAD*R)

PRESSURE = P1*(P2*(P3*P4 + B*RC*P5) + P6)

END

C

C ===== TORQUE =====

C

SUBROUTINE TORQUE(TORK)

C

C This subroutine evaluates the total rotor torque.

C

C -----

IMPLICIT DOUBLE PRECISION (A-H,O-Z)

EXTERNAL FACTRL,SFJ,SFK,SFV,SFP

COMMON / GLOBAL / PI,GC
 COMMON / ROTOR / RO,RI,DEL,ND
 COMMON / SYSTEM / VMFR,ARAD,ADEG,WRAD,WRPM,POUT
 COMMON / EQNCONST / A,B,C,D,RC

DOUBLE PRECISION T1,T2,TORK

C -----

$T1 = (8./15.)*(VMFR/GC)$

$VO = \text{TANVEL}(RO)$

$VI = \text{TANVEL}(RI)$

$T2 = (RO*RO - RI*RI)/2.$

$TORK = T1*(RO*VO - RI*VI + 2*RC*C*T2)$

END

C

C ===== THETA =====

C

SUBROUTINE THETA(R1,U1,V1,R2,U2,V2,DTIME,DTHETA)

C

C This subroutine calculates the angular position at each radial
 C position.

C

C -----

IMPLICIT DOUBLE PRECISION (A-H,O-Z)

DOUBLE PRECISION R1,R2,U1,U2,V1,V2,DTIME,DTHETA

C -----

$DTIME = 2.*(R1 - R2)/(U1 + U2)$

$DTHETA = ((R1 - R2)/(R1*R2))*((R2*V1 + R1*V2)/(U1 + U2))$

RETURN

END

C

C ----- EOP -----

Appendix G

Data Files

The following pages contain data files that were produced by the program listed in Appendix F. What is contained in this appendix is a small sampling of the data files that were produced, but this appendix does contain the majority of the data used in the analysis presented in Chapter 7.

FLOW-100.DAT

===== FLUID =====

Density [lbm/ft^3]: 0.25000E+00
Viscosity [lbm/ft-s]: 0.12000E-04
Kin.Viscosity [ft^2/s]: 0.48000E-04

===== ROTOR =====

Outer Radius [in]: 3.00000
Inner Radius [in]: 1.00000
Disk Spacing [in]: 0.06250
Number of Disks: 0

===== TURBINE =====

Tangency Angle [deg]: 0.10000E+02
Mass Flow Rate [lbm/s]: -0.67858E-02
Outer Pressure [psig]: 0.13691E-02
Inner Pressure [psig]: 0.00000E+00

===== PERFORMANCE =====

Angular Velocity [1/s]: 0.00000E+00
 [rpm]: 0.00000E+00
Torque [in-lbf]: -0.11392E-02
Power [hp]: 0.00000E+00

===== CONSTANTS =====

A [ft^2/s]: -0.41472E+00
B [ft^2/s]: 0.14265E+01
C [ft^2/s]: 0.00000E+00
Rc [1/ft^2]: -0.80000E+01
D [psi]: 0.24990E-02

INTERNAL CONDITIONS

R (in)	Theta (deg)	U (ft/s)	Vbar (ft/s)	P (psig)
3.00000	0.000	-0.16589E+01	0.94079E+01	0.13691E-02
2.90000	10.838	-0.17161E+01	0.94185E+01	0.13130E-02
2.80000	21.700	-0.17774E+01	0.94508E+01	0.12570E-02
2.70000	32.613	-0.18432E+01	0.95059E+01	0.12008E-02
2.60000	43.603	-0.19141E+01	0.95851E+01	0.11443E-02
2.50000	54.700	-0.19906E+01	0.96900E+01	0.10874E-02
2.40000	65.934	-0.20736E+01	0.98227E+01	0.10299E-02
2.30000	77.339	-0.21637E+01	0.99856E+01	0.97161E-03
2.20000	88.951	-0.22621E+01	0.10182E+02	0.91228E-03
2.10000	100.810	-0.23698E+01	0.10415E+02	0.85171E-03
2.00000	112.963	-0.24883E+01	0.10689E+02	0.78967E-03
1.90000	125.459	-0.26193E+01	0.11011E+02	0.72588E-03
1.80000	138.357	-0.27648E+01	0.11386E+02	0.66004E-03
1.70000	151.725	-0.29274E+01	0.11824E+02	0.59179E-03
1.60000	165.641	-0.31104E+01	0.12334E+02	0.52073E-03
1.50000	180.196	-0.33177E+01	0.12932E+02	0.44637E-03
1.40000	195.503	-0.35547E+01	0.13634E+02	0.36815E-03
1.30000	211.695	-0.38282E+01	0.14464E+02	0.28537E-03
1.20000	228.941	-0.41472E+01	0.15454E+02	0.19718E-03
1.10000	247.448	-0.45242E+01	0.16644E+02	0.10251E-03
1.00000	267.486	-0.49766E+01	0.18096E+02	-0.24093E-18

FLOW-101.DAT

===== FLUID =====

Density [lbm/ft³]: 0.25000E+00
Viscosity [lbm/ft-s]: 0.12000E-04
Kin.Viscosity [ft²/s]: 0.48000E-04

===== ROTOR =====

Outer Radius [in]: 3.00000
Inner Radius [in]: 1.00000
Disk Spacing [in]: 0.06250
Number of Disks: 0

===== TURBINE =====

Tangency Angle [deg]: 0.10000E+02
Mass Flow Rate [lbm/s]: -0.33929E-02
Outer Pressure [psig]: 0.35109E-03
Inner Pressure [psig]: 0.00000E+00

===== PERFORMANCE =====

Angular Velocity [1/s]: 0.00000E+00
 [rpm]: 0.00000E+00
Torque [in-lbf]: -0.46740E-03
Power [hp]: 0.00000E+00

===== CONSTANTS =====

A [ft²/s]: -0.20736E+00
B [ft²/s]: 0.43263E+00
C [ft²/s]: 0.00000E+00
Rc [1/ft²]: -0.16000E+02
D [psi]: 0.51679E-03

===== INTERNAL CONDITIONS =====

R (in)	Theta (deg)	U (ft/s)	Vbar (ft/s)	P (psig)
3.00000	0.000	-0.82944E+00	0.47040E+01	0.35109E-03
2.90000	10.660	-0.85804E+00	0.45574E+01	0.33188E-03
2.80000	21.005	-0.88869E+00	0.44305E+01	0.31348E-03
2.70000	31.080	-0.92160E+00	0.43223E+01	0.29576E-03
2.60000	40.926	-0.95705E+00	0.42318E+01	0.27859E-03
2.50000	50.584	-0.99533E+00	0.41586E+01	0.26188E-03
2.40000	60.094	-0.10368E+01	0.41023E+01	0.24553E-03
2.30000	69.493	-0.10819E+01	0.40629E+01	0.22944E-03
2.20000	78.822	-0.11311E+01	0.40404E+01	0.21352E-03
2.10000	88.120	-0.11849E+01	0.40354E+01	0.19769E-03
2.00000	97.427	-0.12442E+01	0.40484E+01	0.18186E-03
1.90000	106.787	-0.13096E+01	0.40808E+01	0.16594E-03
1.80000	116.246	-0.13824E+01	0.41340E+01	0.14984E-03
1.70000	125.855	-0.14637E+01	0.42102E+01	0.13347E-03
1.60000	135.671	-0.15552E+01	0.43123E+01	0.11672E-03
1.50000	145.757	-0.16589E+01	0.44441E+01	0.99474E-04
1.40000	156.188	-0.17774E+01	0.46105E+01	0.81591E-04
1.30000	167.052	-0.19141E+01	0.48184E+01	0.62915E-04
1.20000	178.457	-0.20736E+01	0.50770E+01	0.43257E-04
1.10000	190.533	-0.22621E+01	0.53987E+01	0.22384E-04
1.00000	203.450	-0.24883E+01	0.58017E+01	-0.60233E-19

FLOW-102.DAT

===== FLUID =====

Density [lbm/ft³]: 0.25000E+00
Viscosity [lbm/ft-s]: 0.12000E-04
Kin.Viscosity [ft²/s]: 0.48000E-04

===== ROTOR =====

Outer Radius [in]: 3.00000
Inner Radius [in]: 1.00000
Disk Spacing [in]: 0.03125
Number of Disks: 0

===== TURBINE =====

Tangency Angle [deg]: 0.10000E+02
Mass Flow Rate [lbm/s]: -0.13572E-01
Outer Pressure [psig]: 0.21906E-01
Inner Pressure [psig]: 0.00000E+00

===== PERFORMANCE =====

Angular Velocity [1/s]: 0.00000E+00
 [rpm]: 0.00000E+00
Torque [in-lbf]: -0.91134E-02
Power [hp]: 0.00000E+00

===== CONSTANTS =====

A [ft²/s]: -0.16589E+01
B [ft²/s]: 0.57062E+01
C [ft²/s]: 0.00000E+00
Rc [1/ft²]: -0.80000E+01
D [psi]: 0.39984E-01

FLOW-102.DAT

===== INTERNAL CONDITIONS =====

R (in)	Theta (deg)	U (ft/s)	Vbar (ft/s)	P (psig)
3.00000	0.000	-0.66355E+01	0.37632E+02	0.21906E-01
2.90000	10.838	-0.68643E+01	0.37674E+02	0.21008E-01
2.80000	21.700	-0.71095E+01	0.37803E+02	0.20112E-01
2.70000	32.613	-0.73728E+01	0.38024E+02	0.19213E-01
2.60000	43.604	-0.76564E+01	0.38340E+02	0.18310E-01
2.50000	54.700	-0.79626E+01	0.38760E+02	0.17399E-01
2.40000	65.934	-0.82944E+01	0.39291E+02	0.16479E-01
2.30000	77.339	-0.86550E+01	0.39943E+02	0.15546E-01
2.20000	88.951	-0.90484E+01	0.40727E+02	0.14597E-01
2.10000	100.810	-0.94793E+01	0.41659E+02	0.13628E-01
2.00000	112.963	-0.99533E+01	0.42757E+02	0.12635E-01
1.90000	125.459	-0.10477E+02	0.44043E+02	0.11614E-01
1.80000	138.358	-0.11059E+02	0.45544E+02	0.10561E-01
1.70000	151.725	-0.11710E+02	0.47294E+02	0.94688E-02
1.60000	165.641	-0.12442E+02	0.49337E+02	0.83317E-02
1.50000	180.196	-0.13271E+02	0.51728E+02	0.71420E-02
1.40000	195.503	-0.14219E+02	0.54537E+02	0.58904E-02
1.30000	211.696	-0.15313E+02	0.57858E+02	0.45659E-02
1.20000	228.941	-0.16589E+02	0.61815E+02	0.31548E-02
1.10000	247.448	-0.18097E+02	0.66578E+02	0.16402E-02
1.00000	267.486	-0.19907E+02	0.72387E+02	-0.46259E-17

FLOW-103.DAT

===== FLUID =====

Density [lbm/ft³]: 0.25000E+00
Viscosity [lbm/ft-s]: 0.12000E-04
Kin.Viscosity [ft²/s]: 0.48000E-04

===== ROTOR =====

Outer Radius [in]: 3.00000
Inner Radius [in]: 1.00000
Disk Spacing [in]: 0.02083
Number of Disks: 0

===== TURBINE =====

Tangency Angle [deg]: 0.10000E+02
Mass Flow Rate [lbm/s]: -0.20358E-01
Outer Pressure [psig]: 0.11090E+00
Inner Pressure [psig]: 0.00000E+00

===== PERFORMANCE =====

Angular Velocity [1/s]: 0.00000E+00
 [rpm]: 0.00000E+00
Torque [in-lbf]: -0.30758E-01
Power [hp]: 0.00000E+00

===== CONSTANTS =====

A [ft²/s]: -0.37325E+01
B [ft²/s]: 0.12839E+02
C [ft²/s]: 0.00000E+00
Rc [1/ft²]: -0.80000E+01
D [psi]: 0.20242E+00

FLOW-103.DAT

===== INTERNAL CONDITIONS =====

R (in)	Theta (deg)	U (ft/s)	Vbar (ft/s)	P (psig)
3.00000	0.000	-0.14930E+02	0.84672E+02	0.11090E+00
2.90000	10.838	-0.15445E+02	0.84767E+02	0.10636E+00
2.80000	21.700	-0.15996E+02	0.85057E+02	0.10181E+00
2.70000	32.613	-0.16589E+02	0.85553E+02	0.97265E-01
2.60000	43.604	-0.17227E+02	0.86266E+02	0.92692E-01
2.50000	54.700	-0.17916E+02	0.87211E+02	0.88084E-01
2.40000	65.934	-0.18662E+02	0.88405E+02	0.83425E-01
2.30000	77.339	-0.19474E+02	0.89871E+02	0.78701E-01
2.20000	88.951	-0.20359E+02	0.91636E+02	0.73895E-01
2.10000	100.810	-0.21328E+02	0.93734E+02	0.68989E-01
2.00000	112.963	-0.22395E+02	0.96204E+02	0.63964E-01
1.90000	125.459	-0.23574E+02	0.99097E+02	0.58797E-01
1.80000	138.358	-0.24883E+02	0.10247E+03	0.53464E-01
1.70000	151.725	-0.26347E+02	0.10641E+03	0.47936E-01
1.60000	165.641	-0.27994E+02	0.11101E+03	0.42179E-01
1.50000	180.196	-0.29860E+02	0.11639E+03	0.36156E-01
1.40000	195.503	-0.31993E+02	0.12271E+03	0.29820E-01
1.30000	211.696	-0.34454E+02	0.13018E+03	0.23115E-01
1.20000	228.941	-0.37325E+02	0.13908E+03	0.15971E-01
1.10000	247.448	-0.40718E+02	0.14980E+03	0.83034E-02
1.00000	267.486	-0.44790E+02	0.16287E+03	-0.24672E-16

FLOW-104.DAT

===== FLUID =====

Density [lbm/ft³]: 0.25000E+00
Viscosity [lbm/ft-s]: 0.12000E-04
Kin.Viscosity [ft²/s]: 0.48000E-04

===== ROTOR =====

Outer Radius [in]: 3.00000
Inner Radius [in]: 1.00000
Disk Spacing [in]: 0.01563
Number of Disks: 0

===== TURBINE =====

Tangency Angle [deg]: 0.10000E+02
Mass Flow Rate [lbm/s]: -0.27143E-01
Outer Pressure [psig]: 0.35050E+00
Inner Pressure [psig]: 0.00000E+00

===== PERFORMANCE =====

Angular Velocity [1/s]: 0.00000E+00
 [rpm]: 0.00000E+00
Torque [in-lbf]: -0.72907E-01
Power [hp]: 0.00000E+00

===== CONSTANTS =====

A [ft²/s]: -0.66355E+01
B [ft²/s]: 0.22825E+02
C [ft²/s]: 0.00000E+00
Rc [1/ft²]: -0.80000E+01
D [psi]: 0.63975E+00

===== INTERNAL CONDITIONS =====

R (in)	Theta (deg)	U (ft/s)	Vbar (ft/s)	P (psig)
3.00000	0.000	-0.26542E+02	0.15053E+03	0.35050E+00
2.90000	10.838	-0.27457E+02	0.15070E+03	0.33614E+00
2.80000	21.700	-0.28438E+02	0.15121E+03	0.32178E+00
2.70000	32.613	-0.29491E+02	0.15209E+03	0.30740E+00
2.60000	43.604	-0.30626E+02	0.15336E+03	0.29295E+00
2.50000	54.700	-0.31851E+02	0.15504E+03	0.27839E+00
2.40000	65.934	-0.33178E+02	0.15716E+03	0.26367E+00
2.30000	77.339	-0.34620E+02	0.15977E+03	0.24874E+00
2.20000	88.951	-0.36194E+02	0.16291E+03	0.23355E+00
2.10000	100.811	-0.37917E+02	0.16664E+03	0.21804E+00
2.00000	112.963	-0.39813E+02	0.17103E+03	0.20216E+00
1.90000	125.459	-0.41909E+02	0.17617E+03	0.18583E+00
1.80000	138.358	-0.44237E+02	0.18218E+03	0.16897E+00
1.70000	151.725	-0.46839E+02	0.18918E+03	0.15150E+00
1.60000	165.641	-0.49766E+02	0.19735E+03	0.13331E+00
1.50000	180.196	-0.53084E+02	0.20691E+03	0.11427E+00
1.40000	195.503	-0.56876E+02	0.21815E+03	0.94247E-01
1.30000	211.696	-0.61251E+02	0.23143E+03	0.73055E-01
1.20000	228.941	-0.66355E+02	0.24726E+03	0.50478E-01
1.10000	247.448	-0.72388E+02	0.26631E+03	0.26243E-01
1.00000	267.487	-0.79626E+02	0.28955E+03	-0.74015E-16

FLOW-105.DAT

===== FLUID =====

Density [lbm/ft³]: 0.25000E+00
Viscosity [lbm/ft-s]: 0.12000E-04
Kin.Viscosity [ft²/s]: 0.48000E-04

===== ROTOR =====

Outer Radius [in]: 3.00000
Inner Radius [in]: 1.00000
Disk Spacing [in]: 0.01250
Number of Disks: 0

===== TURBINE =====

Tangency Angle [deg]: 0.10000E+02
Mass Flow Rate [lbm/s]: -0.33929E-01
Outer Pressure [psig]: 0.85571E+00
Inner Pressure [psig]: 0.00000E+00

===== PERFORMANCE =====

Angular Velocity [1/s]: 0.00000E+00
[rpm]: 0.00000E+00
Torque [in-lbf]: -0.14240E+00
Power [hp]: 0.00000E+00

===== CONSTANTS =====

A [ft²/s]: -0.10368E+02
B [ft²/s]: 0.35664E+02
C [ft²/s]: 0.00000E+00
Rc [1/ft²]: -0.80000E+01
D [psi]: 0.15619E+01

FLOW-105.DAT

===== INTERNAL CONDITIONS =====

R (in)	Theta (deg)	U (ft/s)	Vbar (ft/s)	P (psig)
3.00000	0.000	-0.41472E+02	0.23520E+03	0.85571E+00
2.90000	10.838	-0.42902E+02	0.23546E+03	0.82064E+00
2.80000	21.700	-0.44434E+02	0.23627E+03	0.78561E+00
2.70000	32.613	-0.46080E+02	0.23765E+03	0.75050E+00
2.60000	43.604	-0.47852E+02	0.23963E+03	0.71522E+00
2.50000	54.700	-0.49766E+02	0.24225E+03	0.67966E+00
2.40000	65.934	-0.51840E+02	0.24557E+03	0.64371E+00
2.30000	77.339	-0.54094E+02	0.24964E+03	0.60726E+00
2.20000	88.951	-0.56553E+02	0.25455E+03	0.57018E+00
2.10000	100.810	-0.59246E+02	0.26037E+03	0.53232E+00
2.00000	112.963	-0.62208E+02	0.26723E+03	0.49355E+00
1.90000	125.459	-0.65482E+02	0.27527E+03	0.45368E+00
1.80000	138.358	-0.69120E+02	0.28465E+03	0.41253E+00
1.70000	151.725	-0.73186E+02	0.29559E+03	0.36987E+00
1.60000	165.641	-0.77760E+02	0.30836E+03	0.32546E+00
1.50000	180.196	-0.82944E+02	0.32330E+03	0.27898E+00
1.40000	195.503	-0.88869E+02	0.34086E+03	0.23009E+00
1.30000	211.696	-0.95705E+02	0.36161E+03	0.17836E+00
1.20000	228.941	-0.10368E+03	0.38634E+03	0.12324E+00
1.10000	247.448	-0.11311E+03	0.41611E+03	0.64069E-01
1.00000	267.486	-0.12442E+03	0.45242E+03	-0.22204E-15

FLOW-106.DAT

===== FLUID =====

Density [lbm/ft³]: 0.25000E+00
Viscosity [lbm/ft-s]: 0.12000E-04
Kin.Viscosity [ft²/s]: 0.48000E-04

===== ROTOR =====

Outer Radius [in]: 3.00000
Inner Radius [in]: 1.00000
Disk Spacing [in]: 0.03125
Number of Disks: 0

===== TURBINE =====

Tangency Angle [deg]: 0.10000E+02
Mass Flow Rate [lbm/s]: -0.67858E-02
Outer Pressure [psig]: 0.56175E-02
Inner Pressure [psig]: 0.00000E+00

===== PERFORMANCE =====

Angular Velocity [1/s]: 0.00000E+00
 [rpm]: 0.00000E+00
Torque [in-lbf]: -0.37392E-02
Power [hp]: 0.00000E+00

===== CONSTANTS =====

A [ft²/s]: -0.82944E+00
B [ft²/s]: 0.17305E+01
C [ft²/s]: 0.00000E+00
Rc [1/ft²]: -0.16000E+02
D [psi]: 0.82687E-02

===== INTERNAL CONDITIONS =====

R (in)	Theta (deg)	U (ft/s)	Vbar (ft/s)	P (psig)
3.00000	0.000	-0.33178E+01	0.18816E+02	0.56175E-02
2.90000	10.660	-0.34322E+01	0.18230E+02	0.53102E-02
2.80000	21.005	-0.35547E+01	0.17722E+02	0.50157E-02
2.70000	31.080	-0.36864E+01	0.17289E+02	0.47321E-02
2.60000	40.926	-0.38282E+01	0.16927E+02	0.44575E-02
2.50000	50.584	-0.39813E+01	0.16634E+02	0.41901E-02
2.40000	60.094	-0.41472E+01	0.16409E+02	0.39284E-02
2.30000	69.493	-0.43275E+01	0.16252E+02	0.36710E-02
2.20000	78.822	-0.45242E+01	0.16162E+02	0.34163E-02
2.10000	88.120	-0.47397E+01	0.16141E+02	0.31630E-02
2.00000	97.427	-0.49766E+01	0.16194E+02	0.29097E-02
1.90000	106.787	-0.52386E+01	0.16323E+02	0.26550E-02
1.80000	116.246	-0.55296E+01	0.16536E+02	0.23975E-02
1.70000	125.855	-0.58549E+01	0.16841E+02	0.21356E-02
1.60000	135.671	-0.62208E+01	0.17249E+02	0.18676E-02
1.50000	145.757	-0.66355E+01	0.17776E+02	0.15916E-02
1.40000	156.188	-0.71095E+01	0.18442E+02	0.13055E-02
1.30000	167.052	-0.76564E+01	0.19274E+02	0.10066E-02
1.20000	178.457	-0.82944E+01	0.20308E+02	0.69212E-03
1.10000	190.533	-0.90484E+01	0.21595E+02	0.35814E-03
1.00000	203.450	-0.99533E+01	0.23207E+02	-0.96374E-18

FLOW-107.DAT

===== FLUID =====

Density [lbm/ft³]: 0.25000E+00
Viscosity [lbm/ft-s]: 0.12000E-04
Kin.Viscosity [ft²/s]: 0.48000E-04

===== ROTOR =====

Outer Radius [in]: 3.00000
Inner Radius [in]: 1.00000
Disk Spacing [in]: 0.02083
Number of Disks: 0

===== TURBINE =====

Tangency Angle [deg]: 0.10000E+02
Mass Flow Rate [lbm/s]: -0.10179E-01
Outer Pressure [psig]: 0.28439E-01
Inner Pressure [psig]: 0.00000E+00

===== PERFORMANCE =====

Angular Velocity [1/s]: 0.00000E+00
 [rpm]: 0.00000E+00
Torque [in-lbf]: -0.12620E-01
Power [hp]: 0.00000E+00

===== CONSTANTS =====

A [ft²/s]: -0.18662E+01
B [ft²/s]: 0.38937E+01
C [ft²/s]: 0.00000E+00
Rc [1/ft²]: -0.16000E+02
D [psi]: 0.41860E-01

===== INTERNAL CONDITIONS =====				
R (in)	Theta (deg)	U (ft/s)	Vbar (ft/s)	P (psig)
3.00000	0.000	-0.74650E+01	0.42336E+02	0.28439E-01
2.90000	10.660	-0.77224E+01	0.41017E+02	0.26883E-01
2.80000	21.005	-0.79982E+01	0.39875E+02	0.25392E-01
2.70000	31.080	-0.82944E+01	0.38900E+02	0.23956E-01
2.60000	40.926	-0.86134E+01	0.38086E+02	0.22566E-01
2.50000	50.584	-0.89580E+01	0.37427E+02	0.21213E-01
2.40000	60.094	-0.93312E+01	0.36921E+02	0.19888E-01
2.30000	69.493	-0.97369E+01	0.36566E+02	0.18584E-01
2.20000	78.822	-0.10180E+02	0.36364E+02	0.17295E-01
2.10000	88.120	-0.10664E+02	0.36318E+02	0.16013E-01
2.00000	97.427	-0.11197E+02	0.36436E+02	0.14730E-01
1.90000	106.787	-0.11787E+02	0.36727E+02	0.13441E-01
1.80000	116.246	-0.12442E+02	0.37206E+02	0.12137E-01
1.70000	125.855	-0.13173E+02	0.37892E+02	0.10811E-01
1.60000	135.671	-0.13997E+02	0.38811E+02	0.94546E-02
1.50000	145.757	-0.14930E+02	0.39997E+02	0.80574E-02
1.40000	156.188	-0.15996E+02	0.41495E+02	0.66089E-02
1.30000	167.052	-0.17227E+02	0.43366E+02	0.50962E-02
1.20000	178.457	-0.18662E+02	0.45693E+02	0.35039E-02
1.10000	190.533	-0.20359E+02	0.48589E+02	0.18131E-02
1.00000	203.450	-0.22395E+02	0.52215E+02	-0.53969E-17

FLOW-108.DAT

===== FLUID =====

Density [lbm/ft³]: 0.25000E+00
Viscosity [lbm/ft-s]: 0.12000E-04
Kin.Viscosity [ft²/s]: 0.48000E-04

===== ROTOR =====

Outer Radius [in]: 3.00000
Inner Radius [in]: 1.00000
Disk Spacing [in]: 0.01563
Number of Disks: 0

===== TURBINE =====

Tangency Angle [deg]: 0.10000E+02
Mass Flow Rate [lbm/s]: -0.13572E-01
Outer Pressure [psig]: 0.89880E-01
Inner Pressure [psig]: 0.00000E+00

===== PERFORMANCE =====

Angular Velocity [1/s]: 0.00000E+00
 [rpm]: 0.00000E+00
Torque [in-lbf]: -0.29913E-01
Power [hp]: 0.00000E+00

===== CONSTANTS =====

A [ft²/s]: -0.33178E+01
B [ft²/s]: 0.69221E+01
C [ft²/s]: 0.00000E+00
Rc [1/ft²]: -0.16000E+02
D [psi]: 0.13230E+00

===== INTERNAL CONDITIONS =====				
R (in)	Theta (deg)	U (ft/s)	Vbar (ft/s)	P (psig)
3.00000	0.000	-0.13271E+02	0.75264E+02	0.89880E-01
2.90000	10.660	-0.13729E+02	0.72919E+02	0.84963E-01
2.80000	21.005	-0.14219E+02	0.70889E+02	0.80252E-01
2.70000	31.080	-0.14746E+02	0.69156E+02	0.75714E-01
2.60000	40.926	-0.15313E+02	0.67709E+02	0.71320E-01
2.50000	50.584	-0.15925E+02	0.66538E+02	0.67042E-01
2.40000	60.094	-0.16589E+02	0.65638E+02	0.62855E-01
2.30000	69.493	-0.17310E+02	0.65007E+02	0.58736E-01
2.20000	78.822	-0.18097E+02	0.64647E+02	0.54660E-01
2.10000	88.120	-0.18959E+02	0.64566E+02	0.50608E-01
2.00000	97.427	-0.19907E+02	0.64775E+02	0.46555E-01
1.90000	106.787	-0.20954E+02	0.65293E+02	0.42480E-01
1.80000	116.246	-0.22118E+02	0.66144E+02	0.38360E-01
1.70000	125.855	-0.23420E+02	0.67364E+02	0.34169E-01
1.60000	135.671	-0.24883E+02	0.68997E+02	0.29881E-01
1.50000	145.757	-0.26542E+02	0.71105E+02	0.25465E-01
1.40000	156.188	-0.28438E+02	0.73768E+02	0.20887E-01
1.30000	167.052	-0.30626E+02	0.77095E+02	0.16106E-01
1.20000	178.457	-0.33178E+02	0.81231E+02	0.11074E-01
1.10000	190.533	-0.36194E+02	0.86380E+02	0.57303E-02
1.00000	203.450	-0.39813E+02	0.92827E+02	-0.12336E-16

FLOW-109.DAT

===== FLUID =====

Density [lbm/ft³]: 0.25000E+00
Viscosity [lbm/ft-s]: 0.12000E-04
Kin.Viscosity [ft²/s]: 0.48000E-04

===== ROTOR =====

Outer Radius [in]: 3.00000
Inner Radius [in]: 1.00000
Disk Spacing [in]: 0.01250
Number of Disks: 0

===== TURBINE =====

Tangency Angle [deg]: 0.10000E+02
Mass Flow Rate [lbm/s]: -0.16965E-01
Outer Pressure [psig]: 0.21943E+00
Inner Pressure [psig]: 0.00000E+00

===== PERFORMANCE =====

Angular Velocity [1/s]: 0.00000E+00
 [rpm]: 0.00000E+00
Torque [in-lbf]: -0.58424E-01
Power [hp]: 0.00000E+00

===== CONSTANTS =====

A [ft²/s]: -0.51840E+01
B [ft²/s]: 0.10816E+02
C [ft²/s]: 0.00000E+00
Rc [1/ft²]: -0.16000E+02
D [psi]: 0.32299E+00

FLOW-109.DAT

===== INTERNAL CONDITIONS =====

R (in)	Theta (deg)	U (ft/s)	Vbar (ft/s)	P (psig)
3.00000	0.000	-0.20736E+02	0.11760E+03	0.21943E+00
2.90000	10.660	-0.21451E+02	0.11394E+03	0.20743E+00
2.80000	21.005	-0.22217E+02	0.11076E+03	0.19593E+00
2.70000	31.080	-0.23040E+02	0.10806E+03	0.18485E+00
2.60000	40.926	-0.23926E+02	0.10580E+03	0.17412E+00
2.50000	50.584	-0.24883E+02	0.10396E+03	0.16368E+00
2.40000	60.094	-0.25920E+02	0.10256E+03	0.15345E+00
2.30000	69.493	-0.27047E+02	0.10157E+03	0.14340E+00
2.20000	78.822	-0.28276E+02	0.10101E+03	0.13345E+00
2.10000	88.120	-0.29623E+02	0.10088E+03	0.12355E+00
2.00000	97.427	-0.31104E+02	0.10121E+03	0.11366E+00
1.90000	106.787	-0.32741E+02	0.10202E+03	0.10371E+00
1.80000	116.246	-0.34560E+02	0.10335E+03	0.93652E-01
1.70000	125.855	-0.36593E+02	0.10526E+03	0.83421E-01
1.60000	135.671	-0.38880E+02	0.10781E+03	0.72952E-01
1.50000	145.757	-0.41472E+02	0.11110E+03	0.62171E-01
1.40000	156.188	-0.44434E+02	0.11526E+03	0.50994E-01
1.30000	167.052	-0.47852E+02	0.12046E+03	0.39322E-01
1.20000	178.457	-0.51840E+02	0.12692E+03	0.27036E-01
1.10000	190.533	-0.56553E+02	0.13497E+03	0.13990E-01
1.00000	203.450	-0.62208E+02	0.14504E+03	-0.43175E-16

FLOW-110.DAT

===== FLUID =====

Density [lbm/ft³]: 0.25000E+00
Viscosity [lbm/ft-s]: 0.12000E-04
Kin.Viscosity [ft²/s]: 0.48000E-04

===== ROTOR =====

Outer Radius [in]: 3.00000
Inner Radius [in]: 1.00000
Disk Spacing [in]: 0.06250
Number of Disks: 0

===== TURBINE =====

Tangency Angle [deg]: 0.10000E+02
Mass Flow Rate [lbm/s]: -0.13572E-01
Outer Pressure [psig]: 0.39354E-02
Inner Pressure [psig]: 0.00000E+00

===== PERFORMANCE =====

Angular Velocity [1/s]: 0.00000E+00
 [rpm]: 0.00000E+00
Torque [in-lbf]: -0.25305E-02
Power [hp]: 0.00000E+00

===== CONSTANTS =====

A [ft²/s]: -0.82944E+00
B [ft²/s]: 0.36635E+01
C [ft²/s]: 0.00000E+00
Rc [1/ft²]: -0.40000E+01
D [psi]: 0.80298E-02

===== INTERNAL CONDITIONS =====				
R (in)	Theta (deg)	U (ft/s)	Vbar (ft/s)	P (psig)
3.00000	0.000	-0.33178E+01	0.18816E+02	0.39354E-02
2.90000	10.929	-0.34322E+01	0.19148E+02	0.37961E-02
2.80000	22.060	-0.35547E+01	0.19521E+02	0.36543E-02
2.70000	33.419	-0.36864E+01	0.19937E+02	0.35097E-02
2.60000	45.032	-0.38282E+01	0.20401E+02	0.33618E-02
2.50000	56.928	-0.39813E+01	0.20919E+02	0.32104E-02
2.40000	69.139	-0.41472E+01	0.21496E+02	0.30549E-02
2.30000	81.702	-0.43275E+01	0.22139E+02	0.28949E-02
2.20000	94.658	-0.45242E+01	0.22858E+02	0.27299E-02
2.10000	108.053	-0.47397E+01	0.23662E+02	0.25592E-02
2.00000	121.940	-0.49766E+01	0.24564E+02	0.23823E-02
1.90000	136.379	-0.52386E+01	0.25578E+02	0.21982E-02
1.80000	151.442	-0.55296E+01	0.26723E+02	0.20062E-02
1.70000	167.209	-0.58549E+01	0.28021E+02	0.18051E-02
1.60000	183.778	-0.62208E+01	0.29501E+02	0.15937E-02
1.50000	201.265	-0.66355E+01	0.31198E+02	0.13706E-02
1.40000	219.807	-0.71095E+01	0.33158E+02	0.11340E-02
1.30000	239.577	-0.76564E+01	0.35442E+02	0.88163E-03
1.20000	260.783	-0.82944E+01	0.38130E+02	0.61093E-03
1.10000	283.694	-0.90484E+01	0.41331E+02	0.31850E-03
1.00000	308.653	-0.99533E+01	0.45200E+02	-0.77099E-18

FLOW-111.DAT

===== FLUID =====

Density [lbm/ft³]: 0.25000E+00
Viscosity [lbm/ft-s]: 0.12000E-04
Kin.Viscosity [ft²/s]: 0.48000E-04

===== ROTOR =====

Outer Radius [in]: 3.00000
Inner Radius [in]: 1.00000
Disk Spacing [in]: 0.03125
Number of Disks: 0

===== TURBINE =====

Tangency Angle [deg]: 0.10000E+02
Mass Flow Rate [lbm/s]: -0.27143E-01
Outer Pressure [psig]: 0.62966E-01
Inner Pressure [psig]: 0.00000E+00

===== PERFORMANCE =====

Angular Velocity [1/s]: 0.00000E+00
 [rpm]: 0.00000E+00
Torque [in-lbf]: -0.20244E-01
Power [hp]: 0.00000E+00

===== CONSTANTS =====

A [ft²/s]: -0.33178E+01
B [ft²/s]: 0.14654E+02
C [ft²/s]: 0.00000E+00
Rc [1/ft²]: -0.40000E+01
D [psi]: 0.12848E+00

===== INTERNAL CONDITIONS =====				
R (in)	Theta (deg)	U (ft/s)	Vbar (ft/s)	P (psig)
3.00000	0.000	-0.13271E+02	0.75264E+02	0.62966E-01
2.90000	10.929	-0.13729E+02	0.76593E+02	0.60738E-01
2.80000	22.060	-0.14219E+02	0.78083E+02	0.58469E-01
2.70000	33.419	-0.14746E+02	0.79747E+02	0.56155E-01
2.60000	45.032	-0.15313E+02	0.81604E+02	0.53789E-01
2.50000	56.928	-0.15925E+02	0.83674E+02	0.51366E-01
2.40000	69.139	-0.16589E+02	0.85982E+02	0.48878E-01
2.30000	81.702	-0.17310E+02	0.88557E+02	0.46318E-01
2.20000	94.658	-0.18097E+02	0.91432E+02	0.43678E-01
2.10000	108.053	-0.18959E+02	0.94649E+02	0.40948E-01
2.00000	121.940	-0.19907E+02	0.98256E+02	0.38116E-01
1.90000	136.379	-0.20954E+02	0.10231E+03	0.35172E-01
1.80000	151.442	-0.22118E+02	0.10689E+03	0.32099E-01
1.70000	167.209	-0.23419E+02	0.11209E+03	0.28882E-01
1.60000	183.778	-0.24883E+02	0.11800E+03	0.25500E-01
1.50000	201.265	-0.26542E+02	0.12479E+03	0.21930E-01
1.40000	219.807	-0.28438E+02	0.13263E+03	0.18143E-01
1.30000	239.577	-0.30625E+02	0.14177E+03	0.14106E-01
1.20000	260.783	-0.33178E+02	0.15252E+03	0.97749E-02
1.10000	283.694	-0.36194E+02	0.16532E+03	0.50960E-02
1.00000	308.653	-0.39813E+02	0.18080E+03	-0.12336E-16

FLOW-112.DAT

===== FLUID =====

Density [lbm/ft³]: 0.25000E+00
Viscosity [lbm/ft-s]: 0.12000E-04
Kin.Viscosity [ft²/s]: 0.48000E-04

===== ROTOR =====

Outer Radius [in]: 3.00000
Inner Radius [in]: 1.00000
Disk Spacing [in]: 0.02083
Number of Disks: 0

===== TURBINE =====

Tangency Angle [deg]: 0.10000E+02
Mass Flow Rate [lbm/s]: -0.40715E-01
Outer Pressure [psig]: 0.31876E+00
Inner Pressure [psig]: 0.00000E+00

===== PERFORMANCE =====

Angular Velocity [1/s]: 0.00000E+00
 [rpm]: 0.00000E+00
Torque [in-lbf]: -0.68323E-01
Power [hp]: 0.00000E+00

===== CONSTANTS =====

A [ft²/s]: -0.74650E+01
B [ft²/s]: 0.32971E+02
C [ft²/s]: 0.00000E+00
Rc [1/ft²]: -0.40000E+01
D [psi]: 0.65042E+00

===== INTERNAL CONDITIONS =====				
R (in)	Theta (deg)	U (ft/s)	Vbar (ft/s)	P (psig)
3.00000	0.000	-0.29860E+02	0.16934E+03	0.31876E+00
2.90000	10.929	-0.30890E+02	0.17233E+03	0.30749E+00
2.80000	22.060	-0.31993E+02	0.17569E+03	0.29600E+00
2.70000	33.419	-0.33178E+02	0.17943E+03	0.28429E+00
2.60000	45.032	-0.34454E+02	0.18361E+03	0.27231E+00
2.50000	56.928	-0.35832E+02	0.18827E+03	0.26004E+00
2.40000	69.139	-0.37325E+02	0.19346E+03	0.24745E+00
2.30000	81.702	-0.38948E+02	0.19925E+03	0.23449E+00
2.20000	94.658	-0.40718E+02	0.20572E+03	0.22112E+00
2.10000	108.053	-0.42657E+02	0.21296E+03	0.20730E+00
2.00000	121.940	-0.44790E+02	0.22108E+03	0.19296E+00
1.90000	136.379	-0.47147E+02	0.23020E+03	0.17806E+00
1.80000	151.442	-0.49766E+02	0.24051E+03	0.16250E+00
1.70000	167.209	-0.52694E+02	0.25219E+03	0.14621E+00
1.60000	183.778	-0.55987E+02	0.26551E+03	0.12909E+00
1.50000	201.265	-0.59720E+02	0.28078E+03	0.11102E+00
1.40000	219.807	-0.63985E+02	0.29842E+03	0.91851E-01
1.30000	239.577	-0.68907E+02	0.31898E+03	0.71412E-01
1.20000	260.783	-0.74650E+02	0.34317E+03	0.49486E-01
1.10000	283.694	-0.81436E+02	0.37198E+03	0.25799E-01
1.00000	308.653	-0.89580E+02	0.40680E+03	-0.86351E-16

FLOW-113.DAT

===== FLUID =====

Density [lbm/ft³]: 0.25000E+00
Viscosity [lbm/ft-s]: 0.12000E-04
Kin.Viscosity [ft²/s]: 0.48000E-04

===== ROTOR =====

Outer Radius [in]: 3.00000
Inner Radius [in]: 1.00000
Disk Spacing [in]: 0.01563
Number of Disks: 0

===== TURBINE =====

Tangency Angle [deg]: 0.10000E+02
Mass Flow Rate [lbm/s]: -0.54287E-01
Outer Pressure [psig]: 0.10075E+01
Inner Pressure [psig]: 0.00000E+00

===== PERFORMANCE =====

Angular Velocity [1/s]: 0.00000E+00
 [rpm]: 0.00000E+00
Torque [in-lbf]: -0.16195E+00
Power [hp]: 0.00000E+00

===== CONSTANTS =====

A [ft²/s]: -0.13271E+02
B [ft²/s]: 0.58616E+02
C [ft²/s]: 0.00000E+00
Rc [1/ft²]: -0.40000E+01
D [psi]: 0.20556E+01

===== INTERNAL CONDITIONS =====				
R (in)	Theta (deg)	U (ft/s)	Vbar (ft/s)	P (psig)
3.00000	0.000	-0.53084E+02	0.30106E+03	0.10075E+01
2.90000	10.929	-0.54915E+02	0.30637E+03	0.97181E+00
2.80000	22.060	-0.56876E+02	0.31233E+03	0.93551E+00
2.70000	33.419	-0.58982E+02	0.31899E+03	0.89848E+00
2.60000	45.032	-0.61251E+02	0.32642E+03	0.86063E+00
2.50000	56.928	-0.63701E+02	0.33470E+03	0.82185E+00
2.40000	69.139	-0.66355E+02	0.34393E+03	0.78205E+00
2.30000	81.702	-0.69240E+02	0.35423E+03	0.74109E+00
2.20000	94.658	-0.72387E+02	0.36573E+03	0.69885E+00
2.10000	108.053	-0.75835E+02	0.37860E+03	0.65516E+00
2.00000	121.940	-0.79626E+02	0.39302E+03	0.60986E+00
1.90000	136.379	-0.83817E+02	0.40925E+03	0.56275E+00
1.80000	151.442	-0.88474E+02	0.42757E+03	0.51358E+00
1.70000	167.209	-0.93678E+02	0.44834E+03	0.46210E+00
1.60000	183.778	-0.99533E+02	0.47202E+03	0.40800E+00
1.50000	201.265	-0.10617E+03	0.49917E+03	0.35088E+00
1.40000	219.807	-0.11375E+03	0.53053E+03	0.29029E+00
1.30000	239.577	-0.12250E+03	0.56707E+03	0.22570E+00
1.20000	260.783	-0.13271E+03	0.61008E+03	0.15640E+00
1.10000	283.694	-0.14477E+03	0.66130E+03	0.81536E-01
1.00000	308.653	-0.15925E+03	0.72320E+03	-0.19737E-15

FLOW-114.DAT

===== FLUID =====

Density [lbm/ft³]: 0.25000E+00
Viscosity [lbm/ft-s]: 0.12000E-04
Kin.Viscosity [ft²/s]: 0.48000E-04

===== ROTOR =====

Outer Radius [in]: 3.00000
Inner Radius [in]: 1.00000
Disk Spacing [in]: 0.01250
Number of Disks: 0

===== TURBINE =====

Tangency Angle [deg]: 0.10000E+02
Mass Flow Rate [lbm/s]: -0.67858E-01
Outer Pressure [psig]: 0.24596E+01
Inner Pressure [psig]: 0.00000E+00

===== PERFORMANCE =====

Angular Velocity [1/s]: 0.00000E+00
 [rpm]: 0.00000E+00
Torque [in-lbf]: -0.31631E+00
Power [hp]: 0.00000E+00

===== CONSTANTS =====

A [ft²/s]: -0.20736E+02
B [ft²/s]: 0.91587E+02
C [ft²/s]: 0.00000E+00
Rc [1/ft²]: -0.40000E+01
D [psi]: 0.50186E+01

===== INTERNAL CONDITIONS =====				
R (in)	Theta (deg)	U (ft/s)	Vbar (ft/s)	P (psig)
3.00000	0.000	-0.82944E+02	0.47040E+03	0.24596E+01
2.90000	10.929	-0.85804E+02	0.47871E+03	0.23726E+01
2.80000	22.060	-0.88869E+02	0.48802E+03	0.22840E+01
2.70000	33.419	-0.92160E+02	0.49842E+03	0.21936E+01
2.60000	45.032	-0.95705E+02	0.51002E+03	0.21011E+01
2.50000	56.928	-0.99533E+02	0.52296E+03	0.20065E+01
2.40000	69.139	-0.10368E+03	0.53739E+03	0.19093E+01
2.30000	81.702	-0.10819E+03	0.55348E+03	0.18093E+01
2.20000	94.658	-0.11311E+03	0.57145E+03	0.17062E+01
2.10000	108.053	-0.11849E+03	0.59156E+03	0.15995E+01
2.00000	121.940	-0.12442E+03	0.61410E+03	0.14889E+01
1.90000	136.379	-0.13096E+03	0.63946E+03	0.13739E+01
1.80000	151.442	-0.13824E+03	0.66808E+03	0.12539E+01
1.70000	167.209	-0.14637E+03	0.70053E+03	0.11282E+01
1.60000	183.778	-0.15552E+03	0.73752E+03	0.99608E+00
1.50000	201.265	-0.16589E+03	0.77995E+03	0.85663E+00
1.40000	219.807	-0.17774E+03	0.82895E+03	0.70873E+00
1.30000	239.577	-0.19141E+03	0.88605E+03	0.55102E+00
1.20000	260.783	-0.20736E+03	0.95324E+03	0.38183E+00
1.10000	283.694	-0.22621E+03	0.10333E+04	0.19906E+00
1.00000	308.653	-0.24883E+03	0.11300E+04	-0.49343E-15

FLOW-015.DAT

===== FLUID =====

Density [lbm/ft³]: 0.25000E+00
Viscosity [lbm/ft-s]: 0.12000E-04
Kin.Viscosity [ft²/s]: 0.48000E-04

===== ROTOR =====

Outer Radius [in]: 3.00000
Inner Radius [in]: 1.00000
Disk Spacing [in]: 0.01042
Number of Disks: 0

===== TURBINE =====

Tangency Angle [deg]: 0.10000E+02
Mass Flow Rate [lbm/s]: -0.81430E-01
Outer Pressure [psig]: 0.51002E+01
Inner Pressure [psig]: 0.00000E+00

===== PERFORMANCE =====

Angular Velocity [1/s]: 0.00000E+00
 [rpm]: 0.00000E+00
Torque [in-lbf]: -0.54657E+00
Power [hp]: 0.00000E+00

===== CONSTANTS =====

A [ft²/s]: -0.29860E+02
B [ft²/s]: 0.13188E+03
C [ft²/s]: 0.00000E+00
Rc [1/ft²]: -0.40000E+01
D [psi]: 0.10407E+02

===== INTERNAL CONDITIONS =====				
R (in)	Theta (deg)	U (ft/s)	Vbar (ft/s)	P (psig)
3.00000	0.000	-0.11944E+03	0.67737E+03	0.51002E+01
2.90000	10.929	-0.12356E+03	0.68933E+03	0.49197E+01
2.80000	22.060	-0.12797E+03	0.70274E+03	0.47360E+01
2.70000	33.419	-0.13271E+03	0.71772E+03	0.45485E+01
2.60000	45.032	-0.13781E+03	0.73443E+03	0.43569E+01
2.50000	56.928	-0.14333E+03	0.75306E+03	0.41606E+01
2.40000	69.139	-0.14930E+03	0.77384E+03	0.39591E+01
2.30000	81.702	-0.15579E+03	0.79701E+03	0.37517E+01
2.20000	94.658	-0.16287E+03	0.82289E+03	0.35379E+01
2.10000	108.053	-0.17063E+03	0.85183E+03	0.33167E+01
2.00000	121.940	-0.17916E+03	0.88430E+03	0.30874E+01
1.90000	136.379	-0.18859E+03	0.92081E+03	0.28489E+01
1.80000	151.442	-0.19906E+03	0.96203E+03	0.26000E+01
1.70000	167.209	-0.21077E+03	0.10088E+04	0.23394E+01
1.60000	183.778	-0.22395E+03	0.10620E+04	0.20654E+01
1.50000	201.265	-0.23888E+03	0.11231E+04	0.17763E+01
1.40000	219.807	-0.25594E+03	0.11937E+04	0.14696E+01
1.30000	239.577	-0.27563E+03	0.12759E+04	0.11426E+01
1.20000	260.783	-0.29860E+03	0.13727E+04	0.79176E+00
1.10000	283.694	-0.32574E+03	0.14879E+04	0.41277E+00
1.00000	308.653	-0.35832E+03	0.16272E+04	-0.11842E-14

FLOW-116.DAT

===== FLUID =====

Density [lbm/ft³]: 0.25000E+00
Viscosity [lbm/ft-s]: 0.12000E-04
Kin.Viscosity [ft²/s]: 0.48000E-04

===== ROTOR =====

Outer Radius [in]: 3.00000
Inner Radius [in]: 1.00000
Disk Spacing [in]: 0.06250
Number of Disks: 0

===== TURBINE =====

Tangency Angle [deg]: 0.10000E+02
Mass Flow Rate [lbm/s]: -0.45239E-01
Outer Pressure [psig]: 0.16963E-01
Inner Pressure [psig]: 0.00000E+00

===== PERFORMANCE =====

Angular Velocity [1/s]: 0.00000E+00
 [rpm]: 0.00000E+00
Torque [in-lbf]: -0.90999E-02
Power [hp]: 0.00000E+00

===== CONSTANTS =====

A [ft²/s]: -0.27648E+01
B [ft²/s]: 0.14547E+02
C [ft²/s]: 0.00000E+00
Rc [1/ft²]: -0.12000E+01
D [psi]: 0.37592E-01

===== INTERNAL CONDITIONS =====

R (in)	Theta (deg)	U (ft/s)	Vbar (ft/s)	P (psig)
3.00000	0.000	-0.11059E+02	0.62720E+02	0.16963E-01
2.90000	10.993	-0.11441E+02	0.64564E+02	0.16425E-01
2.80000	22.318	-0.11849E+02	0.66553E+02	0.15870E-01
2.70000	34.000	-0.12288E+02	0.68703E+02	0.15296E-01
2.60000	46.070	-0.12761E+02	0.71031E+02	0.14703E-01
2.50000	58.559	-0.13271E+02	0.73559E+02	0.14088E-01
2.40000	71.505	-0.13824E+02	0.76311E+02	0.13449E-01
2.30000	84.948	-0.14425E+02	0.79318E+02	0.12785E-01
2.20000	98.937	-0.15081E+02	0.82613E+02	0.12094E-01
2.10000	113.524	-0.15799E+02	0.86237E+02	0.11372E-01
2.00000	128.771	-0.16589E+02	0.90240E+02	0.10617E-01
1.90000	144.748	-0.17462E+02	0.94682E+02	0.98241E-02
1.80000	161.538	-0.18432E+02	0.99634E+02	0.89904E-02
1.70000	179.238	-0.19516E+02	0.10519E+03	0.81108E-02
1.60000	197.960	-0.20736E+02	0.11146E+03	0.71795E-02
1.50000	217.843	-0.22118E+02	0.11858E+03	0.61898E-02
1.40000	239.050	-0.23698E+02	0.12674E+03	0.51334E-02
1.30000	261.783	-0.25521E+02	0.13618E+03	0.40005E-02
1.20000	286.293	-0.27648E+02	0.14723E+03	0.27784E-02
1.10000	312.896	-0.30161E+02	0.16030E+03	0.14516E-02
1.00000	342.002	-0.33178E+02	0.17602E+03	-0.38549E-17

FLOW-117.DAT

===== FLUID =====

Density [lbm/ft³]: 0.25000E+00
Viscosity [lbm/ft-s]: 0.12000E-04
Kin.Viscosity [ft²/s]: 0.48000E-04

===== ROTOR =====

Outer Radius [in]: 3.00000
Inner Radius [in]: 1.00000
Disk Spacing [in]: 0.03125
Number of Disks: 0

===== TURBINE =====

Tangency Angle [deg]: 0.10000E+02
Mass Flow Rate [lbm/s]: -0.90478E-01
Outer Pressure [psig]: 0.27141E+00
Inner Pressure [psig]: 0.00000E+00

===== PERFORMANCE =====

Angular Velocity [1/s]: 0.00000E+00
 [rpm]: 0.00000E+00
Torque [in-lbf]: -0.72799E-01
Power [hp]: 0.00000E+00

===== CONSTANTS =====

A [ft²/s]: -0.11059E+02
B [ft²/s]: 0.58188E+02
C [ft²/s]: 0.00000E+00
Rc [1/ft²]: -0.12000E+01
D [psi]: 0.60148E+00

===== INTERNAL CONDITIONS =====				
R (in)	Theta (deg)	U (ft/s)	Vbar (ft/s)	P (psig)
3.00000	0.000	-0.44237E+02	0.25088E+03	0.27141E+00
2.90000	10.993	-0.45762E+02	0.25826E+03	0.26280E+00
2.80000	22.318	-0.47397E+02	0.26621E+03	0.25392E+00
2.70000	34.000	-0.49152E+02	0.27481E+03	0.24474E+00
2.60000	46.070	-0.51042E+02	0.28412E+03	0.23524E+00
2.50000	58.559	-0.53084E+02	0.29423E+03	0.22540E+00
2.40000	71.505	-0.55296E+02	0.30525E+03	0.21519E+00
2.30000	84.948	-0.57700E+02	0.31727E+03	0.20457E+00
2.20000	98.937	-0.60323E+02	0.33045E+03	0.19350E+00
2.10000	113.524	-0.63195E+02	0.34495E+03	0.18195E+00
2.00000	128.771	-0.66355E+02	0.36096E+03	0.16986E+00
1.90000	144.748	-0.69848E+02	0.37873E+03	0.15718E+00
1.80000	161.538	-0.73728E+02	0.39854E+03	0.14385E+00
1.70000	179.238	-0.78065E+02	0.42075E+03	0.12977E+00
1.60000	197.960	-0.82944E+02	0.44582E+03	0.11487E+00
1.50000	217.843	-0.88474E+02	0.47431E+03	0.99037E-01
1.40000	239.050	-0.94793E+02	0.50697E+03	0.82135E-01
1.30000	261.783	-0.10208E+03	0.54474E+03	0.64007E-01
1.20000	286.293	-0.11059E+03	0.58890E+03	0.44455E-01
1.10000	312.896	-0.12065E+03	0.64121E+03	0.23226E-01
1.00000	342.002	-0.13271E+03	0.70410E+03	-0.61679E-16

FLOW-118.DAT

===== FLUID =====

Density [lbm/ft³]: 0.25000E+00
Viscosity [lbm/ft-s]: 0.12000E-04
Kin.Viscosity [ft²/s]: 0.48000E-04

===== ROTOR =====

Outer Radius [in]: 3.00000
Inner Radius [in]: 1.00000
Disk Spacing [in]: 0.02083
Number of Disks: 0

===== TURBINE =====

Tangency Angle [deg]: 0.10000E+02
Mass Flow Rate [lbm/s]: -0.13572E+00
Outer Pressure [psig]: 0.13740E+01
Inner Pressure [psig]: 0.00000E+00

===== PERFORMANCE =====

Angular Velocity [1/s]: 0.00000E+00
 [rpm]: 0.00000E+00
Torque [in-lbf]: -0.24570E+00
Power [hp]: 0.00000E+00

===== CONSTANTS =====

A [ft²/s]: -0.24883E+02
B [ft²/s]: 0.13092E+03
C [ft²/s]: 0.00000E+00
Rc [1/ft²]: -0.12000E+01
D [psi]: 0.30450E+01

===== INTERNAL CONDITIONS =====

R (in)	Theta (deg)	U (ft/s)	Vbar (ft/s)	P (psig)
3.00000	0.000	-0.99533E+02	0.56448E+03	0.13740E+01
2.90000	10.993	-0.10297E+03	0.58108E+03	0.13304E+01
2.80000	22.318	-0.10664E+03	0.59898E+03	0.12854E+01
2.70000	34.000	-0.11059E+03	0.61833E+03	0.12390E+01
2.60000	46.070	-0.11485E+03	0.63928E+03	0.11909E+01
2.50000	58.559	-0.11944E+03	0.66203E+03	0.11411E+01
2.40000	71.505	-0.12442E+03	0.68680E+03	0.10894E+01
2.30000	84.948	-0.12983E+03	0.71386E+03	0.10356E+01
2.20000	98.937	-0.13573E+03	0.74352E+03	0.97961E+00
2.10000	113.524	-0.14219E+03	0.77614E+03	0.92113E+00
2.00000	128.771	-0.14930E+03	0.81217E+03	0.85994E+00
1.90000	144.748	-0.15716E+03	0.85214E+03	0.79575E+00
1.80000	161.538	-0.16589E+03	0.89671E+03	0.72822E+00
1.70000	179.238	-0.17565E+03	0.94669E+03	0.65697E+00
1.60000	197.960	-0.18662E+03	0.10031E+04	0.58154E+00
1.50000	217.843	-0.19907E+03	0.10672E+04	0.50137E+00
1.40000	239.050	-0.21328E+03	0.11407E+04	0.41581E+00
1.30000	261.783	-0.22969E+03	0.12257E+04	0.32404E+00
1.20000	286.293	-0.24883E+03	0.13250E+04	0.22505E+00
1.10000	312.896	-0.27145E+03	0.14427E+04	0.11758E+00
1.00000	342.002	-0.29860E+03	0.15842E+04	-0.34540E-15